



HAL
open science

Planification de réseaux WDM translucides avec qualité de transmission garantie

Sawsan Al Zahr

► **To cite this version:**

Sawsan Al Zahr. Planification de réseaux WDM translucides avec qualité de transmission garantie. domain_other. Télécom ParisTech, 2007. English. NNT: . pastel-00004014

HAL Id: pastel-00004014

<https://pastel.hal.science/pastel-00004014>

Submitted on 9 Jan 2009

HAL is a multi-disciplinary open access archive for the deposit and dissemination of scientific research documents, whether they are published or not. The documents may come from teaching and research institutions in France or abroad, or from public or private research centers.

L'archive ouverte pluridisciplinaire **HAL**, est destinée au dépôt et à la diffusion de documents scientifiques de niveau recherche, publiés ou non, émanant des établissements d'enseignement et de recherche français ou étrangers, des laboratoires publics ou privés.

École Nationale Supérieure des Télécommunications
École Doctorale d'Informatique, Télécommunications et Électronique de Paris

THESE

Pour obtenir le grade de

Docteur de l'École Nationale Supérieure des Télécommunications
Spécialité : Informatique et Réseaux

Présentée par

Sawsan Al Zahr

Planification de Réseaux WDM Translucides avec
Qualité de Transmission Garantie

Soutenue à Paris, le 23 novembre 2007 devant le jury

Marco Ajmone Marsan

Rapporteur

Jean-Michel Dumas

Rapporteur

Gérard Hébuterne

Examineur

Pascal Berthomé

Examineur

Maurice Gagnaire

Directeur de thèse

Nicolas Puech

Co-directeur de thèse

WDM Translucent Networks Planning with Guaranteed Quality of Transmission

by

Sawsan Al Zahr

Thesis submitted to the

École Nationale Supérieure des Télécommunications

in partial fulfillment of the requirements of the degree of

Doctor of Philosophy
Networks and Computer Science

Examining committee:

Marco Ajmone Marsan	Reviewer
Jean-Michel Dumas	Reviewer
Gérard Hébuterne	Examiner
Pascal Berthomé	Examiner
Maurice Gagnaire	Ph.D. advisor
Nicolas Puech	Ph.D. co-advisor

Paris, November 23, 2007

Copyright © 2007 by Sawsan Al Zahr

All right reserved. No part of this thesis may be reproduced, in any form or by any means, without the author's prior written consent and information.

À Siham et Nicolas,
*pour leur confiance et leur soutien,
pour leur amour inconditionnel.*

À Nisrine,
*pour que la complicité qui nous unit
continue encore longtemps.*

Remerciements

À mon directeur de thèse, Monsieur Maurice Gagnaire, *pour m'avoir accueillie dans son équipe et pour avoir encadré mes travaux de recherche depuis mon stage de D.E.A et durant mes trois années de thèse. Pour son appui, ses conseils et le temps qu'il m'a consacré, mais aussi pour les responsabilités qu'il m'a données, je l'assure de ma profonde reconnaissance.*

À Monsieur Nicolas Puech *pour avoir co-encadré mon travail durant les trois années de thèse. Je le remercie pour ses conseils avisés, pour le temps qu'il m'a accordé mais surtout pour ses encouragements inlassables.*

À Messieurs Jean-Michel Dumas de l'école nationale supérieure d'ingénieurs de Limoges, Marco Ajmone Marsan de Politecnico di Torino, Gérard Hébuterne de l'institut national des télécommunications, et Pascal Berthomé de l'université de Paris-Sud, *pour m'avoir fait l'honneur de participer à mon jury et pour l'intérêt qu'ils ont porté à mon travail.*

À Messieurs Jean-Michel Dumas et Marco Ajmone Marsan *pour avoir accepté d'être rapporteurs de ma thèse. Leurs commentaires et leurs questions m'ont donné de nouvelles pistes de réflexion.*

À Monsieur Thierry Zami d'Alcatel-Lucent R&I *pour m'avoir initiée à la transmission sur fibre et pour avoir répondu à toutes mes questions avec beaucoup de gentillesse.*

À Mesdames et Messieurs Florence Besnard, Sophie Bérenger, Céline Bizart, Hayette Sousou, Bernard Robinet, Stéphane Bonenfant et Frantz Cayol, *pour*

leur aide, mais surtout pour avoir rendu mon séjour à l'école facile et agréable. Je leur exprime ma profonde reconnaissance.

À Sana Horrich, Nagi Attalah et Rawad Zgheib pour m'avoir chaleureusement entourée. Ils étaient toujours présents pour écarter les doutes et partager les joies. Je les remercie pour leur simple présence.

À Mireille Sarkiss pour m'avoir supportée aussi longtemps, en toutes circonstances, pour m'avoir écoutée et soutenue de nombreuses fois, pour tout ce qu'on a vécu ensemble et qui nous a tant rapproché, pour que cette amitié continue malgré la distance et les années.

À Rosy Aoun pour son amitié, pour sa gaieté et sa bonne humeur, pour avoir rendu la dernière année de ma thèse aussi agréable qu'elle peut l'être. Merci Rosy et bonne continuation !

À Ihsan Fsaifes pour son amitié, son soutien, et pour nos longues discussions toujours enrichissantes. Je le remercie également pour la lecture de mon rapport.

À Elias Doumith avec qui, j'ai pu partager les doutes et les avancées de nos travaux, les mauvais mais surtout de très bons moments. Son amitié m'est très précieuse et m'est toujours de grand réconfort.

À ma sœur Nisrine de m'avoir ouvert les portes fermées pour pouvoir venir en France et continuer mes études de troisième cycle.

Paris, le 10 janvier 2008

Résumé

Introduction

Grâce au multiplexage en longueur d'onde permettant une utilisation efficace de la bande passante offerte par la fibre, les réseaux de fibre optique à haut débit se mettent progressivement en place. Les réseaux optiques à multiplexage en longueur d'onde ou WDM (Wavelength Division Multiplexing) offrent la possibilité de satisfaire, à coût réduit, à la demande croissante de services de télécommunications. L'introduction de la transparence dans le but d'augmenter la capacité de transmission et la flexibilité des systèmes conduit à de nouveaux problèmes d'optimisation pour plusieurs raisons. Premièrement, les coûts des équipements optiques sont encore mal connus en raison du caractère récent des technologies utilisées dans ces équipements. Deuxièmement, l'incertitude de la demande, liée notamment à la concurrence dans le marché des télécommunications et l'adoption de nouvelles applications, rendent difficile la planification de ces réseaux. Enfin, les nouvelles technologies optiques introduisent de nouvelles contraintes qui doivent être prises en compte dans la phase de planification du réseau.

Au cours des deux dernières décennies, de nombreuses études ont été réalisées autour du problème de routage et d'affectation de longueurs d'onde dans les réseaux tout-optiques (transparents). La majorité de ces études néglige la dégradation du signal optique due à la traversée des divers équipements installés le long du chemin optique. Cependant, le signal optique subit tout au long de son parcours plusieurs effets perturbateurs liés à la transmission sur fibre, à savoir l'atténuation, la dispersion et les effets non-linéaires [1][2]. Après avoir traversé plusieurs équipements

et systèmes, le signal optique peut être trop affaibli par rapport à la sensibilité des photo-détecteurs, mais aussi trop dégradé en terme de déphasage.

Au milieu des années 1990, les travaux en matière de planification de réseaux transparents ont fait apparaître une nouvelle tendance consistant à évaluer et à prendre en compte les dégradations subies par le signal optique tout au long de son parcours. Ces travaux prennent en compte principalement la dispersion chromatique (Chromatic Dispersion, CD), la dispersion modale de polarisation (Polarisation Mode Dispersion, PMD) et l'émission spontanée amplifiée (Amplified Spontaneous Emission, ASE) qui a un impact direct sur le rapport signal optique à bruit (Optical Signal to Noise Ratio, OSNR). Des travaux récents prennent en compte également les effets non-linéaires comme, par exemple, l'auto-modulation de phase (Self Phase Modulation, SPM), la modulation de phase croisée (Cross Phase Modulation, XPM), le mélange à quatre ondes (Four Waves Mixing, FWM) ou encore l'interférence entre canaux optiques (Cross Talk).

Dans les réseaux WDM opaques, le signal optique est régénéré systématiquement dans chaque nœud du réseau et par conséquent, la question de la qualité du signal ne se pose pas. Cependant, la régénération électrique à chaque nœud du réseau coûte très cher aux opérateurs. Une solution alternative se situe à mi-chemin entre les réseaux opaques et les réseaux transparents. Cette solution consiste à offrir la possibilité de régénérer le signal dans un nœud intermédiaire du chemin optique si la qualité du signal optique ne satisfait plus aux contraintes de qualité imposées par l'opérateur. De tels réseaux sont qualifiés de translucides.

Dans cette thèse, nous nous intéressons au problème du routage, de l'affectation de longueurs d'onde, et du placement de régénérateur dans les réseaux optiques translucides. Deux problèmes majeurs doivent alors être résolus : i) l'évaluation de la qualité de transmission associée à un chemin optique donné ; ii) le choix de l'emplacement des régénérateurs dans le réseau.

Évaluation de la Qualité du Signal Optique

Dans les systèmes de télécommunications numériques, la qualité du signal peut être prise en compte de manière globale à travers le taux d'erreur binaire (Bit Error Rate, BER). Ce dernier désigne le rapport entre le nombre de bits erronés durant un

intervalle de temps τ et le nombre total des bits transmis durant le même intervalle τ . Quelle que soit la cause des erreurs (déformation des impulsions, niveau de bruit trop élevé ou mauvaise récupération de l'horloge), le BER permet de savoir si la qualité de transmission est suffisante pour assurer un service donné. En pratique, un BER inférieur à 10^{-9} voire 10^{-15} est requis pour les services nécessitant une qualité de service garantie, en l'occurrence la voix.

Le temps d'acquisition pose un problème dans la mesure du BER. En effet, même avec un débit de 10 Mbps/canal, l'obtention d'une mesure fiable d'un taux d'erreur de l'ordre de 10^{-15} nécessite un délai de plusieurs jours. Comme il est concrètement impossible de faire des mesures interactives sur un délai aussi grand ou parce que l'on souhaite en connaître des valeurs prospectives, il est intéressant de pouvoir disposer d'un moyen d'estimer le BER. La méthode du facteur \mathcal{Q} , que l'on utilise dans cette thèse, est une méthode d'estimation du BER lorsque ce dernier est trop faible pour être mesuré directement.

Le facteur \mathcal{Q} est relié au BER par la relation :

$$\text{BER} = \frac{1}{2} \operatorname{erfc} \left(\frac{\mathcal{Q}}{\sqrt{2}} \right) \quad (1)$$

où erfc est la fonction d'erreur complémentaire. Il s'agit ici du facteur \mathcal{Q} optimal du signal ; il est tel que les taux d'erreur sur les "0" et sur les "1" soient identiques. Grâce à l'équation 1, on peut connaître l'ordre de grandeur du BER d'un signal aux caractéristiques données. En pratique, on effectue cette mesure avec une très forte puissance sur le détecteur pour que les dégradations dues au récepteur restent négligeables. Il est important de rappeler que cette méthode s'appuie sur l'hypothèse que la distribution de bruit pour chaque symbole est Gaussienne. Cette hypothèse est une bonne approximation pour des systèmes ayant pour principale limitation le bruit provenant de l'émission spontanée amplifiée des amplificateurs optiques. En revanche, dans d'autres cas de figure tels qu'après le passage par un régénérateur, cette hypothèse n'est plus valable car le bruit subit une redistribution due à la non-linéarité du régénérateur par rapport à la puissance d'entrée.

On notera également l'importance de la position du seuil de décision. Pour le même signal, on peut obtenir plusieurs décades de différence sur le BER suivant cette position. Il existe deux positions privilégiées : le seuil en position optimale suivant le niveau du bruit optique et le seuil au milieu des niveaux électriques des

symboles “0” et “1”. Cette dernière position est optimale lorsque le niveau du bruit optique est faible car c’est alors le bruit thermique du détecteur, identique pour les deux symboles binaires, qui devient significatif.

Dans le chapitre 2, nous présentons les principaux concepts des réseaux WDM, les composants et systèmes utilisés dans un réseau WDM de longue portée ainsi que les principales dégradations physiques affectant le signal optique.

Les Principales Dégradations du Signal Optique

Dans cette thèse, le calcul du facteur Q tient compte de quatre effets perturbateurs liés à la transmission sur fibre, à savoir la dispersion chromatique, la dispersion modale de polarisation, la phase non-linéaire et l’émission spontanée amplifiée. L’originalité de cette approche est non seulement la prise en compte de ces quatre dégradations mais aussi la prise en compte de leurs interactions. En l’occurrence, le niveau admissible de la dispersion chromatique dépend du niveau des effets non-linéaires.

Les Différents Types de Dispersion

Considérons une impulsion optique de faible durée (typiquement < 1 ns), dont les composantes spectrales sont centrées autour de ω_0 . $\beta(\omega)$ est sa constante de propagation. On établit alors que la vitesse de propagation de cette impulsion, nommée vitesse de groupe, est $1/\beta_1$. Cependant, β_1 dépend à son tour de nombreux paramètres tels que le mode transversal, sa polarisation ou la longueur centrale ω_0 . Cette dispersion de vitesse peut entraîner une déformation très gênante de l’impulsion optique lors de la transmission.

Dispersion Chromatique

La vitesse de groupe $1/\beta_1$ est fonction de la pulsation ω . Ainsi, deux impulsions de longueurs d’onde centrales différentes ne voyagent pas à la même vitesse. C’est la dispersion chromatique qui caractérise l’étalement du signal lié à sa largeur spectrale et s’exprime en picoseconde par nanomètre par kilomètre ($\text{ps.nm}^{-1}.\text{km}^{-1}$).

$$D = \frac{d\beta_1}{d\lambda} = -\frac{2\pi c}{\lambda^2} \beta_2 \approx \frac{\lambda}{c} \frac{d^2 n}{d\lambda^2} \quad (2)$$

Deux régimes peuvent être distingués suivant le signe de D :

- La dispersion est dite anormale si $D > 0$; les grandes longueurs d’onde vont plus vite que les courtes.

-
- La dispersion est dite normale si $D < 0$; les grandes longueurs d'onde vont moins vite que les courtes.

La dispersion chromatique crée des différences de vitesse de propagation entre les différents canaux d'un signal WDM. Elle induit aussi des différences de vitesse au sein des composantes spectrales d'un même canal. Ainsi, pour des signaux haut débit dont le spectre optique est relativement large, les impulsions se déforment sous l'influence de la dispersion chromatique. Cette déformation s'accroît le long de la propagation sur la fibre. Plus le paramètre D est élevé en valeur absolue, plus les effets de la dispersion chromatique sont marqués. Ces effets, additifs durant la propagation, peuvent être éliminés si la dispersion chromatique cumulée au bout de la transmission est quasiment nulle. Ainsi, en disposant périodiquement de modules de fibre dont la dispersion s'oppose à celle des fibres de ligne, on peut augmenter considérablement la portée du système.

Dans notre approche, nous considérons des cartes de gestion de la dispersion chromatique. Ces cartes déploient des sections de fibre qui induisent une forte dispersion négative pour opposer l'effet de la dispersion chromatique induite par les fibres de ligne. Ces cartes compensent la dispersion chromatique graduellement le long d'un lien entre deux nœuds et ramènent la dispersion à zéro au niveau de chaque nœud intermédiaire du chemin optique (voir Chapitre 3).

Dispersion Modale de Polarisation

Dans une fibre idéale, il existe un seul mode de polarisation optique. En pratique, une fibre possède deux modes de polarisation privilégiés. Dans le cas d'une fibre parfaitement isotrope, ces deux modes auraient une même vitesse de groupe mais les variations aléatoires de l'ellipticité du cœur et les contraintes mécaniques externes brisent cette symétrie. Ainsi, ces deux modes de polarisation ne présentent pas la même vitesse de groupe et les différents axes de polarisation privilégiés de la fibre ne sont pas constants sur toute sa longueur. Le délai différentiel de groupe (Differential Group Delay, DGD) désigne l'étalement du signal dans le temps dû à la dispersion modale de polarisation. Ce délai est donné comme suit :

$$\Delta\tau = \Delta\beta/\omega \quad (3)$$

où $\Delta\beta$ désigne la différence de la constante de propagation et ω désigne la fré-

quence angulaire. Le DGD dépend de la racine carrée de la distance parcourue. Une valeur typique du DGD est $0.5 \text{ ps}/\sqrt{\text{km}}$ qui signifie qu'après 100 km de propagation, le délai cumulé sera de l'ordre de 50 ps. Cette valeur doit être comparée au temps bit ; ce dernier vaut 100 ps dans les systèmes 10 Gbps. La dispersion modale de polarisation devient un facteur limitant dans les systèmes de transmission haut débit.

La Phase Non-Linéaire

La phase non-linéaire est due à l'effet Kerr traduit par l'équation suivante :

$$\phi_{NL} = n_2 k_0 L |E|^2 \quad (4)$$

où n_2 est le coefficient non-linéaire de l'indice de réfraction, $k_0 = 2\pi/\lambda$, L est la longueur de la fibre et $|E|^2$ est l'intensité optique. Dans les systèmes utilisant la modulation par sauts de phase, la phase non-linéaire peut conduire à des élargissements fréquentiels des impulsions. Les variations instantanées dans la phase du signal peuvent engendrer des variations instantanées dans les fréquences autour de la fréquence centrale du signal. Ces variations sont dues au changement de l'intensité du signal. En conséquence, différentes parties de l'impulsion subissent différents sauts de phase. Cet effet est proportionnel à la puissance du signal et par conséquent, la phase non-linéaire devient un facteur très limitant dans les systèmes utilisant des puissances très élevées.

L'Émission Spontanée Amplifiée

Le principe d'un amplificateur optique est basé sur l'émission stimulée. Elle s'accompagne d'une émission spontanée qui ajoute au signal amplifié des photons totalement incohérents. Une partie de ces photons est couplée avec le mode du signal dans la fibre de transmission de telle sorte qu'elle l'accompagne après l'amplification. Cette émission a lieu tout au long du milieu amplificateur. En conséquence, les photons spontanément émis en début de la fibre amplificatrice seront eux-même amplifiés. C'est pourquoi on parle d'émission spontanée amplifiée.

L'importance du bruit ajouté est quantifiée via le rapport signal optique à bruit (OSNR). Les amplificateurs optiques sont placés périodiquement sur un lien pour amplifier la puissance du signal optique. Chaque amplificateur ajoute du bruit au

signal et donc l'OSNR se dégrade graduellement tout au long du lien. L'OSNR à la sortie d'un amplificateur est donné par l'équation :

$$OSNR = \frac{P_{in}}{NF \times h\nu \times \Delta f} \quad (5)$$

où NF représente la figure de bruit de l'amplificateur optique, h est la constante de Plank, ν est la fréquence optique et Δf est la bande de la mesure de la figure de bruit. Quand on considère des systèmes WDM avec une cascade d'amplificateurs, l'émission spontanée amplifiée devient un facteur limitant car la figure de bruit s'accumule le long de la cascade.

Prediction du BER

Dans le but d'obtenir une estimation de la valeur du facteur \mathcal{Q} pour chaque chemin optique dans le réseau, nous avons développé un outil appelé BER-Predictor. Cet outil calcule la valeur du facteur \mathcal{Q} , dans tous les nœuds intermédiaires le long d'un chemin optique jusqu'à la destination en fonction des pénalités induites par les effets physiques considérés. La valeur estimée du BER est déterminée par la valeur calculé du facteur \mathcal{Q} .

Dans le chapitre 3, nous présentons le modèle physique du système de transmission considéré dans ce travail. Nous décrivons les différentes étapes du BER-Predictor, à savoir l'initialisation des paramètres du système et le calcul du facteur \mathcal{Q} . Étant donné la topologie du réseau et les caractéristiques des systèmes déployés dans le réseau, BER-Predictor fournit une estimation de la valeur du BER prévue au bout d'un chemin optique donné. BER-Predictor opère en trois étapes distinctes :

Étape 1. Un chemin optique est défini par son chemin physique et la longueur d'onde attribuée à ce chemin. Le réseau est défini par la topologie physique et les caractéristiques physiques de ses équipements et ses systèmes (fibres, amplificateurs optiques, brasseurs optiques, etc.) La topologie du réseau constitue une donnée d'entrée de l'outil BER-Predictor ; elle se présente sous la forme d'un fichier texte dont chaque ligne décrit un lien du réseau (les deux nœuds adjacents, la longueur du lien, les longueurs des spans¹). Les caractéristiques physiques des équipements et des systèmes du réseau sont fournis à BER-Predictor en fichier texte dans lequel chaque ligne décrit un équipement ou un

¹Le mot "span" désigne la section de fibre reliant deux amplificateurs optiques adjacents.

système spécifique. La première étape de BER-Predictor consiste à initialiser tous les paramètres relatifs à la transmission.

Étape 2. Le long de son trajet, le signal optique traverse différents équipements et systèmes optiques. Chaque équipement ou système induit une pénalité sur la puissance du signal. La deuxième étape de BER-Predictor consiste à simuler la propagation du signal optique du nœud source au nœud destinataire. Cette simulation est réalisée en calculant de nouvelles valeurs des paramètres de la transmission (la puissance du signal, la dispersion chromatique, le bruit, etc.) à la sortie de chaque équipement traversé.

Étape 3. Les valeurs de la dispersion chromatique, de la dispersion modale de polarisation, de la phase non-linéaire et de l'émission spontanée amplifiée, qui ont été calculées dans la deuxième étape, sont utilisées dans cette troisième étape pour calculer la valeur du facteur Q . L'expression analytique du facteur Q a été développée dans le cadre du projet RYTHME² aux sein des laboratoires d'Alcatel-Lucent R&I. Cette expression repose sur la modélisation mathématique des phénomènes physiques et leur validation en vraie grandeur sur une boucle optique expérimentale. Comme indiqué plus haut, la valeur du facteur Q détermine la valeur du BER estimée à la sortie de chaque nœud traversé et ce jusqu'à destination.

Limites de la Transparence dans les Réseaux WDM

Afin de souligner les limites de la transparence dans un réseau WDM réel, une étude préliminaire est présentée dans le chapitre 4. Dans ce chapitre, nous étudions l'évolution de la qualité de transmission en fonction de la longueur des connexions. À ce stade de la thèse, nous nous intéressons principalement à la qualité de transmission ; le problème du routage, de l'affectation de longueurs d'onde et du placement de régénérateurs n'est pas encore traité à ce stade-là.

Pour ce faire, nous considérons le plus court chemin entre tous les couples source-destinations possible dans le réseau et nous calculons la valeur du facteur Q pour chaque chemin possible. Nous classons les valeurs du facteur Q obtenues en fonction de la longueur des chemins. Cette procédure est effectuée systématiquement

²Le projet RYTHME (Réseaux hYbrides Transparents Hiérarchiques à Multiplexage En longueurs d'onde) est un projet national de recherche dont l'ENST fait partie.

pour deux réseaux différents, à savoir le réseau Européen EBN (European Backbone Network) et le réseau Américain NSFNet (National Science Foundation Network). Ces réseaux se différencient en termes de longueur moyenne des liens et degré physique moyen des nœuds. Une comparaison entre les résultats obtenus pour les deux réseaux permet de tirer une conclusion sur l'impact de la topologie du réseau sur la qualité de transmission.

Dans la partie 4.2, nous faisons l'hypothèse que la courbe de dispersion des fibres ainsi que la courbe du gain des amplificateurs sont plates par rapport à la longueur d'onde. En d'autres termes, la qualité de transmission sur une connexion donnée ne dépend pas de la longueur d'onde empruntée par la connexion. En considérant un seuil de facteur Q de 15.59 dB (BER de 10^{-9}), les résultats de simulation montrent la faisabilité de connexions transparentes de 1800 km et 2200 km dans respectivement l'EBN et le NSFNet (voir la figure 4.9).

Dans la partie 4.3, nous nous intéressons à l'impact de la non-platitude spectrale de la courbe de dispersion et de la courbe du gain. Dans cette partie, nous comparons les résultats obtenus pour chaque réseau en considérant deux longueurs d'onde de la bande C, à savoir $\lambda_1 = 1538.48$ nm et $\lambda_2 = 1554.13$ nm. Dans le cas du réseau EBN, les résultats de simulation montrent que les deux longueurs d'onde permettent de réaliser une portée de 2080 km. En revanche, dans le réseau NSFNet, λ_1 permet d'atteindre une portée de 2000 km contre 1500 km faisable avec λ_2 (voir la figure 4.15). Ces résultats nous conduisent à deux conclusions importantes : i) la topologie du réseau ayant un impact sur la qualité de transmission globale ; ii) dans la bande C (1530 - 1570 nm), il existe des longueurs d'onde permettant de réaliser des performances meilleures que celles réalisées par d'autres longueurs d'onde (voir la figure 4.16).

Comme indiqué plus haut, l'utilisation de l'amplificateur présente l'inconvénient d'une amplification inégale des différentes longueurs d'onde due à la non-platitude spectrale du gain. Afin de faire face à ce problème, nous optons pour l'utilisation d'un égaliseur de gain dynamique (DGE pour Dynamic Gain Equalizer). Ce dernier intervient pour réaliser une égalisation des niveaux des différentes longueurs d'onde du spectre incident dans la bande C.

Jusqu'à présent, aucun schéma d'égalisation en ligne n'a été considéré : l'égalisation du gain a lieu uniquement au niveau des nœuds. Dans la partie 4.4, nous

études l'impact de l'égalisation en ligne sur la qualité de transmission dans le réseau. Dans un premier temps, nous déployons un égaliseur tous les spans (après chaque amplificateur). Les résultats de simulation montrent que l'égalisation n'a pas de grande influence dans le cas du réseau EBN (voir la figure 4.19(b)). En revanche, on peut constater une nette amélioration dans le cas du réseau NSFNet et en particulier pour les distances supérieures à 3500 km (voir la figure 4.19(d)). A partir de ces résultats, on constate que l'égalisation du gain en ligne permet de réaliser une meilleure harmonie dans les performances des différentes longueurs d'onde. L'impact du pas d'égalisation (le nombre d'amplificateurs entre deux égaliseurs) est discuté à la fin de cette partie (voir la figure 4.20).

À l'aide du logiciel BER-Predictor, nous établissons une base de données contenant le facteur Q associé à chaque chemin optique qu'il est possible d'établir dans le réseau. Cette base de données est établie hors ligne à partir de la description de la topologie du réseau considéré et la description de la technologie utilisée dans ce réseau. Elle est consultée à chaque fois qu'il est nécessaire d'évaluer le facteur Q d'un chemin optique donné.

Réseaux WDM Translucides

La principale contribution de cette thèse est d'étudier la faisabilité de réseaux optiques translucides. Étant donné la topologie physique d'un réseau et un ensemble de demandes de connexions permanentes, comment satisfaire à ces demandes en garantissant une certaine qualité de transmission ? Dans le chapitre 5, nous présentons un état de l'art des travaux réalisés dans ce domaine. Nous classons ces travaux sous deux grandes catégories : i) la prise en compte de la qualité de transmission dans le routage et l'affectation de longueurs d'onde de sorte à minimiser le nombre de demandes rejetées faute de qualité de signal [3] [4] [5]; ii) la planification des réseaux translucides dans lesquels des régénérateurs sont installés pour satisfaire aux contraintes de qualité de transmission [6] [7] [8] [9].

Dans ce contexte, nous proposons un nouvel algorithme permettant de traiter le problème du dimensionnement de réseaux translucides. Le logiciel qui implémente cet algorithme est appelé LERP pour *Lightpath Establishment and Regenerator Placement*. L'originalité de cet algorithme est de combiner de manière itérative la phase

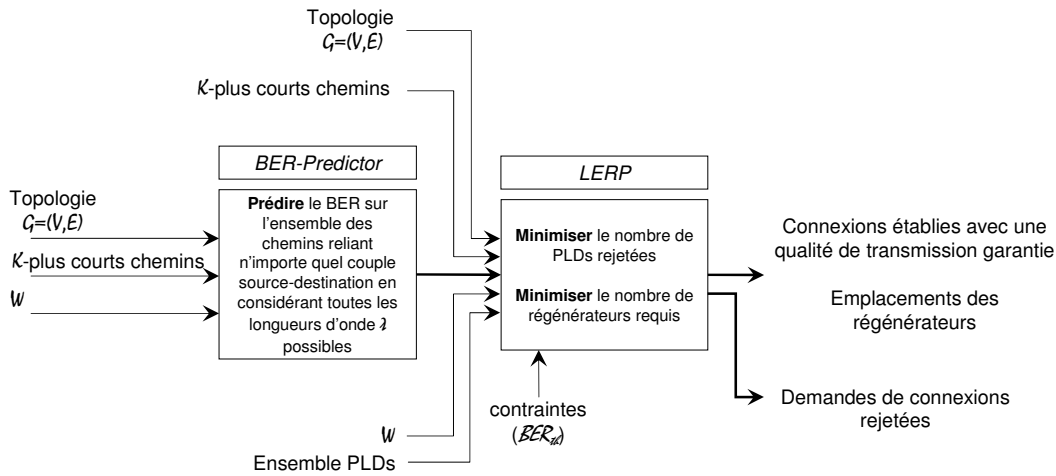


Fig. 1: Routage, affectation de longueurs d'onde, et placement de régénérateurs avec une qualité de transmission garantie.

de routage et d'affectation de longueurs d'onde avec la phase de placement de régénérateurs afin d'optimiser les ressources du réseau tout en minimisant le nombre nécessaire de régénérateurs. En d'autres termes, l'objectif de cet algorithme est de minimiser le nombre de demandes rejetées faute de ressources du réseau ainsi que le nombre de régénérateurs requis pour satisfaire aux contraintes de qualité définies par l'opérateur. Le chapitre 6 présente une description détaillée de notre algorithme et ses variantes.

Routage et Placement de Régénérateurs

La figure 1 représente une description schématique de la solution proposée au problème de la planification de réseaux translucides avec qualité de transmission garantie. Nous définissons ce problème comme suit :

Étant donné :

- une topologie représentée par le graphe $\mathcal{G} = (\mathcal{V}, \mathcal{E})$, où \mathcal{V} représente l'ensemble des sommets (nœuds du réseau) et \mathcal{E} représente l'ensemble des arcs (liens du réseau) ;
- un ensemble de demandes de connexions permanentes PLDs (Permanent Light-path Demands) ;
- un ensemble de longueurs d'onde W disponible par fibre optique ;
- un seuil admissible du BER dans le réseau BER_{th} .

Trouver :

-
- une solution de routage et d'affectation de longueurs d'onde qui minimise le nombre de demandes de connexions rejetées ;
 - une solution de placement de régénérateurs qui minimise le nombre de régénérateurs requis pour satisfaire aux contraintes de qualité exigées.

Une première version de LERP, appelé sLERP pour *simple LERP*, consiste à traiter séparément le problème du routage et de l'affectation de longueurs d'onde et le problème du placement de régénérateurs. La première étape de sLERP repose sur un algorithme de routage et d'affectation de longueur d'onde séquentiel amélioré. L'ordre de traitement des demandes de connexion ayant un grand impact sur le taux de rejet dans le réseau, nous adoptons un algorithme assorti d'une recherche aléatoire pour définir un ordre de traitement judicieux. Cet algorithme consiste à considérer la combinatoire d'un grand ensemble de solutions possibles où chaque solution correspond à un scénario incrémental aléatoire. En d'autres termes, si l'ensemble de demandes est constitué de D demandes, $D!$ (factorielle de D) scénarios incrémentaux différents sont possibles. Parmi ces $D!$ scénarios, nous choisissons celui dont la solution correspond au taux de rejet minimal. Pour des grandes valeurs de D ($D > 10$), nous considérons un sous ensemble de $D!$.

Une série de simulations, présentée dans la partie 6.3.4, montre l'intérêt de l'utilisation d'une méthode de recherche aléatoire par rapport à un algorithme séquentiel classique. Notre algorithme amélioré permet de réaliser un gain de l'ordre de 20% en terme de nombre de demandes rejetées faute de ressources d'une part et un gain de l'ordre de 22% en terme de nombre moyen de canaux optiques consommés par demande d'autre part (voir les figures 6.3 et 6.4). En effet, cette méthode de recherche aléatoire permet d'obtenir des résultats très proches de ceux obtenus avec une méthode exacte (voir la partie 6.3.5). A la différence de la méthode exacte, la recherche aléatoire permet de traiter de problèmes de plus grande taille [10].

À l'issue de la première étape du routage et de l'affectation de longueurs d'onde, nous disposons de la liste des demandes acceptées associées aux chemins optiques qui leur ont été affectés. La deuxième étape considère successivement les chemins optiques de ces demandes acceptées et décide l'emplacement des régénérateurs éventuels dans les nœuds intermédiaires ; la régénération a lieu dès qu'on constate que le signal ne satisfait plus à la contrainte de qualité imposée.

LERP repose sur une première phase identique à celle de sLERP. Il diffère de sLERP dans sa deuxième phase qui est plus sophistiquée et repose sur un module appelé QoT-Test. Considérant une connexion reliant une source s à une destination d ayant une qualité de transmission insuffisante (facteur Q inférieur au seuil admissible) dans un nœud intermédiaire i :

- Nous installons un régénérateur au nœud $(i - 1)$.
- Nous découpons le chemin optique en deux sous-chemins. Le premier relie la source s au nœud régénérant $(i - 1)$ et le dernier constitue une nouvelle demande reliant le nœud régénérant $(i - 1)$ à la destination d . Les ressources du chemin $(s, i - 1)$ sont réservées et la nouvelle demande $(i - 1, d)$ est placée dans une nouvelle matrice de demandes.
- Une fois toutes les connexions analysées en terme de qualité, nous considérons la matrice de demandes résiduelles et nous procédons au routage de ces demandes en appliquant de nouveau l'algorithme du routage et de l'affectation de longueurs d'onde.

Cette procédure recursive est répétée jusqu'à ce que toutes les connexions soient établies en satisfaisant à la qualité de transmission exigée. A ce stade, nous reconsidérons les demandes rejetées dans la première phase. Ces demandes peuvent en effet avoir une chance d'être établies dans la mesure où les régénérateurs installés dans le réseau ont relaxé la contrainte de la continuité de longueur d'onde. La figure 2 présente le synopsis de LERP.

On peut constater l'intérêt de LERP par rapport à sLERP à partir des résultats de simulation présentés dans la partie 6.4.4. La figure 6.7 montre que pour un scénario donné (matrice de demandes et nombre de longueurs d'onde par fibre), LERP utilise moins de régénérateurs que sLEPR. Par exemple, pour quatre longueurs d'onde disponibles par fibre ($W = 4$), LERP peut réaliser un gain de 13% en terme du nombre de régénérateurs requis. De plus, LERP permet de satisfaire plus de demandes que sLERP grâce à la dernière phase permettant de reconsidérer les demandes qui ont été initialement rejetées (voir la figure 6.8). Dans notre exemple ($W = 4$), LERP permet d'optimiser l'utilisation des ressources en réalisant un gain d'environ 12% en terme du nombre de chemins établis dans le réseau.

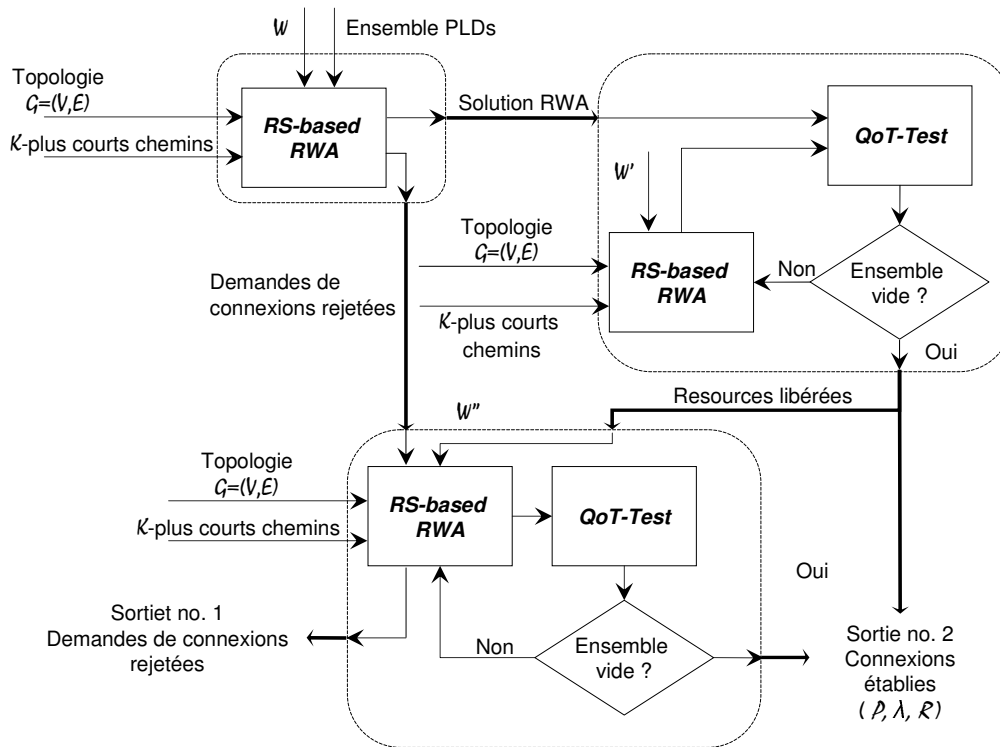


Fig. 2: Synopsis de LERP.

Égalisation du Gain et Stratégies de Coloration

Dans le chapitre 4, nous avons étudié l'impact de la non-platitude spectrale du système de transmission sur la qualité du signal. Nous avons vu qu'on peut faire face à la non-platitude spectrale de la courbe du gain en utilisant des égaliseurs de gain dynamiques. Dans la partie 6.5, nous étudions l'impact de l'utilisation d'égaliseurs de gain dynamiques sur le nombre de régénérateurs requis dans le réseau pour satisfaire aux contraintes de la qualité de transmission. Dans cette partie, nous avons adopté un schéma d'égalisation déployant un égaliseur tous les cinq spans. Les résultats de simulation montrent que l'utilisation d'un schéma d'égalisation en ligne permet de réaliser un gain de 30% et de 40% respectivement pour de petites et de grandes charges de trafic (voir les figures 6.10 et 6.11). Nous avons également étudié le bénéfice d'un compromis entre la régénération électrique et l'égalisation dynamique du gain. Les résultats de simulation ont montré que l'égalisation dynamique du gain est essentiellement intéressante pour de fortes charges de trafic (voir figure 6.13). Ce résultat est intuitif puisqu'un égaliseur est un équipement mutuel; il est capable de traiter plusieurs canaux optiques en parallèle. À l'opposé d'un égaliseur, un régéné-

rateur électrique est un équipement dédié, capable de traiter un seul canal optique à la fois.

Les résultats obtenus dans la partie 4.3 nous ont conduit à proposer de nouvelles stratégies d'affectation de longueurs d'onde, à savoir min-BER-fit (MBF) et best-BER-fit (BBF). Ces nouvelles stratégies tiennent compte de la qualité de transmission inhérente au choix de la longueur d'onde. MBF choisit la longueur d'onde ayant les meilleures performances parmi les longueurs d'onde disponibles alors que BBF choisit celle ayant juste le minimum pour satisfaire les contraintes de qualité. Les résultats de simulation montrent que MBF et BBF offrent respectivement un gain de 66% et 50% pour de faibles charges de trafic. Pour de forte charges de trafic, BBF permet d'obtenir un gain de 15% alors que le gain obtenu avec MBF monte à 11.5% seulement (voir les figures 6.15 et 6.16). En outre, les résultats de simulation montrent que de telles stratégies peuvent compenser l'absence d'égaliseurs dans le réseau (voir la figure 6.18) et donc conduire à une réduction importante du coût du réseau.

Les outils proposés dans cette thèse, LERP et ses variantes, ont des applications potentielles pour les opérateurs et les équipementiers. En effet, la qualité de transmission est évaluée sur la base de caractéristiques réalistes de matériel de transmission actuellement disponibles sur le marché.

Travaux Futures

Dans la partie 6.6.3, nous présentons une étude préliminaire de l'impact de la topology du réseau sur la distribution des régénérateurs. Pour ce faire, nous avons considéré 10 matrices de trafic différentes de 400 demandes permanentes générées selon une loi uniforme. Les figures 6.19 et 6.20 montrent le nombre moyen des régénérateurs requis dans chaque nœud du réseau. Les résultats de simulations montrent que les nœuds 6 et 7, ayant le plus grand degré physique (5), nécessitent le plus grand nombre de régénérateurs. En outre, les liens reliant les nœuds 6 et 7 à leurs voisins sont très longs par rapport à la longueur moyenne des liens dans le réseau (982 km), en particulier les liens 7 – 14, 7 – 11 et 6 – 12. Cette observation nous conduit à concevoir une nouvelle approche du problème du placement de régénérateurs ; cette nouvelle approche repose sur un placement préliminaire des régénérateurs en se basant sur la topology physique du réseau.

L'expression analytique adoptée dans cette thèse pour le calcul du facteur \mathcal{Q} prend en compte un scénario de pire cas relativement à l'interférence entre canaux optiques (crosstalk ou XT). En d'autres termes, nous avons fait l'hypothèse que toutes les longueurs d'onde disponibles par fibre (W) propagent simultanément dans le réseau. Dans l'optique d'affiner la prise en compte de l'XT, nous envisageons une nouvelle stratégie d'affectation de longueurs d'onde visant à réduire l'XT.

Au cours de cette thèse, nous avons étudié deux schémas de protection dans les réseaux translucides, à savoir un schéma de protection 1 + 1 et un schéma de protection 1 : 1 [11]. Le problème de la protection partagée dans le contexte des réseaux translucides nécessite une étude étendue et approfondie.

Ces perspectives font partie d'un nouveau projet européen DICONET pour Dynamic Impairment Constraint Networking for Transparent Mesh Optical Networks, dans lequel, je suis personnellement impliquée.

Mots Clés

Fibre optique, longueur d'onde, amplification optique, multiplexage en longueur d'onde, canal optique, circuit optique, commutation de circuits, réseaux optiques, transparence, réseaux opaques, réseaux tout-optiques, réseaux translucides, conversion de longueur d'onde, transmission sur fibre, dispersion chromatique, dispersion modale de polarisation, effets non-linéaires, émission spontanément amplifiée, qualité de transmission, facteur \mathcal{Q} , régénération, égalisation du gain, planification, routage, affectation de longueurs d'onde, placement de régénérateurs, optimisation, modèles linéaires à nombres entiers, heuristiques.

Abstract

The problem of routing and wavelength assignment (RWA) in all-optical WDM networks has been deeply investigated in the literature. Most of these studies neglect the impact of transmission impairments on the feasibility of all-optical connections. Actually, the optical signal undergoes along its route various transmission impairments like attenuation, dispersion, nonlinearities, etc. In fully opaque WDM networks, the quality of transmission is always considered as acceptable since 3R (Re-amplifying, Re-shaping, and Re-timing) regeneration is performed systematically at each node in the network. However, providing electrical regeneration at each node is very expensive. Translucent WDM networks are considered today as a promising solution to meet the fully opaque network performance at much lower cost. In such networks, 3R regenerators are used at intermediate nodes only when it is necessary, leading to partially transparent networks.

In this thesis, we deal with the problem of routing, wavelength assignment, and regenerator placement in translucent WDM networks; we propose an original tool called lightpath establishment and regenerator placement (LERP). The aim of LERP is to provide a routing and wavelength assignment solution that optimizes the network resources utilization while guaranteeing a predefined quality of transmission. The quality of transmission is ensured by means of 3R electrical regenerators placed at network nodes when it is necessary to improve the optical signal budget. The quality of the optical signal is evaluated through Q factor. The Q factor value is computed by means of a prediction tool, also developed during this thesis, called BER-Predictor. BER-Predictor takes into account the effect of four main physical impairments due to transmission over fiber, namely chromatic dispersion, polariza-

tion mode dispersion, nonlinear phase shift, and amplified spontaneous emission. LERP aims to minimize both the number of rejected lightpath demands and the number of regenerators required to satisfy the quality of transmission requirements.

In WDM transmission systems, the quality of transmission observed on a given lightpath depends on the considered wavelength. For instance, a lightpath connecting two distant nodes in the network may be feasible using wavelength λ_1 and unfeasible using wavelength λ_2 . One approach to compensate for the non-flatness of the amplifiers's gain is to deploy inline gain equalizers. For this approach, we study the impact of a tradeoff between electrical regeneration and gain equalization on the network cost. In addition, we investigate another approach to deal with the non-flatness problem by proposing two new impairment-aware wavelength assignment strategies, namely min-BER-fit (MBF) and best-BER-fit (BBF). We show that these strategies can compensate for the absence of gain equalizers in the network and lead to a significant reduction in the number of required regenerators.

Contents

1	Introduction	3
1.1	Context	3
1.2	Motivation and Contribution	5
1.3	Organization of the Dissertation	6
2	WDM Transmission Systems: Characteristics and Performance	9
2.1	Optical Transmission: Technology and Devices	9
2.1.1	Optical Fiber	9
2.1.1.1	Multi-Mode Fiber	10
2.1.1.2	Single-Mode Fiber	10
2.1.2	Optical Transmitters	11
2.1.2.1	Light-Emitting Diodes	11
2.1.2.2	Lasers	12
2.1.3	Optical Receivers	13
2.1.4	Multiplexing Techniques	13
2.1.5	Line Rates	14
2.1.6	LH and ULH Transmission	14
2.1.6.1	Long Haul (LH)	15
2.1.6.2	Ultra Long Haul (ULH)	15
2.1.7	Optical Amplifiers	15
2.1.7.1	Semiconductor Laser Amplifiers	16
2.1.7.2	Optical Doped Fiber Amplifiers	16
2.1.7.3	Raman Optical Amplifiers	16

2.1.8	WDM Communication Link	17
2.1.9	Switching Elements	20
2.1.9.1	Optical Add/Drop Multiplexers	21
2.1.9.2	Opaque Switching Node	21
2.1.9.3	Transparent Switching Node	23
2.1.9.4	Translucent Switching Node	24
2.2	Optical Transmission: Impairments and Performance	25
2.2.1	Signal Quality Measurement	25
2.2.2	Receiver Sensitivity and Power Penalty	27
2.2.3	Impairments Due to Transmission Over Fiber	29
2.2.3.1	Attenuation	29
2.2.3.2	Dispersion	30
2.2.3.3	Nonlinear Effects	33
2.2.3.4	Amplified Spontaneous Emission	36
2.3	Summary	36
3	Quality of Transmission Evaluation: the Physical Model	41
3.1	Introduction	41
3.2	BER-Predictor Structure	42
3.3	Fiber Related Issues	44
3.3.1	Dispersion Management Strategy	46
3.4	Amplifier Related Issues	50
3.4.1	EDFA Commonly Available Features	50
3.4.2	Optical Power Schemes in Transmission Links	51
3.4.3	Gain Saturation	53
3.4.4	Gain Equalization	54
3.5	Optical Cross-Connect Related Issues	56
3.6	Q factor Computation	57
3.7	Summary	57
4	Limits of the Physical Layer: a Preliminary Study	61
4.1	Simulations Assumptions	63
4.1.1	Network Topology	63
4.1.2	Physical Characteristics	63
4.2	Limits of Transparency for Flat Systems	65

4.3	Impact of the System Flatness	68
4.4	Impact of Gain Equalization	72
4.5	Summary	77
5	RWA Considering Physical Layer Constraints	81
5.1	Routing and Wavelength Assignment	81
5.1.1	Separate Routing and Wavelength Assignment	83
5.1.1.1	Routing Algorithms	83
5.1.1.2	Wavelength Assignment Algorithms	86
5.1.2	Joint Routing and Wavelength Assignment	87
5.2	Physical Impairments Aware Routing	88
5.2.1	Opaque versus Transparent versus Translucent Networks	88
5.2.2	Impairment-Aware RWA in Transparent Networks	89
5.2.2.1	Study of Huang et al.	89
5.2.2.2	Study of Cardillo et al.	92
5.2.2.3	Study of Deng et al.	93
5.2.3	Impairment-Aware RWA in Translucent Networks	94
5.2.3.1	Study of Kim et al.	94
5.2.3.2	Study of Ramamurthy et al.	95
5.3	Summary	98
6	Regenerator Placement and Wavelength Assignment Strategies	103
6.1	Introduction	103
6.2	Description of the Problem	105
6.3	Routing and Wavelength Assignment	106
6.3.1	Notations	106
6.3.2	Sequential RWA (seqRWA)	108
6.3.3	Random Search Based RWA (RS-based RWA)	110
6.3.4	seqRWA versus RS-based RWA	111
6.3.5	RS-based RWA versus ILP Formulation	112
6.4	Regenerator Placement	113
6.4.1	Simple Lightpath Establishment and Regenerator Placement	113
6.4.2	Lightpath Establishment and Regenerator Placement	113
6.4.3	Illustrative Example	116
6.4.4	sLERP versus LERP	117

6.5	Impact of Dynamic Gain Equalization	118
6.5.1	Numerical example	119
6.5.2	Numerical Simulations	120
6.6	Impairment-Aware Wavelength Assignment Strategies	124
6.6.1	Numerical example	124
6.6.2	Numerical Simulations	125
6.6.3	Aggregated versus Distributed Regenerator Placement	128
6.7	Summary	129
7	Conclusions and Future Work	133
7.1	Conclusions	133
7.2	Perspectives	135
	List of Publications	137
	Glossary	139
	Bibliography	156

List of Figures

1	Planification de réseaux WDM translucides	xix
2	Synopsis de LERP.	xxii
2.1	Attenuation versus wavelength for optical fiber.	10
2.2	Typical configuration of a WDM point-to-point communication system.	17
2.3	A WDM system that has wavelength conversion capabilities.	18
2.4	A WDM system demonstrating a channel dropping	18
2.5	Optical Add/Drop Multiplexer (OADM).	21
2.6	Opaque switching node architecture.	22
2.7	Transparent switching node architecture.	23
2.8	Translucent switching node architecture.	24
2.9	Diagram of an optoelectronic receiver.	26
2.10	Probability density function for the observed photocurrent	28
2.11	Illustration of pulse spreading due to PMD	31
2.12	Illustration of pulse spreading due to CD	32
3.1	Lightpath carried by λ_1 and connecting node A to node C	46
3.2	Typical dispersion map of a transmission link	47
3.3	Dispersion map of a transmission link with accumulated dispersion reset to zero at each intermediate node.	48
3.4	Schematic of a fiber amplifier control part.	51
3.5	Gain saturation in an optical amplifier.	53
3.6	Effect of non-flat amplifier gains at different wavelength.	55

4.1	The European backbone network (EBN) topology.	62
4.2	The American NSF backbone network (NSFNet) topology.	62
4.3	The C-Band region.	64
4.4	40 wavelengths in the C-Band with 100 GHz channel spacing.	64
4.5	CD w.r.t. distance in a flat system.	66
4.6	PMD w.r.t. distance in a flat system.	66
4.7	Φ_{NL} w.r.t. distance in a flat system.	66
4.8	OSNR w.r.t. distance in a flat system.	66
4.9	\mathcal{Q} factor values w.r.t. distance.	67
4.10	Inadmissibility ratio w.r.t. distance.	67
4.11	PMD w.r.t. distance in a non-flat system.	69
4.12	CD w.r.t. distance in a non-flat system.	69
4.13	ϕ_{NL} w.r.t. distance in a non-flat system.	70
4.14	OSNR w.r.t. distance in a non-flat system.	70
4.15	\mathcal{Q} factor w.r.t. distance in a non-flat system.	71
4.16	Reach distance w.r.t. wavelength for different BER-thresholds.	72
4.17	Impact of the gain equalization scheme on the values of ϕ_{NL}	73
4.18	Impact of the gain equalization scheme on the values of OSNR	74
4.19	Impact of the gain equalization scheme on the values of \mathcal{Q} factor	75
4.20	Impact of the equalizer placement on the values of \mathcal{Q} factor.	76
5.1	Integrated model of impairment-aware RWA algorithms.	90
6.1	Lightpath establishment and regenerator placement	106
6.2	The American NSF backbone network (NSFNet) topology.	110
6.3	Number of rejected demands.	111
6.4	Used WDM channels per demand.	111
6.5	Synopsis of LERP.	114
6.6	11-node network topology.	116
6.7	Number of required regenerators.	117
6.8	Number of rejected demands.	117
6.9	Solutions computed without/with in-line gain equalization.	120
6.10	Number of regenerators w.r.t. traffic load without/with equalization.	121
6.11	Gain in the number of regenerators w.r.t. traffic load.	121

6.12	Number of regenerators w.r.t. BER-threshold without/with equalization.	122
6.13	Network cost gain w.r.t. device cost ratio	123
6.14	Solutions to Example 6.5.1 computed by the three WA strategies. . .	125
6.15	Number of regenerators w.r.t. traffic load.	126
6.16	Gain against FF strategy w.r.t. traffic load.	126
6.17	Number of regenerators w.r.t. BER_{th}	127
6.18	Number of regenerators w.r.t. traffic load.	127
6.19	Geographical distribution of the regenerators w.r.t. WA strategies. .	128
6.20	Location distribution of regenerators for different traffic matrices. . .	128

List of Tables

3.1	Physical impairments due to WB technology.	56
3.2	Physical impairments due to MEM technology.	57
3.3	Physical impairments due to WSS technology.	57
4.1	Topological features of the EBN and the NSFNet networks.	63
4.2	Physical characteristics of SMF and DCF fibers at 1550 nm.	65
4.3	Physical characteristics of boosters and line amplifiers	65
6.1	The set of PLDs to be set up	117
6.2	A set of three traffic demands	119
6.3	Q factor value w.r.t. the used wavelength	119

*“... And he said:
Your children are not your children.
They are the sons and daughters of Life’s longing for itself.
They come through you but not from you,
and though they are with you, yet they belong not to you.
You may give them your love but not your thoughts,
for they have their own thoughts...”*
The Prophet – Gibran Khalil Gibran (1883 - 1931)

*“Love is like the wind,
we do not know from where it comes...”*
– Honoré de Balzac (1799 - 1850)

1 Introduction

1.1 Context

Wavelength division multiplexing (WDM) networks provide huge bandwidth to keep up with the explosive growth of traffic demands. All-optical - or *transparent* - WDM networks are nowadays achievable thanks to the development of optical switching and optical amplification. In such networks, data is transmitted from source to destination in optical form. Switching operations are performed in the optical domain without undergoing any optical-to-electrical conversion. Provisioning of all-optical WDM networks outlines two main challenges:

- the absence of all-optical buffering;
- the impact of transmission impairments on network performance (optical signal to noise ratio (OSNR) at the receiver's side).

The first all-optical switches test-beds, designed at the early 1990's, have tried to compensate for the absence of optical buffering by the use of fiber delay lines. Very rapidly, the limit of such an approach has been observed, fiber delay line being not equivalent to random access memory (RAM). Alternative solutions have been then investigated; these solutions consist in the establishment of end-to-end optical circuits using the same wavelength from source to destination. On another hand, long-haul all-optical transmission is subject to phase distortion. Current optical amplifiers are efficient to boost the level of the optical signal but not to compensate for the phase distortion. In a first approach, phase distortion increases with distance and data rate. In addition to phase distortion that directly impacts clock recovery

at destination, other physical layer impairments such as optical crosstalk must also be taken into account.

Most studies related to all-optical network design, reported in the literature, assume perfect physical layer conditions by neglecting transmission impairments. However, the optical signal undergoes various transmission impairments such as attenuation, chromatic dispersion, polarization mode dispersion, nonlinear effects, noise sources, etc. Current networks using electrical switching (ATM, Frame Relay, SDH, SONET) or electrical routing (IP), are referred as fully opaque networks. In such networks, the quality of the optical signal is easily mastered thanks to 3R regeneration (re-amplifying, re-shaping, and re-timing) provided at each node. Meanwhile, providing regeneration at each node is costly. In this context, all-optical networks aim at two objectives. First, they tend to prevent any electrical regeneration in order to reduce the network investment for the carrier. Second, they try to provide a large range of services in terms of data rates and protocols on the same infrastructure. Such a property is known as transparency.

Recent research work in the field of optical network planning focuses on the problem of routing and wavelength assignment (RWA) considering physical layer constraints. Several studies reported in the literature focus on developing impairment-aware RWA algorithms in all-optical networks whereas other studies support the idea of sparse regeneration in large-scale WDM networks in order to ensure admissible quality of transmission at destination. Since the year 2000, various studies taking into account physical layer impairments have tried to consider the effective performance of transmission equipment available on the market. From these studies, it appears that according to the state of technology, pure transparency in large scale carrier networks such as the north American backbone or the European backbone is not achievable. This thesis, positioned in this perspective, is dedicated to the design of partially transparent networks known as translucent networks. A translucent network is not made of mix of opaque and all-optical switching nodes. It corresponds to an all-optical network wherein 3R electrical regeneration capabilities may be coupled to each switching node. Electrical regenerators are used at intermediate nodes only when it is necessary to improve the signal budget. It has been shown that translucent networks can achieve performance measures close to those obtained in fully opaque networks at a much lower cost.

1.2 Motivation and Contribution

In this thesis, we deal with the problem of translucent optical networks design. At the beginning of this thesis, the great majority of related investigations clearly separate the problem into two independent phases. First, a set of connection demands is satisfied with a set of lightpaths to be established in the network. This phase is mainly an optimization problem concerning the limited capacity of each fiber-link (in number of parallel optical channels). Second, the feasibility of each lightpath is investigated considering the physical characteristics of the various devices and systems used in the optical network. In addition, due to the complexity of physical layer impairments modeling, most studies consider individually the impact of the various physical layer impairments. For instance, a lightpath is estimated as acceptable if it is acceptable regarding to chromatic dispersion, and if it is acceptable regarding to polarization mode dispersion, and so on. Our approach is original in the way it jointly considers the RWA phase and the quality of transmission (QoT) evaluation phase. A second originality of our work is to simultaneously deal with four transmission impairments, namely chromatic dispersion, polarization mode dispersion, nonlinear phase shift, and amplified spontaneous emission.

In this context, we propose an original dimensioning tool called LERP for light-path establishment and regenerator placement. The aim of LERP is to provide a routing and wavelength assignment solution that optimizes the network resources utilization while guaranteeing a predefined quality of transmission. The quality of transmission is ensured by means of 3R electrical regenerators placed at network nodes when it is necessary to improve the optical signal budget. The optical signal quality is evaluated via a prediction tool, also developed during this thesis, called BER-Predictor that takes into account the aforementioned transmission impairments. LERP aims at minimizing both the number of rejected lightpath demands and the number of regenerators required to satisfy the quality of transmission requirements. In the continuation of the LERP tool specification, complementary studies have been carried out:

- In WDM transmission systems, the quality of transmission observed on a given lightpath may differ according to the considered wavelength. More precisely, a lightpath connecting two distant nodes in the network may be feasible using wavelength λ_1 and non-feasible using wavelength λ_2 . One approach to compensate for the non-flatness of the amplifiers' gain is to deploy inline dynamic gain

equalizers. In this thesis, we investigate the economical impact of a tradeoff between electrical regeneration and gain equalization.

- In most of studies related to optical network design, wavelength assignment aims to minimize the connection rejection ratio but does not consider quality of transmission issues. Because of the non-flatness of WDM transmission systems, we propose two innovating impairment-aware wavelength assignment strategies, namely min-BER-fit (MBF) and best-BER-Fit (BBF). We show that these strategies have a significant impact on the network capacity.

1.3 Organization of the Dissertation

This dissertation is organized as follows. Chapter 2 provides an overview of the essential concepts related to optical networking as well as the main transmission impairments that affect the quality of transmission in WDM optical networks. In Chapter 3, we describe the BER-Predictor tool. A preliminary study is given in Chapter 4 to outline the limits of transparency in real optical backbone networks. Chapter 5 assesses the state of the art of routing and wavelength assignment considering physical layer impairments. In Chapter 6, we investigate the LERP tool and the new impairment-aware wavelength assignment strategies (MBF and BBF). We also consider the economical benefit of a tradeoff between electrical regeneration and gain equalization. Chapter 7 presents the conclusions and perspectives of this thesis.

*"The opposite of a correct statement is a false statement but
the opposite of a profound truth may well be another profound truth."*

– Niels Boher (1885 - 1962)

2 WDM Transmission Systems: Characteristics and Performance

As the wavelength division multiplexing (WDM) industry continues to evolve towards tera-bit transmission systems that incorporate tightly spaced transmission channels, phenomena like *attenuation*, *dispersion*, and *nonlinearities* become limiting factors for long-distance transmission systems. The aim of this chapter is to provide an overview of the essential concepts related to optical networking as well as the main transmission impairments that affect the quality of transmission in WDM optical networks.

2.1 Optical Transmission: Technology and Devices

2.1.1 Optical Fiber

Early experiments in the mid 1960s by Kao and Hockham [12] have proved that optical transmission over fiber is feasible. However, optical fiber transmission systems have really took off in the early 1970s thanks to low-loss optical fiber manufactured by Corning [13] and Lucent Bell Labs [14]. This silica-based optical fiber has three low-loss windows in the 800, 1300, and 1550 nm infrared wavelength bands [1] [15]. The lowest loss is around 0.18 dB/km in the 1550 nm band, and about 0.5 dB/km in the 1300 nm band (see Figure 2.1). Losses are primarily due to impurities (water vapor) in the fiber glass and Rayleigh scattering (the medium is not absolutely uniform). To overcome the fiber losses, electrical regenerators, also called repeaters, are used between fiber sections.

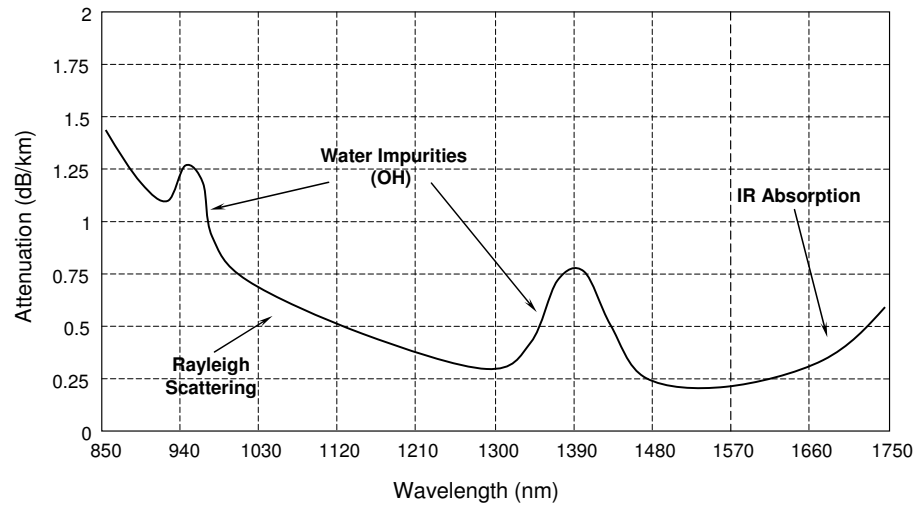


Figure 2.1: Attenuation versus wavelength for optical fiber.

2.1.1.1 Multi-Mode Fiber

Early fibers were the so-called multi-mode fibers (MMFs). Multi-mode fibers have core diameters between 50 and 85 μm . Such diameters are large compared to the operating wavelength of the optical signal and therefore, multi-mode fibers support multiple propagation modes traveling through the fiber at different speeds. At the end of the fiber, the different modes arrive at different times resulting in a pulse spreading. This form of spreading, known as intermodal dispersion, restricts the transmission distances on multi-mode fibers [1]. Typically, the early transmission systems operated at bit rates ranging from 32 to 140 Mbps with regenerators every 10 km. Multi-mode fiber systems are still in use for low-cost computer interconnection at a few hundred megabits per second over a few kilometers.

2.1.1.2 Single-Mode Fiber

To deal with intermodal dispersion, the next generation of optical systems, deployed in the mid 1980s, uses standard single-mode fibers (SMFs) in the 1300 nm band [16]. Single-mode fibers have a relatively small core diameters (about 8 to 10 μm) which is of the same order of magnitude as the transmitted wavelength. Consequently, all the energy of the optical signal travels in the form of a single mode.

Using single-mode fiber effectively eliminates intermodal dispersion and enables a significant increase in the bit rates and distances between regenerators. These systems operate at bit rates of a few hundred megabits per second and have a regen-

erator spacing of 50 km. Studies [17] [18] [19] [20] describe some of the early optical fiber transmission systems.

In the late 1980s, a new generation of optical fiber transmission systems was deployed. These systems use the 1550 nm wavelength band to take advantage of the lower loss in this window, with respect to the 1300 nm window. Low losses in the 1550 nm window enabled larger regenerator spacing (typically, every 100 km).

Another form of dispersion in optical fiber, namely chromatic dispersion, becomes a limiting factor as far as increasing the bit rates is concerned. Chromatic dispersion (discussed in Section 2.2.3.2) depends on the wavelength and results in a spreading pulse at the end of the fiber. Standard single-mode fibers have almost no chromatic dispersion in the 1300 nm band, but have a significant dispersion in the 1550 nm band. The high chromatic dispersion at 1550 nm has motivated the development of dispersion-shifted fibers (DSFs) [21]. Dispersion-shifted fibers are carefully designed to have zero dispersion in the 1550 nm wavelength window. An advanced description of different fiber types can be found in [1].

Some equipment vendors employ bi-directional transmission on a single fiber, using filters and circulators to separate the two directions at the network nodes. Other vendors use two separate fibers for each direction of transmission. In the remaining of this thesis, only unidirectional transmission is considered, as it is the case in metro and long-haul networks.

Optical fiber cables are usually installed underground fiber ducts connecting cities. The ducts often run parallel to existing infrastructure networks, *e.g.*, roads, railways, or gas pipelines.

2.1.2 Optical Transmitters

Other key devices for optical fiber transmission are light sources. In current transmission systems, the transmitter is modulated in amplitude according to the value of successive bits. Such a modulation is called non return to zero (NRZ) modulation.

2.1.2.1 Light-Emitting Diodes

Light-emitting diodes (LEDs) have been used until the 1990s as cheap optical sources for the local area network (LAN) environment. They are based on spontaneous emission that occurs within the entire bandwidth of the gain medium. The light generated at the output of a LED is characterized by broad spectrum and a low

directivity. In addition, LEDs are limited to a low power light transmission, typical output powers being of the order of -20 dBm. They cannot be directly modulated at data rates higher than a few hundred megabits per second [1].

2.1.2.2 Lasers

Lasers are the most common light sources in optical communication systems. A laser is essentially an optical amplifier enclosed within a reflective cavity generating a light beam on a specific wavelength. *Semiconductor* lasers use semiconductors as gain medium, whereas *fiber* lasers use doped fiber as gain medium. Semiconductor lasers do not need any optical pumping unlike fiber lasers which use a semiconductor laser as a pump¹. Furthermore, semiconductor lasers are highly efficient in converting input electrical (pump) energy into output optical energy. Both semiconductor and fiber lasers are capable of achieving high output powers, typically between 0 and 10 dBm. In current optical networks, semiconductor lasers are widely deployed.

The early lasers were multi-longitudinal mode (MLM) Fabry-Perot lasers. Because of the large spectral widths of MLM lasers, typically around 10 nm, it was desirable to design a laser that oscillates in a single-longitudinal mode (SLM) only [1]. A single-longitudinal mode can be achieved by providing a distributed light feedback. The most common means to distribute light feedback is to provide a periodic variation in the width of the cavity (*corrugation*). Any laser that uses a corrugated waveguide to achieve a single-longitudinal mode can be termed as distributed feedback laser. However, the acronym DFB laser is used only when the corrugation region occurs within the gain region of the cavity. When the corrugation region is outside the gain region, the laser is termed as distributed Bragg reflector (DBR) [1].

DFB lasers are inherently more complex and expensive than Fabry-Perot lasers. However, they are used in almost all high-speed transmission today because of their high level integration in optoelectronic circuits. More details about laser's types and technologies can be found in [15] [1].

¹A pump is a local power source that couples its power to an incident optical signal, thereby amplifying the incident signal by transferring its power either directly or through doped impurities to the optical signal.

2.1.3 Optical Receivers

Three functional elements compose an optical receiver: photo-detector, front-end amplifier, and decision circuit [1]. The photo-detector generates an electrical current proportional to the incident optical power. The front-end amplifier increases the power of the generated electrical signal to a usable level. In digital communication systems, the front-end amplifier is followed by a circuit decision that estimates data. The design of this decision circuit depends on the modulation scheme used to transmit data. An optical amplifier may be optionally placed before the photo-detector to act as a pre-amplifier.

2.1.4 Multiplexing Techniques

The need for multiplexing is driven by the fact that, in most applications, it is much more economical to transmit data at higher rates over a single fiber than it is to transmit data at lower rates over multiple fibers. There are fundamentally two ways to increase the transmission capacity over fiber. The first one is to increase the bit rate by using higher-speed electrical devices. Many low-speed data streams are multiplexed into a higher-speed stream at the transmission bit rate by means of electrical time division multiplexing (TDM). The multiplexer typically interleaves the low-speed streams to obtain the higher-speed stream. Today, the highest transmission rate in commercially available systems is around 10 Gbps. Nowadays, 40 Gbps TDM transmission systems are available on the market. To push TDM technology beyond these rates, researchers are working on methods to optically perform the multiplexing and demultiplexing functions. This approach is called optical time division multiplexing (OTDM). Laboratory experiments have demonstrated the multiplexing/demultiplexing of several 10 Gbps streams into/from a 250 Gbps stream, although commercial implementation of OTDM is still several years away [22] [23] [24] [25].

Another way to increase the capacity of the fiber consists in using wavelength division multiplexing (WDM) which is equivalent to traditional frequency division multiplexing (FDM). WDM is a multi-carrier modulation (MCM) technique that multiplexes multiple optical signals into a single optical fiber. Each of these optical channels is modulated, according to the state of the technology, with NRZ modulation to transport independent data flows. For data rates per optical channel under 40 Gbps, these optical channels do not interfere with each other if the distance between

two adjacent channels is at least twice the inverse of the bit duration of the fastest channel. Today, WDM systems are widely deployed in long-haul and undersea networks, and they are deployed in metropolitan networks as well. In summary, WDM enables to optimize bandwidth utilization of optical fibers, limiting by the cost of civil engineering. Today's networks use a combination of TDM and WDM. Indeed, with WDM, multiple TDM channels can be sent simultaneously along a fiber. Each TDM channel occupies a wavelength on the ITU-specified grid, separated at channel spacing of, for instance, 100 GHz. Different commercial systems propose 50 GHz or even 25 GHz channel spacing [26]. With these narrow spacings the transmission is qualified dense WDM (DWDM). Such systems allow a limited number of channels (around 4 to 6 channels) to be transmitted simultaneously and are well suited to shorter reach applications (access networks).

2.1.5 Line Rates

The individual channels in WDM systems are TDM signals at rates of typically 2.5 Gbps or 10 Gbps. These transmission speeds, or line rates, correspond to the synchronous digital hierarchy (SDH) standardized data rates such as STM-16, STM-64, and STM-256. In SDH, all data channels are bidirectional, two contra-directional fibers being used between adjacent network nodes.

Traditionally, each rise in equipment transmission rate by a factor of 4 is accompanied by a cost increase of 250% [27] [28], giving a financial incentive to groom traffic up to the highest transmission rate. Although WDM is bit rate independent, this is not the case for electrical regenerators that operate at a specified bit rate. In other terms, upgrading an optical transmission system in terms of capacity is very expensive. The emergence of optical amplification enables to solve this problem, such amplifiers being also bit rate independent [29]. Recent advances have achieved 0.8 bits/s/Hz spectral efficiency with 40 Gbps line rates at a 50 GHz channel spacing [30].

2.1.6 LH and ULH Transmission

Currently, there are two available platforms for optical core network transmission, based on the following prevailing industry segmentation:

2.1.6.1 Long Haul (LH)

Long haul (LH) transmission systems have a capacity up to 1.6 Tbps via upgradable stages. Such a data rate corresponds to 160 parallel wavelengths at 10 Gbps each. Therefore, a possible upgrade route is to deploy a 40-channel LH transmission system and then upgrade to 80 and 160 channels when necessary by adding extra components to utilize further bands of the transmission capacity. LH transmission systems have a reach distance ranging from 400 to 600 km, depending on the fiber type. An NRZ modulation scheme is common for LH transmission systems, and amplifiers are required typically every 100 km [31].

2.1.6.2 Ultra Long Haul (ULH)

The newer ultra long haul (ULH) transmission systems have a reach distance of over 2000 km (4000 km reach distance is reported in some commercially available systems [32]). A return to zero (RZ) modulation scheme is employed to achieve longer-distance transparent transmission [31]. Raman amplification [33] is required about every 100 km. Dispersion slope compensation [28] and dynamic gain equalization [34] are required to achieve such long distances (see Chapter 3 and Chapter 4). ULH technology has the potential to increase the level of optical transparency in core network. However, since a ULH system involves more sophisticated technologies, it is significantly more expensive than a LH system.

2.1.7 Optical Amplifiers

In an optical transmission system, the optical signals are attenuated as they propagate through the fiber. Losses are due to the fiber and other optical components traveled by the signal. Beyond a certain distance, as losses accumulate, the signal becomes too weak to be detected. Before this happens, the signal strength has to be restored. Prior to the advent of optical amplifiers, the only option to strengthen the transmitted signal was to regenerate the signal, that is, receive the signal, and retransmit it.

Optical amplifiers (OAs) offer advantages over regenerators. Unlike regenerators, optical amplifiers are insensitive to the bit rate and modulation format used by the system. Consequently, a transmission system using optical amplifiers can be easily upgraded, for example, to a higher bit rate without replacing any amplifier. In contrast, in a transmission system using regenerators, such an upgrade would require

the replacement of all the regenerators. Furthermore, optical amplifiers have fairly large gain bandwidths and thus, a single amplifier can simultaneously amplify several WDM channels. In contrast, a regenerator is specific for each channel. Therefore, optical amplifiers have become an essential component in LH and ULH transmission systems[28]. An optical amplifier works on the same principle as that of a laser. In short, incident light is amplified by sustained stimulated emission. The amplification is achieved by a pumping process whereby either electrical or optical pumping boosts the incident signal power in a gain medium or just in a fiber.

In the following, we consider three types of amplifiers: semiconductor optical amplifier, optical doped fiber amplifiers, and fiber Raman amplifiers [1].

2.1.7.1 Semiconductor Laser Amplifiers

Semiconductor laser amplifiers (SLAs) are laser diodes, without end mirrors, which have fiber attached to both ends. They amplify any optical signal that comes from either fiber and transmit the amplified signal out of the second fiber. SLAs may be used in 1300 nm and 1550 nm systems. Main disadvantages of these amplifiers are high-coupling losses and a high noise figure.

2.1.7.2 Optical Doped Fiber Amplifiers

Optical doped fiber amplifiers (ODFAs) are lengths of fiber doped with an element (rare earth) that can amplify light. The most common doping element is erbium, which provides gain for wavelengths of 1525 – 1560 nm. At the end of the fiber, a laser transmits a strong signal at a lower wavelength (called the pump wavelength) back up the fiber. This pump signal excites the dopant atoms into a higher energy level. This allows the data signal to stimulate the excited atoms to release photons. Most erbium doped fiber amplifiers (EDFAs) are pumped by lasers with a wavelength of either 980 or 1480 nm. The 980 nm wavelength has shown gain efficiencies around 10 dB/mW, while the 1480 nm wavelength provides efficiencies around 5 dB/mW. Typical gains are of the order of 25 dB.

2.1.7.3 Raman Optical Amplifiers

Raman optical amplifiers (ROAs) use stimulated Raman scattering (SRS) occurring in silica fibers when an intense pump beam propagates through it [15] (SRS is discussed in Section 2.2.3.3). The Raman gain spectrum is fairly broad [1]. The peak

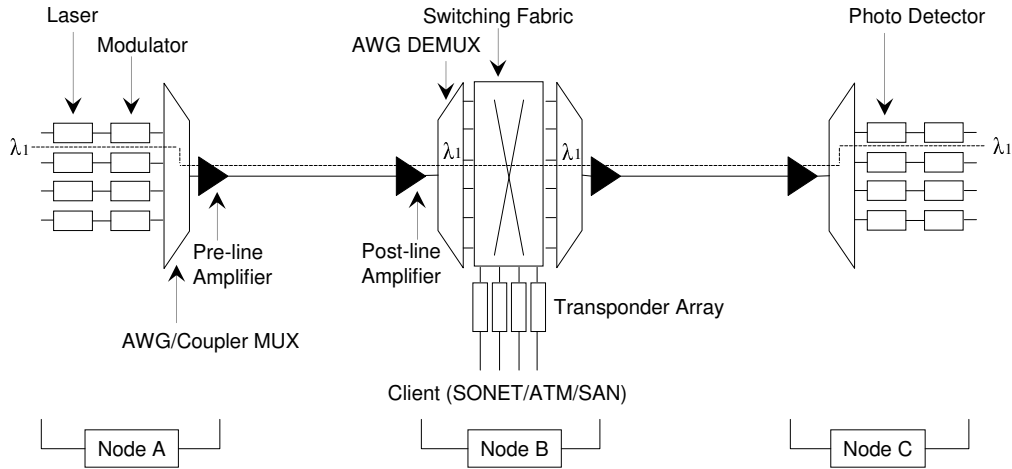


Figure 2.2: Typical configuration of a WDM point-to-point communication system.

of the gain is centered about 13 THz below the frequency of the pump signal used. In the near-infrared region of interest, this corresponds to a wavelength separation of about 100 nm. Therefore, by pumping a fiber using high-power pump laser, we can provide gain to other signals, with a peak gain obtained 13 THz below the pump frequency. For instance, using pumps around 1460 – 1480 nm provides Raman gain in the 1550 – 1600 nm window.

Raman amplifiers have lower noise figure and they handle wider bands than EDFAs. Today, Raman amplifiers are used to complement EDFAs by providing additional gain in LH and ULH transmission systems. The biggest challenge in realizing Raman amplifiers lies in the pump source it-self. These amplifiers require high-power pump sources of the order of 1 W or more at the right wavelength.

2.1.8 WDM Communication Link

Figure 2.2 illustrates a typical configuration of a WDM point-to-point transmission system. In this example, node A transmits data to node C through an intermediate node, node B. At node A, an array of electrical devices injects data into different wavelengths. These devices corresponds typically, in the metro area and long-distance area, to SDH interfaces. In many cases, the SDH infrastructure is used to transport IP (Internet Protocol) over ATM (Asynchronous Transfer Mode) traffic. Electrical data, under the form of a continuous flow of SDH frames, modulate a semiconductor laser. The modulated signals generated by parallel lasers are then multiplexed to be injected in the optical fiber. Generally, lasers are modulated ex-

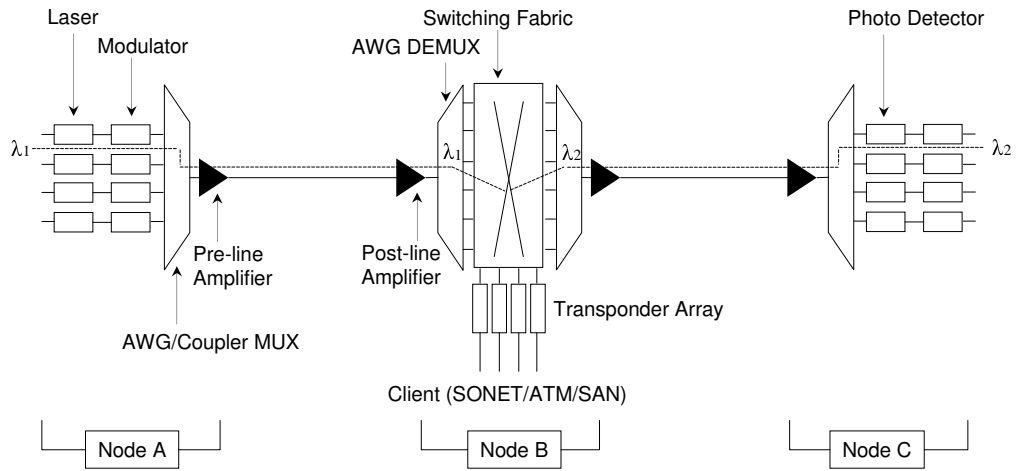


Figure 2.3: A WDM system that has wavelength conversion capabilities.

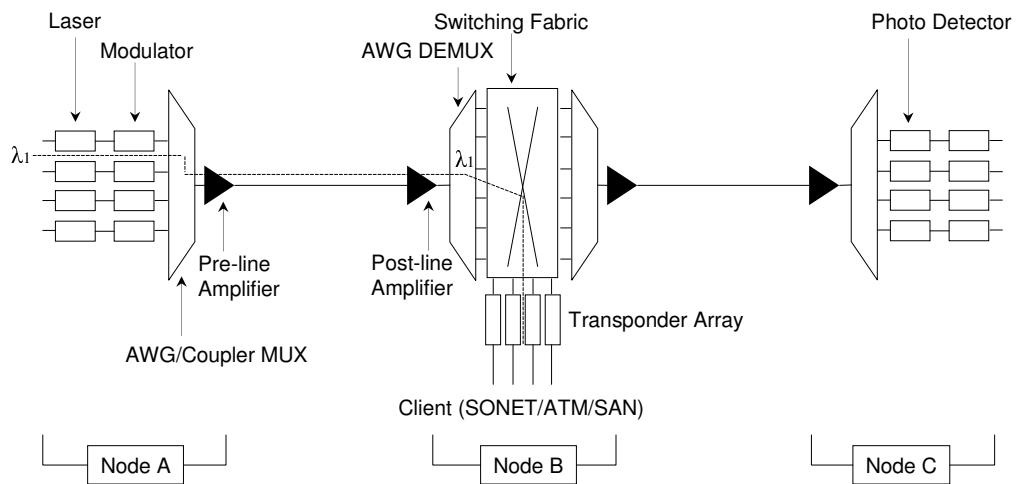


Figure 2.4: A WDM system demonstrating a channel dropping at an intermediate node.

ternally in order to avoid the chirp phenomenon. By simplification, all the optical channels are generated at a source node (node A in our example) with a common optical power.

WDM multiplexers are based on arrayed waveguide gratings (AWGs) which are low-cost and highly integrable devices. The composite signal is then amplified before being transmitted into the fiber by a pre-amplifier (doped fiber or Raman). Along the transmission fiber, the signal is evenly amplified (typically, every 100 km) using inline amplifiers. Depending on the distance, the bit rate, and the fiber type, inline amplifiers may also include a dispersion compensation modules (different dispersion management strategies are discussed in Section 3.3.1).

At the intermediate node B, the signal is first amplified by a post-amplifier. The amplified signal is de-multiplexed into individual channels that are inserted at the different ports of a switching fabric. This switching fabric may be either all-optical or optoelectronic. An all-optical switch has the functionality of completely switching or routing the data channels in the optical domain. An optoelectronic switch operates in the electrical domain by converting the optical signals into electrical bit streams at the input of the switch, the reverse operation being carried out at the output of the switch. It has to be noted that, thanks to this optoelectronic conversion, a logical channel from A to C may change of wavelength at node B (Figure 2.3).

A switching fabric has also the possibility to add (drop) individual channels. Dropping a channel imposes an optoelectronic conversion, either to feed an electrical device directly, or to convert the transmission carrier (around 1550 nm) into a client wavelength (usually a shorter wavelength, *e.g.*, 1310 nm). The transponders are the equipment providing such a conversion. Figure 2.4 shows an example of dropping channels at intermediate nodes. In summary, the switching fabric does the task of adding, dropping, switching optical channels or just passing them through the node. Section 2.1.9 provides an overview on different switching fabric types.

At the output of node B, the channels are inserted into a multiplexer to form a composite WDM signal. This signal is amplified by a pre-amplifier. At node C, the signal is amplified by the post-amplifier and de-multiplexed into individual signals. These optical signals are detected by an array of photo-detectors. The obtained electrical signals are directed to the destination clients of the network. Transponders usually perform the function of detecting and converting the network signal into a client signal. Individual electrical streams could be further de-multiplexed in the time

domain to give slower rate streams as it is the case, for instance, in SDH equipment.

In this work, an all-optical connection, that is established from a source node to a destination node using a given wavelength, is referred as *lightpath*; this notion of lightpath is introduced by [35]. A *semi-lightpath* is defined as a concatenation of lightpaths to connect a source node to a destination node; the wavelength used along the semi-lightpath being eventually converted either optically or electrically at intermediate nodes.

2.1.9 Switching Elements

Up to now, WDM transmission systems including optical amplification have only enabled to increase the capacity and the range of point-to-point optical links. Before the emergence of optical switching, such technological advances have not allowed to introduce flexibility and intelligence at the optical layer. Thanks to optical switching, the optical layer is now able to route either statically or dynamically end-to-end lightpaths. In this perspective, the integration of the optical control plane of the physical layer with the electrical control planes at the upper layers (SDH, ATM, IP, Frame Relay, Ethernet, etc.) becomes a real challenge.

In opaque switching equipment made of add/drop multiplexers (ADMs) and of a digital switching fabric, the information is processed electronically. Significant research efforts are being carried out to optically perform some networking functions in switching elements, typically called optical ADMs (OADM) and optical switching fabrics. The ultimate goal of this trend is the realization of all-optical networks wherein signals are processed optically without undergoing any optical-to-electrical (O/E) or electrical-to-optical (E/O) conversion. The motivation for all-optical networks is twofold. On one hand, eliminating O/E and E/O conversions significantly reduces the cost of the network, since the cost of transponders used to perform these conversions represents today between 50% and 75% of the network cost [36]. On the other hand, transparent switching fabrics, which are independent of the modulation format and the data rate inherent to each optical carrier, will enable a soft transition towards higher capacity networks.

Despite these advantages, all-optical networks are far from becoming a reality basically because the technologies used to perform key networking functions in the optical domain are limited. Actually, given the current state of the art of technology, transparency introduces significant problems in terms of quality of transmission

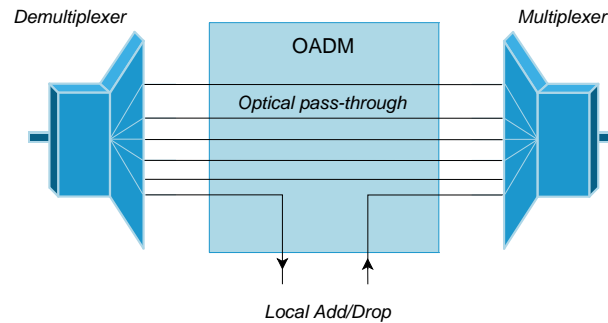


Figure 2.5: Optical Add/Drop Multiplexer (OADM).

(QoT). In the short and mid term, transparency will then be progressively introduced in carriers' networks in limited areas where the QoT remains acceptable at the receiver's side. Such evolutions lead the manufacturers to design hybrid switching nodes associating both optical and electrical processing. In the following, such nodes are qualified as *translucent*.

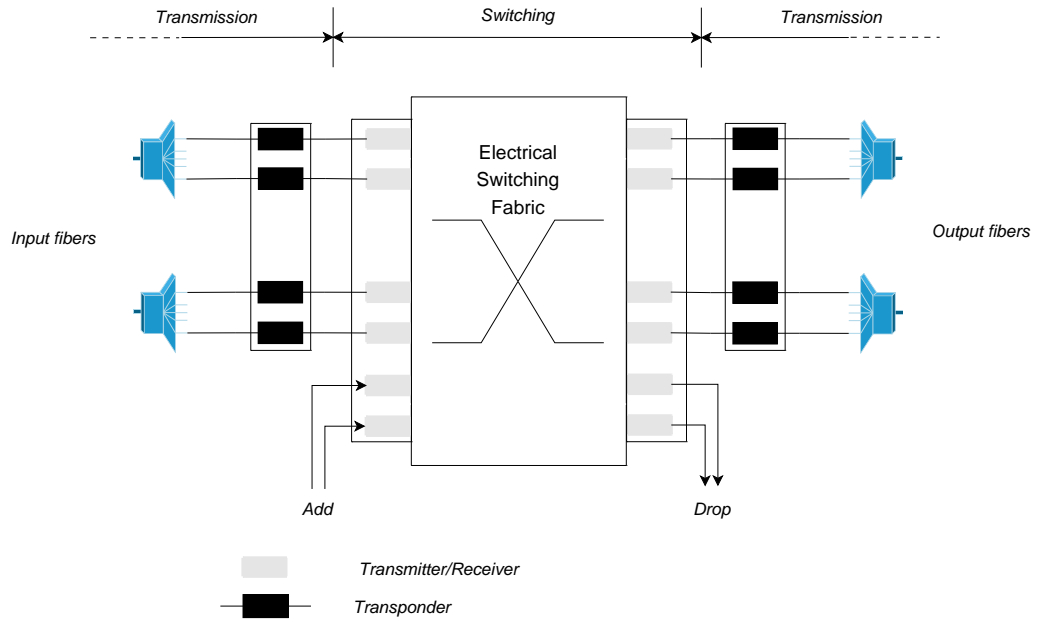
2.1.9.1 Optical Add/Drop Multiplexers

Optical add/drop multiplexers (OADMs) provide a cost effective means for handling pass-through traffic in both metro and long-haul networks. An OADM is an equipment with one input port and one output port enabling to extract one or several optical channels from an incoming multiplex, or to insert locally generated optical channels in the incoming multiplex (Figure 2.5). The first OADMs have been used along optical WDM rings; there are also adopted in mesh topologies. The first OADMs were static since the optical channels either inserted or extracted were predetermined. Today, flexible OADM called reconfigurable OADM (ROADM) are able to select dynamically the optical channels to be inserted or to be extracted [37].

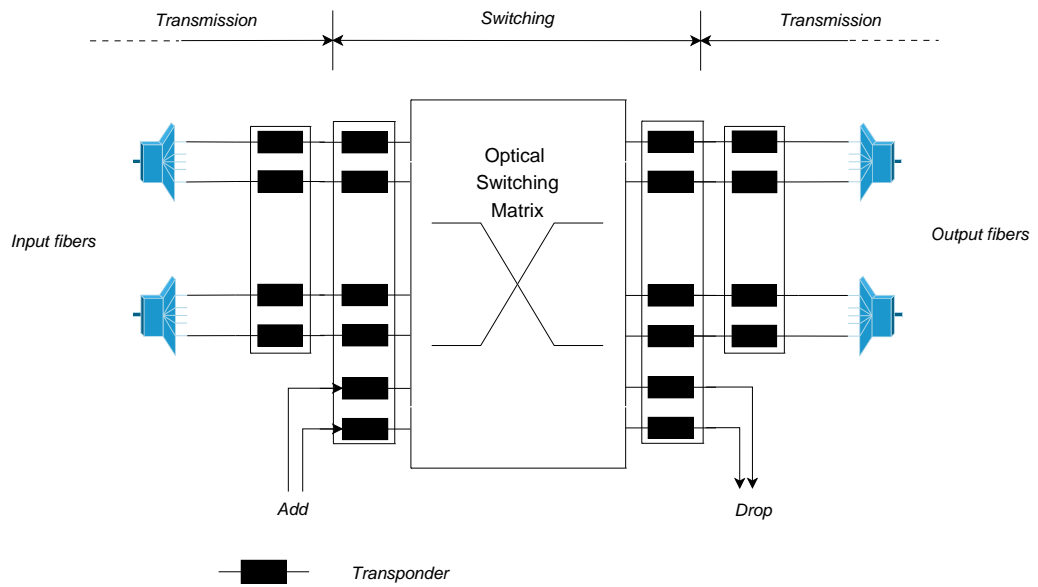
2.1.9.2 Opaque Switching Node

Figure 2.6 shows two different architectures of opaque switching nodes. Actually, in the opaque configurations, the switching matrix can be done either electrically or optically. An electrical switching fabric routes logical data flows in the electrical domain (Figure 2.1.9.2).

Although all-optical switches are technically feasible, traffic management in all-optical networks is subject to the wavelength continuity constraint because of the



(a) Opaque switching node using electrical core.



(b) Opaque switching node using optical core.

Figure 2.6: Opaque switching node architecture.

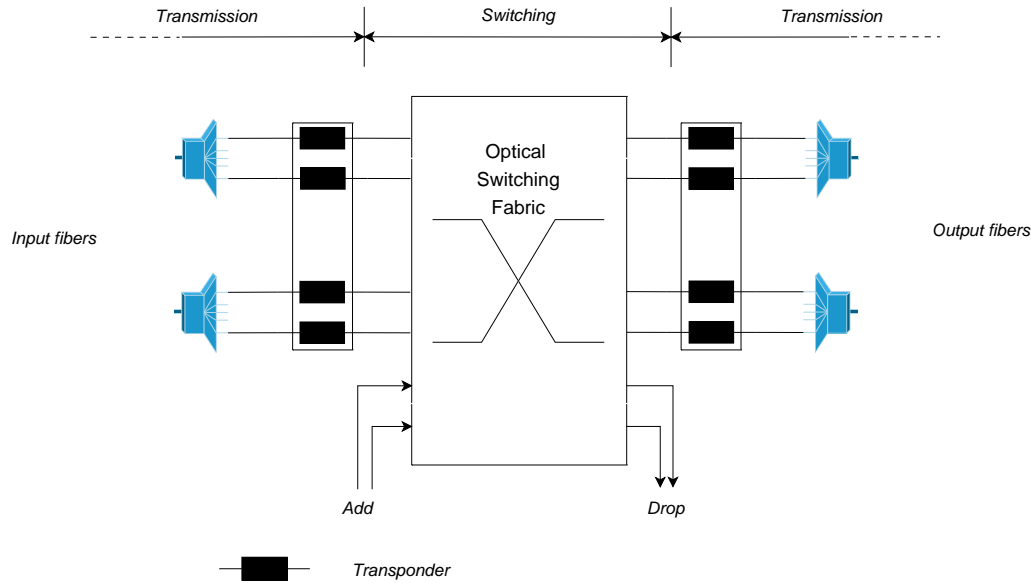


Figure 2.7: Transparent switching node architecture.

lack of all-optical conversion. All-optical converters have been developed in research laboratories but their cost remains today unaffordable for the carriers. This is the reason why another type of opaque switching node is currently considered. In such nodes, the switching fabric in fact transparent, but the input and output ports require O/E and E/O conversions, respectively (Figure 2.6(b)). Upgrading such nodes to higher bit rates is much less costly than in the case of fully-opaque node described in Figure 2.1.9.2. Indeed, increasing the capacity of the node only requires the replacement of the transponders used at the input and output ports whereas it also requires the replacement of the switching fabric in the case of fully-opaque node.

2.1.9.3 Transparent Switching Node

A transparent switching node routes the logical data flows in the optical domain thanks to an optical switching fabric. These logical data flows transit through the node without any O/E conversion. In the absence of all-optical wavelength converters, the wavelength continuity constraint is imposed. Such nodes, known as O-O-O switches, are fully rate-adaptive. Meanwhile, this rate adaptivity is upper-bounded by the power and the number of parallel optical channels transiting through the node. Indeed, above a certain power level, a phenomenon known as intra-channel crosstalk, degrades the QoT of these channels. Figure 2.7 shows a typical configuration of a

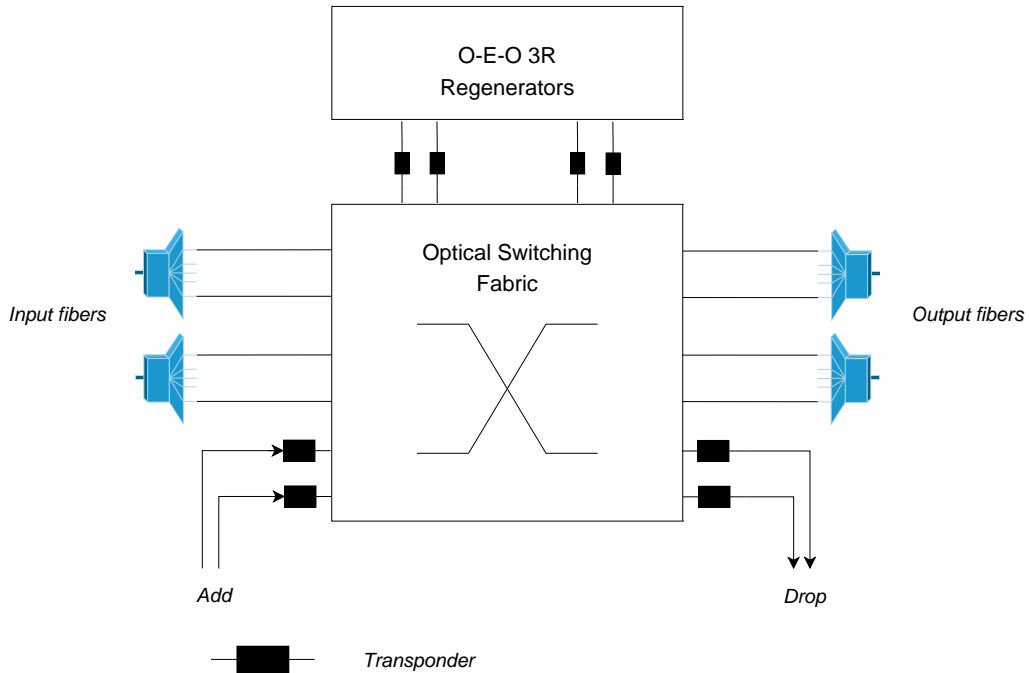


Figure 2.8: Translucent switching node architecture.

transparent switching node.

Four main approaches are considered for O-O-O switches. Optical cross-connects (OXC) are the most mature of these approaches. An OXC is able to route statically semi-permanent lightpaths. The main drawback of OXC is their coarse grain granularity. Optical circuit switches (OCS) rely on the same hardware as OXC but are able to switch dynamically the lightpaths thanks to a control plane. Optical packet switches (OPS) strongly improve the granularity of optical switches in sharing in TDM each lightpath. Optical burst switching (OBS) is the most recent and most prospective approach. Unlike an OPS switch that is connection-oriented, an OBS is connectionless-oriented and the packets' size being variable. In this thesis, we only refer to semi-permanent lightpaths routed via OXC.

2.1.9.4 Translucent Switching Node

In high-speed all-optical networks, transmission impairments like attenuation, dispersion and nonlinearities accumulate along the lightpath and result in unacceptable bit error ratio (BER) at the receiver's side. In this context, many current research work focus on the design of *translucent* optical networks. In such networks, electrical

regenerators are used at intermediate nodes for QoT purposes. Typically, if the BER at transit nodes along a lightpath falls under a certain admissible threshold, one or several electrical regenerators² are placed along the lightpath. Two main contexts must be distinguished in terms of regenerator placement: network planning and traffic engineering. In the former case, lightpaths are established for the long term via OXCs. Regenerator placement in this context occurs during the network planning phase. In the latter case, lightpaths are established on the fly via OCSs, regenerators being already placed in the network. Under dynamic traffic, the regenerator placement problem is then limited to a routing problem. In this thesis, we only deal with the problem of regenerator placement at the OXCs.

Since our objective is to tend the best as possible to a fully-transparent network, we adopt the node architecture described in Figure 2.8. In such an architecture, the switching node consists of an OXC connected with a pool of regenerators connected via transponders. Optical signals achieving the QoT requirements, transit through the node optically without undergoing any O-E-O conversion. If the signal quality does not meet the QoT requirements, the signal may eventually be regenerated before being retransmitted to destination. According to the state of the art, different architectures of translucent switching nodes can be considered [38].

2.2 Optical Transmission: Impairments and Performance

2.2.1 Signal Quality Measurement

In digital communications³, the standard measure of quality is the bit error ratio (BER) - also referred to as bit error rate. The BER is defined as the number of erroneous bits over a period \mathcal{T} divided by the total number of bits received over this period.

The transmission system must ensure that the bits are transmitted from their source to their destination with an acceptable BER value (BER values ranging from 10^{-15} to 10^{-9} are considered as acceptable values). In practice, most carriers consider 10^{-12} as a target BER value for their network. Before the emergence of optical amplification at the end of 1990s, telecommunication optical systems were regenerated electrically in average every 50 km. Nowadays, thanks to optical amplification,

²In the remaining of this thesis, the term "regenerator" will be used to refer to 3R (Reamplification, Reshaping, and Retiming) electrical regenerator.

³Our study is limited to digital optical networks.

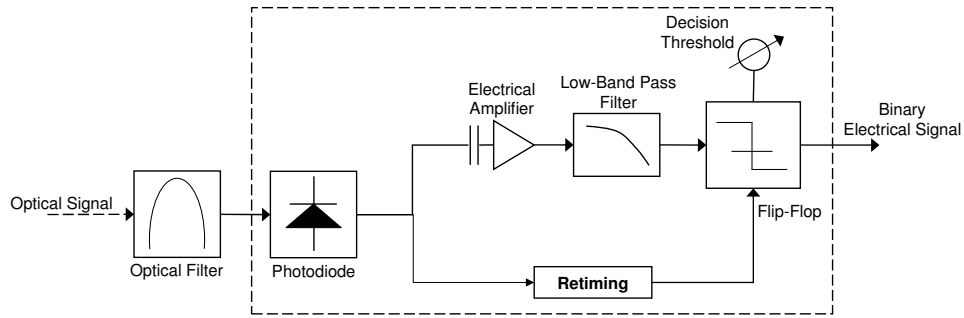


Figure 2.9: Diagram of an optoelectronic receiver.

such a target BER value remains acceptable between two adjacent opaque nodes. In Europe, an average distance of 500 km separates electrical nodes (ATM switches, IP routers, SONET/SDH cross-connects). The main challenge for the next decades consists in providing transparent optical systems over distances of several thousands of kms. For such distances, the power of transmission remaining of the same order as traditional systems (typically -1 dBm), measured BER at destination becomes greater than 10^{-9} . Two options are possible to solve this problem: either using greater power transmission or compensating for additional erroneous at destination. The second option has been chosen by the carriers since it may reuse the principle of forward error correction (FEC) [39]. FEC codes have been widely adopted in wireless systems since the eighties to prevent data retransmission. FEC codes are very efficient to detect and correct burst of errors. Their main drawback is due to the high overload they induce in the transmission system. In optics, this drawback can be neglected according to the huge capacity of an optical fiber.

The receiver decides which bit (0 or 1) was transmitted in each bit interval by sampling the photocurrent as shown in Figure 2.9. Due to the presence of noise currents, the receiver can make a wrong decision resulting in an erroneous bit.

Let P_0 and P_1 denote the received optical power during a 0 bit and a 1 bit, respectively. Let I_0 and I_1 denote the photocurrent sampled by the receiver during a 0 bit and a 1 bit, respectively, and let σ_0^2 and σ_1^2 represent the corresponding noise variances. The noise signals are assumed to be Gaussian, thus, the bit decision problem faced by the receiver may be formulated as follows. The photocurrent for a 0 bit is a sample of a Gaussian random variable with mean I_0 and variance σ_0^2 , and similarly for the 1 bit. The receiver must look at this sample and decide whether the transmitted bit is 0 or 1.

Figure 2.10 shows typical probability density functions for both the 0 and the 1 bits. The receiver aims at choosing a decision strategy that minimizes the BER. The optimal decision strategy can be shown to be the one that, given the observed photocurrent I , chooses the bit (0 or 1) that was the “most likely” to be transmitted. It consists in comparing the observed photocurrent I to a decision threshold I_{th} . If $I \geq I_{th}$, it decides that a 1 bit was transmitted, otherwise, it decides that a 0 bit was transmitted.

Assuming that 0 and 1 bits are equally likely, we have:

$$\text{BER} = \frac{1}{2} \left[\frac{1}{\sqrt{2\pi\sigma_0^2}} \int_{I_{th}}^{+\infty} e^{-\frac{(I-I_0)^2}{2\sigma_0^2}} dI + \frac{1}{\sqrt{2\pi\sigma_1^2}} \int_0^{I_{th}} e^{-\frac{(I_1-I)^2}{2\sigma_1^2}} dI \right] \quad (2.1)$$

Using the definition of the complimentary error function *erfc*, we can write Equation 2.1 as follows:

$$\text{BER} = \frac{1}{4} \left[\text{erfc} \left(\frac{I_{th} - I_0}{\sigma_0\sqrt{2}} \right) + \text{erfc} \left(\frac{I_1 - I_{th}}{\sigma_1\sqrt{2}} \right) \right] \quad (2.2)$$

The photocurrent threshold value can be further optimized to reduce the BER. This is obtained when both densities sketched in Figure 2.10 cross. The threshold value is given approximatively by:

$$I_{th} = \frac{\sigma_0 I_1 + \sigma_1 I_0}{\sigma_0 + \sigma_1} \quad (2.3)$$

This approximative value is very close but not exactly equal to the optimal value of the threshold [1].

One method to estimate the BER is the well known \mathcal{Q} factor defined in Equation 2.4. The \mathcal{Q} factor provides a quantitative description of the absolute quality of an optical signal. The \mathcal{Q} factor is related to the BER according to Equation 2.5.

$$\mathcal{Q} = \frac{I_1 - I_0}{\sigma_0 + \sigma_1} \quad (2.4)$$

$$\text{BER} = \frac{1}{2} \text{erfc} \left(\frac{\mathcal{Q}}{\sqrt{2}} \right) \quad (2.5)$$

2.2.2 Receiver Sensitivity and Power Penalty

The receiver’s sensitivity is defined as the minimal power required to achieve a certain BER value; typical transmission systems require a BER value between 10^{-9} and

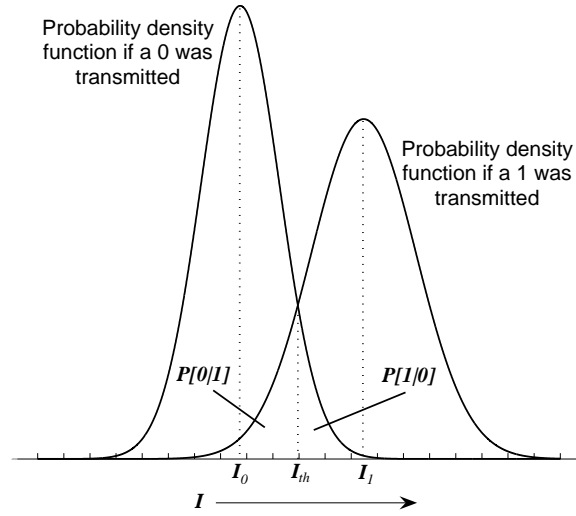


Figure 2.10: Probability density function for the observed photocurrent

10^{-15} . Actually, the value of the sensitivity enables the evaluation of the receiver's performance as well as the physical impairments induced by the transmission system:

- The optical signal measured at the transmitter's output allows to evaluate the receiver's performance. Such a measure is known as a back-to-back configuration. Obviously, the lower the sensitivity, the better the receiver.
- In order to evaluate the physical impairment induced by a certain optical component, the sensitivity is measured in the presence of this specific component. The deviation between this measure and the back-to-back measure is defined as the *power penalty* associated to the impairment induced by the considered component.

One way to define the power penalty induced by an impairment is to define it as the reduction of optical signal to noise ratio (OSNR) due to this specific impairment. Let P'_1 , P'_0 , σ'_1 , and σ'_0 denote the received powers and noise standard deviations, respectively in the presence of impairments. Assuming an optimized threshold setting and according to Equations 2.4 and 2.5, the power penalty $P_{penalty}$ is given by:

$$P_{penalty} = -10 \log \left(\frac{\frac{I'_1 - I'_0}{\sigma'_1 + \sigma'_0}}{\frac{I_1 - I_0}{\sigma_1 + \sigma_0}} \right) \quad (2.6)$$

At this stage, we distinguish between two important cases. The first case corresponds to unamplified systems where the dominant component is the receiver's thermal noise, for which $\sigma_1 = \sigma_0 = \sigma_{th}$. In this case, or any situation where the noise is independent of the signal power, the power penalty is given by:

$$P_{penalty} = -10 \log \left(\frac{P'_1 - P'_0}{P_1 - P_0} \right) \quad (2.7)$$

The other case corresponds to amplified systems where the dominant noise component is the amplified spontaneous emission. In this case, the noise variance depends on the signal power ($\sigma_1^2 \propto P_1$). Therefore, assuming that $P_0 \ll P_1$, we can assume that $\sigma_0 \ll \sigma_1$. An optimized receiver would set its threshold close to the 0 level, whereas a simple receiver would still set its decision threshold at the average received power and would have a somewhat higher BER. However, the power penalties turn out to be the same in both cases. This penalty is given by:

$$P_{penalty} = -5 \log \left(\frac{P'_1}{P_1} \right) \quad (2.8)$$

Transmission system design requires careful budgeting of the power penalties due to the different transmission impairments. One way for designing such a system is to determine the ideal value of the \mathcal{Q} factor that is needed. For a BER of 10^{-12} typically assumed in high-speed transmission systems, we need $\mathcal{Q} = 7$, or $\mathcal{Q}_{dB} = 20 \log \mathcal{Q} = 17$ dB. This would be the case if there were no transmission impairments leading to power penalties. In practice, the various transmission impairments result in power penalties that must be added to this ideal value to obtain the required value of \mathcal{Q} that the system must be designed to yield.

2.2.3 Impairments Due to Transmission Over Fiber

2.2.3.1 Attenuation

Attenuation in optical fiber leads to a reduction of the signal power as the signal propagates. When determining the maximum distance that a signal can propagate for a given transmitter power and a given receiver sensitivity, one must consider attenuation. Let P_L be the power of the optical pulse at distance L from the transmitter and α be the attenuation coefficient of the fiber. Attenuation is characterized by:

$$P_L = P_{in} e^{-\alpha L} \quad (2.9)$$

where P_{in} is the optical power at the transmitter. It is customary to express the loss in units of dB/km. Thus, a loss of α_{dB} dB/km means that for $L = 1$ km, the ratio P_L/P_{in} satisfies

$$10 \log_{10} \frac{P_L}{P_0} = -\alpha_{dB} \quad (2.10)$$

For a link length of L km, P_L must be greater than or equal to the receiver's sensitivity P_r . From Equation 2.10, we get the maximum distance that can be reached without re-amplification:

$$L_{max} = \frac{10}{\alpha_{dB}} \log_{10} \frac{P_0}{P_r} \quad (2.11)$$

The maximum distance between the transmitter and the receiver (or the distance between consecutive amplifiers⁴) depends more heavily on the coefficient α than on the optical power P_{in} injected by the transmitter. For standard single-mode fibers (SMF), the value of the coefficient α is about 0.2 dB/km. In current optical systems, the value of L_{max} is about 80 km. New fiber optic technologies should lead to better values of L_{max} .

2.2.3.2 Dispersion

Dispersion is the name given to any effect wherein different components of the transmitted signal travel at different velocities, arriving at different times at the receiver. A signal pulse emitted over a fiber arrives broadened at the other end as a consequence of this effect. This broadening leads to inter-symbol interference (ISI), which in turn leads to power penalties. Dispersion is a cumulative effect: the longer the link, the greater the amount of dispersion.

Several forms of dispersion arise in optical communication systems, the most important being *intermodal dispersion*, *polarization mode dispersion*, and *chromatic dispersion*. Since our study is limited to single-mode fibers (also called mono-mode fibers), we will only deal with polarization mode dispersion (PMD) and chromatic dispersion (CD).

⁴The amplifier sensitivity is usually equal to the receiver sensitivity, while the amplifier output is usually equal to the optical power at a transmitter.

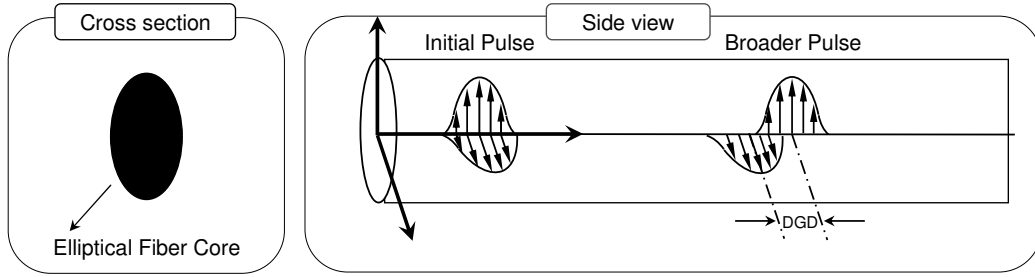


Figure 2.11: Illustration of pulse spreading due to PMD

Polarization Mode Dispersion

In an ideal optical fiber, the core has a perfectly circular cross-section. In this case, the fundamental mode has two orthogonal polarizations (orientations of electric field) that travel at the same velocity. The signal that is transmitted over the fiber is randomly polarized, *i.e.*, is a random superposition of both polarizations. This would not matter in an ideal fiber because both polarizations would propagate identically.

However, a realistic fiber is not truly a cylindrical waveguide, but must be considered as an imperfect cylinder. The variations in the geometry of the fiber leads to a phenomenon called *birefringence* whereby the propagating pulse loses the balance between the two orthogonally polarized modes. Hence, the signal's polarizations travel with different group velocities which results in pulse spread. This pulse spread is referred to as polarization mode dispersion or PMD.

Figure 2.11, shows the pulse spreading due to PMD. The energy of the pulse is assumed to be split between the two orthogonally polarized modes, shown by horizontal and vertical pulses. Due to the fiber birefringence, one of these polarizations travels at slower velocity than the other. The pulse has been broadened due to PMD and its energy is now spread over a larger time period.

The time spread, or differential group delay (DGD), due to PMD after the pulse has propagated through a unit length of the fiber is given by:

$$\Delta\tau = \Delta\beta/\omega \quad (2.12)$$

where $\Delta\beta$ denotes the difference in propagation constants and ω denotes the angular frequency. A typical value of the DGD is $\Delta\tau = 0.5$ ps/km, which suggests that after propagating through 100 km of fiber, the accumulated time spread will be 50 ps. Such a value should be compared to the bit period of 100 ps for a 10 Gbps systems

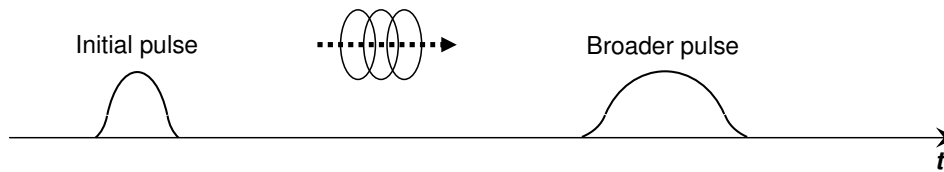


Figure 2.12: Illustration of pulse spreading due to CD

and shows that PMD becomes a serious obstructor in very high speed systems.

However, assuming fixed propagation constants for each polarization mode is unrealistic since the fiber birefringence changes over the length of the fiber⁵. Consequently, the PMD effects are not as bad as foreseen by this model since the time delays in different segments of the fiber vary randomly and tend to cancel each other. The DGD is shown to depend on the inverse of the square root of the link length. Typical value lies in the range of 0.1 to 1 ps/ $\sqrt{\text{km}}$.

Chromatic Dispersion

The chromatic dispersion is the phenomenon by which different spectral components of a pulse travel at different velocities in the fiber. Chromatic dispersion (CD) arises in the fiber for two reasons and thus it may be classified into two categories: *material dispersion* and *waveguide dispersion*.

Material dispersion is due to the fact that the refractive index of silica (the material used to make optical fiber) is frequency dependent. Consequently, frequency components travel at different speeds in silica which results in pulse broadening that cumulates along the lightpath.

The origin of waveguide dispersion is that the light energy of a mode propagates partly in the core and partly in the cladding of the fiber. Also, the effective index of a mode lies between the refractive indices of the cladding and the refractive indices of the core. The actual value of the effective index between these two limits depends on the proportion of power that is contained in the cladding and the core.

The power distribution of a mode between the core and the cladding of the fiber is frequency dependent. When the frequency is low, more power gets in the cladding. Therefore, even without material dispersion, if the wavelength changes, the power distribution changes so that the effective index of the mode changes.

As shown in Figure 2.12, the shape of a pulse propagating in an optical fiber is

⁵The birefringence also changes over time due to temperature and other environment changes.

not preserved due to the presence of chromatic dispersion. The key parameter in the evolution of the pulse shape is the second derivative of the propagation constant β with respect to the angular frequency:

$$\beta_2 = \frac{d^2\beta}{d\omega^2}$$

Chromatic dispersion is commonly described by the *chromatic dispersion parameter* D which is related to β_2 according to:

$$D = -\frac{2\pi c}{\lambda^2}\beta_2 = -\frac{\lambda}{c}\frac{d^2n}{d\lambda^2} \quad (2.13)$$

where n is the effective index. D is measured in ps/(nm.km) since it expresses the temporal spread (ps) per unit propagation distance (km), per unit pulse spectral width (nm). For most optical fibers, there is a so called *zero-dispersion wavelength*, for which the parameter β_2 is equal to zero. For positive values of β_2 , the chromatic dispersion is said to be *normal* whereas it is said to be *anomalous* for $\beta_2 < 0$.

2.2.3.3 Nonlinear Effects

Nonlinearities in fiber may lead to attenuation, distortion, and cross-channel interference. In a WDM system, these effects impose constraints on the spacing between adjacent wavelength channels, and they limit the maximum power per channel, the maximum bit rate, and the system reach. There are two categories of nonlinear effects that arise in optical fibers.

First, the refractive index depends on the *intensity* of the applied electrical field, which in turn is proportional to the square of the field amplitude. The most important nonlinear effects in this category are *self-phase modulation*, *cross-phase modulation*, and *four-wave mixing*.

The second category of nonlinearities are due to several types of scattering effects whereby the energy gets transferred from one light wave to another longer wavelength. The lost energy is absorbed by the molecular vibrations in the medium. The two main effects in this category are *stimulated Raman scattering* and *stimulated Brillouin scattering*.

Self-Phase Modulation

Self-phase modulation (SPM) is due to variations in the power of an optical signal and results in variations in the phase of the signal. The amount of phase shift

introduced by SPM is given by:

$$\phi_{NL} = n_2 k_0 L |E|^2 \quad (2.14)$$

where n_2 is the nonlinear coefficient for the index of refraction, $k_0 = 2\pi/\lambda$, L is the length of the fiber, and $|E|^2$ is the optical intensity. In phase-shift-keying (PSK) systems, SPM may lead to a degraded performance since the receiver relies on the phase information. SPM also leads to spectral broadening of pulses. Instantaneous variation in the signal phase caused by changes in the signal intensity will result in instantaneous variations of frequency around the signal's central frequency. Hence, different parts of the pulse undergo different phase shifts, which gives rise to chirping of the pulses. Pulse chirping in turn enhances the pulse broadening effects of chromatic dispersion. This chirping effect is proportional to the transmitted signal power so that SPM effects are more important in systems using high transmitted powers.

Cross-Phase Modulation

In WDM systems, the intensity-dependent nonlinear effects are enhanced since the combined signal from all the channels can be quite intense, even when individual channels are operated at moderate powers. Thus, the intensity-dependent phase shift, and the consequent chirping, induced by SPM alone is enhanced because of the intensities of the signals in other channels. This effect is referred to as *cross-phase modulation* (XPM).

XPM is a shift in the phase of a signal caused by the change in intensity of another signal propagating at a different wavelength. XPM can lead to asymmetric spectral broadening, and combined with dispersion, may also affect the pulse shape in the time domain.

Although XPM may limit the performance of the optical systems, it may have advantageous applications as well. XPM can be used to modulate a pump signal at one wavelength from a modulated signal on a different wavelength. Such techniques can be used in wavelength conversion devices.

Four Wave Mixing

In WDM systems using the angular frequencies $\omega_1, \dots, \omega_n$, the intensity dependence of the refractive index not only induces phase shifts within a channel but also gives

rise to signals at new frequencies such as $2\omega_i - \omega_j$ and $\omega_i + \omega_j - \omega_k$. This phenomenon, referred to as *four-wave mixing* (FWM), may result in inter-channels crosstalk. In contrast with SPM and XPM, which are significant mainly in high-bit rate systems, the FWM effect is independent of the bit rate but is critically dependent on the channel spacing. Hence, the effects of FWM must be considered even for moderate bit rate systems when the channels are closely spaced.

Stimulated Raman Scattering

Stimulated Raman scattering (SRS) is caused by the interaction of light with molecular vibrations. Light incident on the molecules creates scattered light at a longer wavelength than that of the incident light. A portion of the light traveling at each frequency in a Raman-active fiber is downshifted across a region of lower frequencies. The light generated at the lower frequencies is called the Stokes wave. The range of frequencies occupied by the Stokes wave is determined by the Raman gain spectrum⁶ which covers a range of around 40 THz below the frequency of the input light. In silica fiber, the Stokes wave has a maximum gain at a frequency of around 13.2 THz less than the input signal.

The fraction of power transferred to the Stokes wave grows rapidly as the power of the input signal is increased. Under very high input power, SRS will cause almost all of the power in the input signal to be transferred to the Stokes wave.

In WDM systems, the shorter wavelength channels will lose some power to each of the higher wavelength channels within the Raman gain spectrum. To reduce the amount of loss, the power of each wavelength channel must be below a certain level (typically 1 mW).

Stimulated Brillouin Scattering

Stimulated Brillouin scattering (SBS) is similar to SRS, except that the frequency shift is caused by sound waves rather than molecular vibrations. Other characteristics of SBS are that the Stokes wave propagates in the opposite direction of the input light, and SBS occurs at relatively low input power for wide pulses (greater than 1 μ s), but has negligible effect for short pulse (less than 1 ns). The intensity of the scattered light is much greater in SBS than in SRS, but the frequency range of

⁶The Raman gain spectrum typically describes the measured Raman gain coefficient for silica fibers as a function of the frequency shift at a pump wavelength of 1.0 μ m.

SBS, in the order of 10 GHz, is much lower than that of SRS. In addition, the gain bandwidth of SBS is only in the order of 100 MHz.

In WDM systems, SBS may induce inter-channel crosstalk. To get around the SBS effect, the input power should be set below a certain threshold.

2.2.3.4 Amplified Spontaneous Emission

Amplified Spontaneous Emission (ASE) is produced when a laser gain medium is pumped to produce a population inversion. Feedback of the ASE by the laser's optical cavity may produce laser operation if the lasing threshold is reached. Excess ASE is an unwanted effect in lasers since it dissipates some of the laser's power. In optical amplifiers, ASE limits the achievable gain of the amplifier and increases its noise level.

Optical amplifiers are placed evenly on the fiber link to boost the signal power. Each amplifier adds its own component of ASE noise. Thus, the OSNR gradually degrades along the fiber length. The OSNR at the amplifier's output is given by:

$$OSNR = \frac{P_{in}}{NF \times h\nu \times \Delta f} \quad (2.15)$$

where NF represents the noise figure of the optical amplifier, h is the Planck's constant⁷, ν is the optical frequency, and Δf is the bandwidth that measures the noise figure. When we consider WDM links with cascaded amplifiers, ASE becomes a serious issue because the cumulation of the noise figure of each amplifier degrades the end-to-end OSNR.

In WDM systems, cross saturation occurs whereby the gain of a WDM channel is saturated by either its own power or cross-talk power from neighboring channels.

2.3 Summary

In this chapter, we have first recalled the typical configuration of WDM transmission systems. The main characteristics of optoelectronic devices used in such systems have been described. We have then depicted the four main types of optical switching nodes: OXC, OCS, OPS, and OBS. This thesis being focused on optical network planning, we have considered three types of OXCs: opaque, transparent and translu-

⁷The value of the Planck's constant is $h = 6.62606896 \times 10^{-34}$ expressed in J.s.

cent. Finally, the end of this chapter has been dedicated to the evaluation of BER in optical transmission systems.

Although chromatic dispersion is the most important phenomenon limiting the performance of optical systems operating at moderate bit rates (2.5 Gbps and below), nonlinear effects become important at higher bit rates. The main nonlinear effects that impair high-speed WDM transmission are self-phase modulation, cross-phase modulation and four-wave mixing.

In this thesis, the simultaneous effects of four transmission impairments is investigated, namely chromatic dispersion, polarization mode dispersion, amplified spontaneous emission, and nonlinear phase shift. To the best of our knowledge, at the date of the beginning of this thesis, none of the network planning studies was taking into account these four parameters simultaneously.

In Chapter 3, we describe into details an original tool enabling to evaluate the BER associated to a lightpath in considering the realistic characteristics of each device of the transmission system. We mean by realistic characteristics the performance figures based on the current state of the technology. This tool, called BER-Predictor, computes the Q factor on the basis of analytical formulation of physical impairments. The numerical value of Q factor allows to estimate the BER value at the destination node of the lightpath.

“Do not worry about your difficulties in Mathematics.

I can assure you mine are still greater.”

– Albert Einstein (1879 - 1955)

3 Quality of Transmission

Evaluation: the Physical Model

3.1 Introduction

The transparency in optical networks is desirable in many respects. For instance, it helps to avoid the bottleneck due to the optoelectronic conversion at each switch, saves cost by reducing the number of transponders, enables to connect various types of equipment to the network and enables terminal upgrades without requiring the entire network reconfiguration thanks to bit rate and data format transparency. Nevertheless, transparency is viable only if the quality of the analog signal, evaluated through the BER, remains acceptable at destination.

In this work, the feasibility of a lightpath is examined through the computation of a numerical value describing the quality of transmission (QoT) called Q factor. Q factor may be numerically approximated by four main transmission impairments namely chromatic dispersion, polarization mode dispersion, nonlinear phase shift, and amplified spontaneous emission. The originality of this study is to consider simultaneously these impairments and thus, to take into account the interactions between them. For instance, the chromatic dispersion level is tolerable depending on the level of nonlinear effects. Q factor is mainly a characteristic parameter of a given lightpath, since the Q factor value depends on the traveled path and the assigned wavelength.

In order to get an estimate of the BER for a given lightpath in a given WDM network, we have developed a prediction tool called BER-Predictor that computes

the Q factor as a function of the penalties induced by the considered transmission impairments. In this chapter, we focus on the design and the functionalities of BER-Predictor. For this end, we have to understand how the network is modeled and how the transmission impairments accumulate through the different devices and systems traversed by the optical signal.

3.2 BER-Predictor Structure

Given a network topology and the physical characteristics of the devices and systems deployed in the network, BER-Predictor provides an estimate of the BER to be expected at the destination node of a specific lightpath. BER-Predictor takes into account the penalties induced by the chromatic dispersion, polarization mode dispersion, nonlinear phase shift, and the amplified spontaneous emission. BER-Predictor mainly consists of three distinct steps:

Step 1. A lightpath is defined by its physical route and the assigned wavelength. The network is defined by its topology and the physical characteristics of its devices and systems (fibers, optical amplifiers, optical cross-connects, etc.). The network topology is provided to BER-Predictor as an input text file wherein each line describes a link of the network (adjacent nodes, length of the link, lengths of the links spans¹). The physical characteristics of the network devices and systems are provided to BER-Predictor as an input text file wherein each line describes a specific device or a specific system. The first step of BER-Predictor consists in setting the input signal powers and transmission parameters with respect to the chosen technologies.

Step 2. Along its route, the optical signal travels different optical devices, essentially fibers, amplifiers, and optical cross-connects. Each device affects the optical signal and induces power penalties. The second step of BER-Predictor consists in simulating the propagation of the optical signal from its source node to its destination node. This is done by computing new values of the transmission parameters (optical power, chromatic dispersion, etc.) at the output of a network device as a function of the transmission parameters values at the input of this device. The computation of each transmission parameter as well as the way the transmission parameters are accumulated will be detailed later in this chapter.

¹Span refers to the fiber that connects two adjacent line amplifiers.

Synopsis 3.1 BER-Predictor synopsis

Input: Network topology (* links and their lengths *),
 Physical parameters (* fiber parameters, amplifier parameters, node parameters, etc. *),
 Lightpath (* route and wavelength *)

Output: The value of Q factor associated to the given lightpath

Begin

Step 1. Initialization

1 Initialize the lightpath:

1.1 \mathcal{N} the number of the nodes traveled by the signal including the source and destination nodes

1.2 \mathcal{V} a vector of length \mathcal{N} representing the physical route $[\nu_1, \dots, \nu_{\mathcal{N}}]$

2 Initialize the physical parameters

Step 2. Propagation of the optical signal through the physical route

3 Construct an "ADD" node (* the source node ν_1 *)

4 Compute the transmission parameters

5 Return the transmission parameters

6

for $i := 1$ to $\mathcal{N} - 1$ do

6.1 Open the file describing the network topology

6.2 Find the specifications of the current link (ν_i, ν_{i+1})

6.2.1 S the number of spans

6.2.2 \mathcal{L}_j the length Span j for $j \in \{1 \dots S\}$

6.3 Deploy a dispersion compensating module

6.4 Compute the transmission parameters

6.5 Use a pre-line amplifier (* an EDFA amplifier of type "BOOSTER" *)

6.6 Compute the transmission parameters

6.7

for $j := 1$ to S do

6.7.1 Deploy a line fiber of length \mathcal{L}_j

6.7.2 Compute the transmission parameters

6.7.3 Use an EDFA amplifier (* the first stage of the of the inline amplifiers *)

6.7.4 Compute the transmission parameters

6.7.5 Deploy a dispersion compensating module

6.7.6 Compute the transmission parameters

6.7.7 Use an EDFA amplifier (* the second stage of the of the inline amplifiers *)

6.7.8 Compute the transmission parameters

endfor

6.8 Return the transmission parameters

6.9

if $(i < \mathcal{N} - 1)$ then

6.9.1 Construct a "TRANSIT" node (* the node ν_i *)

else

6.9.2 Construct a "DROP" node (* the destination mode $\nu_{\mathcal{N}}$ *)

endif

6.10 Compute the transmission parameters

6.11 Return the transmission parameters

endfor

Step 3. Computation of the value of Q factor

7 Compute the four penalties π_{CD} , π_{PMD} , π_{PhNL} , and π_{ASE}

8 Compute the value of Q factor defined as function of these penalties

9 Return the value of Q factor for the given lightpath

End.

Step 3. The values of chromatic dispersion, polarization mode dispersion, nonlinear phase shift and amplified spontaneous emission that have been computed in the second step of BER-Predictor are used to compute the Q factor. The analytical relation between Q factor and the four aforementioned parameters has been derived both from equations describing the physical phenomena, and experimental measurements (see [40] [41] and [42]).

Synopsis 3.1 summarizes the steps of BER-Predictor. In the following of this chapter, we detail the computation of each transmission parameter as well as the accumulation of the transmission impairments along the route.

3.3 Fiber Related Issues

From the point of view of BER-Predictor, the fiber is a simple entity, *i.e.*, is independent from other BER-Predictor entities. Given a link of the network, BER-Predictor considers the fiber link span by span. In order to characterize a span and to compute the transmission parameters, we provide BER-Predictor with the type and the characteristics of the fiber, the considered wavelength and the input signal power. The computation of the transmission parameters after having traveled a fiber is detailed in Synopsis 3.2.

As explained in Chapter 2, chromatic dispersion and Kerr effect are the two major impairments induced by transmission over fiber. Considering the signal that is modulated at a given wavelength, the different spectral components of this signal propagate along the optical fiber at different speeds resulting in signal distortion at the fiber output. This phenomenon, called chromatic dispersion, is linear and accumulates along the fiber(s). The total amount of dispersion accumulated at the end of the fiber characterizes the impairments induced by dispersion. In order to overcome these impairments, carriers insert along the transmission link sections of fiber with strong negative dispersion known as dispersion compensating modules (DCM). These DCMs are usually located at the beginning, and along the transmission link (typically, in the inter-stage of optical amplifiers).

As far as nonlinearities are concerned, the physical effect, known as Kerr effect, comes from the dependence of the refractive index on the power of the light propagating along the fiber. Minimizing nonlinear effects and guaranteeing a minimum optical power at the receiver's side are two contrary objectives. For instance, optical

Synopsis 3.2 Computation of the transmission parameters after traveling a fiber

Input: Type of the fiber (* X , $X \in \{ \text{SMF}_1, \text{SMF}_2, \text{LEAF}, \text{DCF} \}$ *),
 Mode of the fiber (* Y , $Y \in \{ \text{Flat}, \text{Non-Flat} \}$ *),
 Physical parameters (* attenuation, dispersion, polarization mode dispersion, etc. *),
 Length of the fiber \mathcal{L} km,
 Considered wavelength λ

Output: Transmission parameters

Begin

Step 1. Compute the overall CD(* getCD *)

```

1
  if (Y == Flat) then
1.1   $\mathcal{D} := \mathcal{D}_X \times \mathcal{L}$ 
    else
1.2  Get the dispersion  $\mathcal{D}_{X,\lambda}$  for the wavelength  $\lambda$ 
1.3   $\mathcal{D} := \mathcal{D}_{X,\lambda} \times \mathcal{L}$ 
    endif
2  Return  $\mathcal{D}$ 

```

Step 2. Computation of the PMD(* getPMD *)

```

3   $\mathcal{PMD} := \mathcal{PMD}_X \times \sqrt{\mathcal{L}}$ 
4  Return  $\mathcal{PMD}$ 

```

Step 3. Computation of the Φ_{NL} (* getPhiNL *)

```

5
  if (Y == Flat) then
5.1   $\text{Attenuation} := \alpha \times \mathcal{L}$ 
    else
5.2  Get the attenuation  $\alpha_{X,\lambda}$  for the wavelength  $\lambda$ 
5.3   $\text{Attenuation} := \alpha_{X,\lambda} \times \mathcal{L}$ 
    endif
6  Compute the effective length of the fiber
6.1   $\text{ConvAtt} := (\ln(10) \times 10^{-4} \times \text{Attenuation}) / \mathcal{L}$ 
6.2   $\mathcal{L}_{\text{eff}} := (1 - \exp(-\text{ConvAtt} \times 10^{-3} \times \mathcal{L})) / \text{ConvAtt}$ 
7   $\Phi_{\text{NL}} := 2\pi \times n_2 / (A_{\text{eff}} \times 10^{-21} \times \lambda \times \mathcal{L}_{\text{eff}})$ 
8  Return  $\Phi_{\text{NL}}$ 

```

Step 4. Computation of the output power (* getOutputPower *)

```

9   $\mathcal{P}_{X,\lambda}^{\text{out}} := \mathcal{P}_{X,\lambda}^{\text{in}} - \text{Attenuation}$ 
10 Return  $\mathcal{P}_{X,\lambda}^{\text{out}}$ 

```

End.

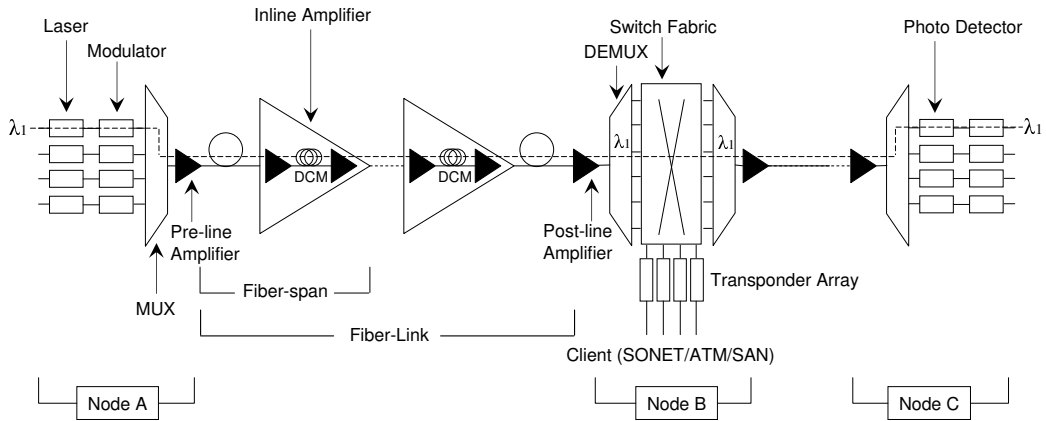


Figure 3.1: Lightpath carried by λ_1 and connecting node *A* to node *C*.

amplifiers are very efficient to boost the optical power but they favor nonlinear effects. In addition, optical amplifiers induce ASE noise. Therefore, the optical input power of a signal appears as a tradeoff between nonlinearities (a low input power is required), noise and receiver's sensitivity (a high input power is required) limitations.

3.3.1 Dispersion Management Strategy

Chromatic dispersion and nonlinearities closely interact so that it becomes almost impossible to compensate their detrimental impact separately. The usual way to mitigate at the same time the impact of chromatic dispersion and nonlinearities is called *dispersion management*: rather than only focusing on the linear compensation of the accumulated dispersion over a fiber-link, the dispersion management allows to gradually compensate the accumulated dispersion by deploying DCMs at specific locations along this link. In the design of a point-to-point transmission link, we distinguish three types of DCM:

- a pre-compensating module, located at the beginning of the link (this DCM, not represented in Figure 3.1, is deployed just before the pre-amplifier);
- a post-compensating module, located at the end of the link (this DCM, not represented in Figure 3.1, is deployed just before the post-amplifier);
- inline compensating modules, inserted between the two stages of the line amplifiers that link two consecutive spans of line fiber as illustrated by Figure 3.1.

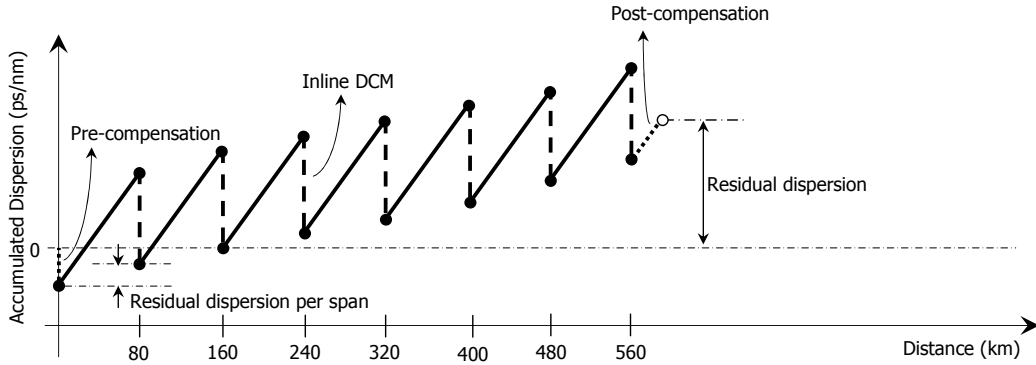


Figure 3.2: Typical dispersion map of a transmission link consisting of 7 spans of 80 km SMF fiber.

A *dispersion map* is the way chromatic dispersion is managed over a transmission link. It can be graphically summarized by plotting the evolution of the accumulated dispersion over distance as illustrated in Figure 3.2. From the scheme depicted in Figure 3.2, we can notice that:

- Firstly, the residual dispersion at the end of the link is not zero. Indeed, in the presence of nonlinearities, the optimal residual dispersion is rarely zero because of the interplay of chromatic dispersion and nonlinearities [43]. Chromatic dispersion tends to be slightly positive, *e.g.*, a few hundreds of ps/nm, depending on the fiber input power, the transmission distance, and the dispersion map itself.
- Secondly, the residual dispersion per span is not zero. Indeed, a full compensation for the dispersion induced by the preceding fiber-span appears to be sub-optimal. At the beginning of each fiber span, the accumulated dispersion and power would be reset to the initial conditions which may lead to some kind of resonant effect impairing even more the transmitted signal. Consequently, it is preferable to let dispersion accumulate slightly along the link and to compensate for higher dispersion at the end of the link.

More complex dispersion management schemes may be also used. For instance, the accumulated dispersion can be periodically reset to a very low value in order to prevent a long post-compensating module. Attenuation induced by a long compensating module would affect the optical signal to noise ratio (OSNR) at the receiver's end.

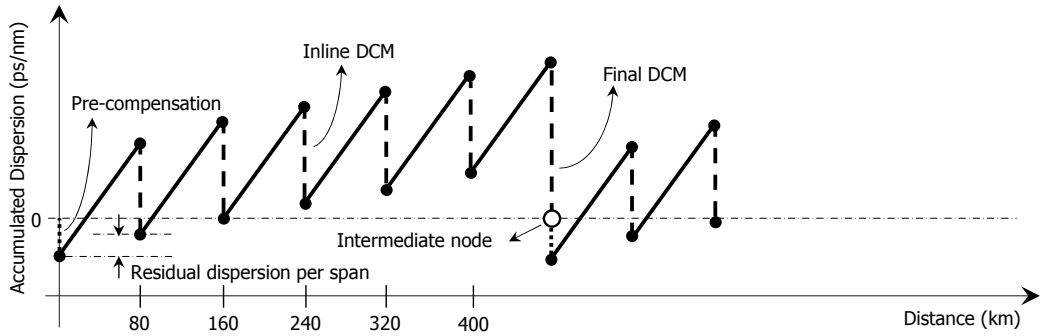


Figure 3.3: Dispersion map of a transmission link with accumulated dispersion reset to zero at each intermediate node.

In meshed networks design, the constraints are not the same as in point-to-point systems design. We have to ensure that the dispersion management will be relevant for all possible lightpaths. More precisely, the residual dispersion at the end of a lightpath has to be compatible with the tolerance range of the receiver. Indeed, in the context of meshed networks, it is impossible to perform an ideal dispersion compensation since the optical channels arriving at a given destination may have traveled different paths, each path being characterized by its own physical impairments. Even in the context of point-to-point systems, an ideal dispersion compensation is unfeasible since the different optical channels arriving at a given destination operate at different wavelengths and chromatic dispersion depends on the operating wavelength. Moreover, an optical network is likely to support different types of line fiber ², each requiring, *a priori*, a specific dispersion management scheme. Four strategies to manage chromatic dispersion in an optical network can be defined:

1. The first strategy consists of a fixed set of parameters (pre-compensation, in-line residual dispersion, and post-compensation) whatever the lightpath. These parameters could be adopted with respect to the fiber type. It means that, provided a non zero in-line residual dispersion, the residual dispersion over a lightpath will depend on the number of fiber-spans. The choice of these parameters has to take into account the tolerance range of the receiver (between -500 ps/nm and $+500$ ps/nm in back to back configuration, *i.e.*, with transmitter and receiver directly connected). Such a strategy has already proved to be feasible for transparent networks.

²Different types of standard single mode fiber (SMF) are deployed in current networks.

2. The second strategy is similar to the first one but the target at the receiver's end is no longer a fixed post-compensation but a fixed residual dispersion. Such a strategy requires a *tunable* DCM at the receiver's end and a feedback information about the signal quality in order to control the tunability of the DCM.
3. The third strategy, which appears to be the easiest to implement, consists in applying a pre-compensation at each node output and in resetting the accumulated dispersion to zero at each node input in order to manage the accumulated dispersion whatever the lightpath. Therefore, the residual dispersion at the receiver's end can be set to fixed value using the same post-compensation DCM whatever the lightpath. Alternatively, a tunable DCM can be used to optimize the transmission performance. Figure 3.3 illustrates the rationale of such a strategy with a residual dispersion per node equal to zero.
4. The fourth strategy is inspired by the previous one. It consists of a non zero residual dispersion per node with a fixed target of post-compensation or residual dispersion.

Synopsis 3.3 Pre-compensating module

Input: Pre-compensation (* \mathcal{D} ps/nm *)
 Dispersion of the compensating fiber (* \mathcal{D}_{DCF} ps/nm.km *)
 Granularity of the compensating fiber (* $\mathcal{D}_{Granularity}$ ps/nm *)

Output: The length of the pre-compensating fiber \mathcal{L}_{Pre} km

Begin

- 1 $\mathcal{D} := Round(\mathcal{D}/\mathcal{D}_{Granularity}) \times \mathcal{D}_{Granularity}$
- 2 $\mathcal{L}_{Pre} := \mathcal{D}/\mathcal{D}_{DCF}$
- 3 Return the length of the pre-compensating fiber \mathcal{L}_{Pre}

End.

In this thesis, we manage chromatic dispersion using the third strategy which consists in resetting the accumulated dispersion to zero at the input of each node. The pre-compensation and inline compensation modules are chosen depending on the fiber type between adjacent nodes³. Thereafter, we consider a dispersion management scheme that uses an inline residual dispersion of 100 ps/nm/span and a pre-compensation of -800 ps/nm for transmission over SMF fiber. The lengths of the pre-compensation fiber and the inline compensation modules are computed as done in Synopsis 3.3 and 3.4, respectively.

³Our studies are limited to the standard single mode fibers (SMF).

Synopsis 3.4 Inline compensating module

Input: Dispersion of the line fiber (* \mathcal{D}_{SMF} ps/nm.km *)
Dispersion of the compensating fiber (* \mathcal{D}_{DCF} ps/nm.km *)
Granularity of the compensating fiber (* $\mathcal{D}_{Granularity}$ ps/nm *)
Dispersion slope (* \mathcal{D}_{Slope} *)

Length of the current span \mathcal{L} km
Current span s_i Number of spans of the link \mathcal{S}

Output: The length of the compensating fiber \mathcal{L}_{DCF} km

Begin

```
1
  if  $s_i == \mathcal{S}$  then
1.1  $\mathcal{D} := \text{GetCumulatedDispersion}$ 
1.2  $\mathcal{D} := -\text{Round}(\mathcal{D}/\mathcal{D}_{Granularity}) \times \mathcal{D}_{Granularity}$ 
  else
1.3  $\mathcal{D} := \mathcal{D}_{SMF} \times \mathcal{L}$ 
1.4  $\mathcal{D} := -\text{Round}((\mathcal{D} - \mathcal{D}_{Slope})/\mathcal{D}_{Granularity}) \times \mathcal{D}_{Granularity}$ 
  endif
2  $\mathcal{L}_{DCF} := \text{Round}(\mathcal{D}/\mathcal{D}_{DCF})$ 
3 Return the length of the compensating fiber  $\mathcal{L}_{DCF}$ 
```

End.

3.4 Amplifier Related Issues

In BER-Predictor, we consider three types of EDFAs with respect to the system application, namely boosters, first stage amplifiers, and second stage amplifiers. Each system application has its own configuration, *i.e.*, gain and noise figure characteristics. In this section, we detail different EDFAs control strategies and how these strategies are related to the use of BER-Predictor. Some standard amplifier features are also introduced.

3.4.1 EDFA Commonly Available Features

Figure 3.4 shows a simplified scheme of an EDFA and its control part. The amplification part⁴ consists of an erbium doped fiber and one or more pumping lasers emitting in the out-of-band spectrum (980 nm or 1480 nm)⁵. The pumping optical power is injected in the doped fiber through a multiplexer. The amplification gain is directly related to the quantity of the pumped optical power injected in the doped fiber. The quantity of the optical power generated in the pumping lasers is related to the pumping current provided to the them by the control part of the amplifier.

Two tap couplers with a photodiode are located at the input and the output of the

⁴The amplification part is not detailed in this figure.

⁵A complete WDM amplifier also presents a spectral filter compensating for the doped fiber gain profile over the C-Band. This filter is designed for a given gain and a given input power.

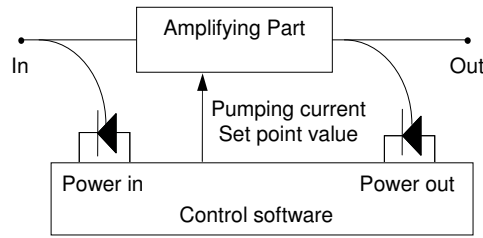


Figure 3.4: Schematic of a fiber amplifier control part.

amplifier in order to measure the optical power to be amplified and the optical power being amplified. Both information can be used by the amplifier control software in order to determine an optimal set-point value for the pumping laser diodes, and then adjusting the amplifier features to the optical input. Three operating modes can be implemented in amplifiers [15]:

Constant current: It is possible to predetermine the behavior of EDFA considering a finite set of amplification values in the C-band. If the amplification is operating in a saturation regime (which is generally true), small power variations (~ 3 dB) at the input will not change the total output power of the amplifier in a constant current mode. However, the output power balance will be changed in a similar magnitude to the input change.

Constant gain: In the constant gain mode, both the input and the output powers are monitored. The gain, defined as the ratio of the output power to the input power, is used to control the pumping current level.

Constant power: In the constant power mode, only the output power is monitored and then used as a feedback signal for pumping current set-point.

3.4.2 Optical Power Schemes in Transmission Links

In EDFA-based transmission systems, for a given lightpath in a given network, the occurring nonlinear effects mainly depend on the optical power injected in the fiber. That is the reason why the output power of optical amplifiers is monitored in WDM transmission systems. Actually, the WDM transmission systems design depends on the following characteristics:

Synopsis 3.5 Optical amplifiers configuration

Input: Function of the amplifier (* $X, X \in \{\text{Booster, Stage1, Stage2}\}$ *)
Mode of the amplifier (* $Y, Y \in \{\text{Flat, Non-Flat}\}$ *)
Noise figure NF
Amplifier gain G (* computed to compensate the preceding fiber loss *)
Input power P_{in} and input noise power P_{in}^{ASE}
Considered wavelength λ

Output: Output power and output noise power (* P_{out} and P_{out}^{ASE} *)

Begin

1

if $Y == \text{Flat}$ **then**

1.1 $P_{out} := P_{in} + G$

1.2 $P_{out}^{ASE} := \text{AddPowers}(P_{in}^{ASE} + G, (NF \times h\nu\delta f))$

else

1.3 Get the noise figure $NF_{X,\lambda}$ for amplifier X and wavelength λ

1.4 Get the gain $G_{X,\lambda}$ for amplifier X and wavelength λ

1.5 $P_{out} := P_{in} + G + G_{X,\lambda}$

1.6 $P_{out}^{ASE} := \text{AddPowers}(P_{in}^{ASE} + G, (NF_{X,\lambda} \times h\nu\delta f))$

endif

2 Return P_{out} and P_{out}^{ASE}

End.

1. Given the output optical power of the previous amplifier, fiber attenuation determines the input optical power of the next amplifier.
2. Optical noise added to the signal is directly related to the optical power per channel at the amplifier input.
3. Nonlinearities in the fiber are directly related to the output power of the amplifiers.
4. The power balance at the amplifier output depends on both the input power balance and the amplifier gain.

Optical amplifiers design must take into account the previous characteristics. This problem is already complex in the context of point-to-point transmission systems under static traffic. It becomes even more complex in the context of meshed networks under dynamic traffic. Main difficulties are due to the variation in the channels powers and load in the fiber; for instance, under dynamic traffic, the characteristics of optical amplifiers should be recomputed at each lightpath setup and tear-down. Another important aspect is the fluctuations of the amplifier regime in case of fiber cut, some of the optical channels passing through the amplifier being suppressed. Hence, the amplification control scheme needs to provide a certain output power per channel 1) whatever the amplifier load (number of channels), 2)

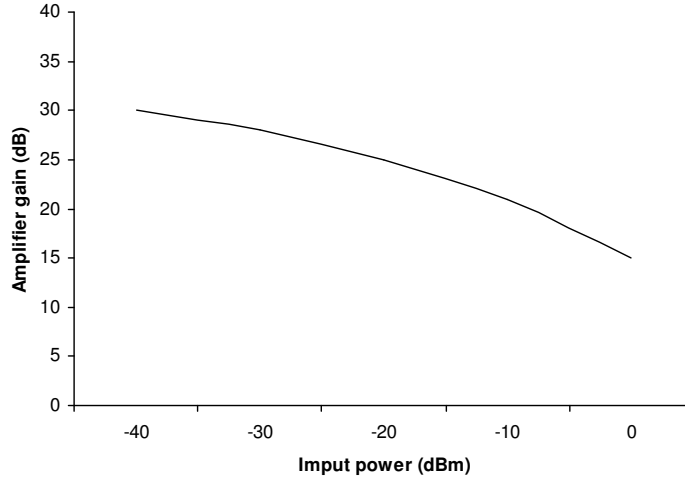


Figure 3.5: Gain saturation in an optical amplifier.

whatever the power fluctuations of channels entering the amplifier (caused by preceding amplifier ageing or fiber bend). Synopsis 3.5 briefly describes the configuration of optical amplifiers in BER-Predictor.

3.4.3 Gain Saturation

An important consideration in designing amplified systems is the saturation of the optical amplifier. Depending on the pump power and the amplifier design itself, the output power of the amplifier is limited. Indeed, above a certain cumulated power level, nonlinear effects become predominant. As a result, when the input power is increased, the amplifier gain drops [1]. This behavior is expressed approximately by the following equation:

$$G = 1 + \frac{P_{sat}}{P_{in}} \ln \frac{G_{max}}{G} \quad (3.1)$$

Here, G_{max} is the maximum admissible (unsaturated) gain and G is the saturated gain of the amplifier. P_{sat} is its internal saturation power and P_{in} is the input power. Figure 3.5 plots the amplifier gain as a function of the input power for a typical EDFA. For low input powers, the amplifier gain is at its unsaturated value, and at very high input power, $G \rightarrow 1$ and the output power $P_{out} = P_{in}$. The output saturation power $P_{out,sat}$ is defined to be the output power at which the amplifier gain dropped by 3 dB. Using Equation 3.1 and the fact that $P_{out} = G \times P_{in}$, and assuming $G \gg 1$, the output saturation power is given by:

$$P_{out,sat} = P_{sat} \ln 2 \quad (3.2)$$

The saturation power is a function of the pump power and other amplifier parameters. It is quite common to have output saturation powers of the order of 10 to 100 mW (10 to 20 dBm). There is no fundamental problem in operating an EDFA in saturation, and power amplifiers usually operate in saturation. The only thing to keep in mind is that the saturated gain will be less than the unsaturated gain.

Synopsis 3.6 Gain saturation

Input: Function of the amplifier (* X , $X \in \{\text{Booster, Stage1, Stage2}\}$ *)
Output power P_{out} (* Table including the output power off all optical channels *)
Number of optical channels C

Output: Output power

Begin

1 **if** $P_{out} > P_X^{sat}$ **then**

1.1 $\varrho := P_{out}/P_X^{sat}$

endif

1.2 **for** $i := C$ **to** 1 **do**

1.2.1 $P_{out}[i] := P_{out}[i]/\varrho$

endfor

End.

In our approach, we consider constant gain amplifiers. In order to control the output power without changing the gain (and then the flatness⁶) of the amplification part, a variable optical attenuator (VOA) can be used at the output side. If the output power exceeds a certain limit, VOA attenuates the power of each channel by ϱ defined as the ratio between the output power value and the limit value (saturation power). Synopsis 3.6 describes the VOA procedure.

3.4.4 Gain Equalization

The flatness of the EDFA pass-band becomes a critical issue in WDM systems with cascaded amplifiers. The amplifier gain is not exactly the same at each wavelength. Small variation in gain between channels in a stage can cause large variations in the power between channels at the output of the chain. For example, if the gain variation between the worst channel and the best channel is 1 dB at each stage, after 10 stages it will be 10 dB, and the worst channel will have a much poorer OSNR

⁶We mean by flatness the dependency of an optical component on the wavelength. Later in this chapter, we detail how BER-Predictor deal with the flatness of the transmission system.

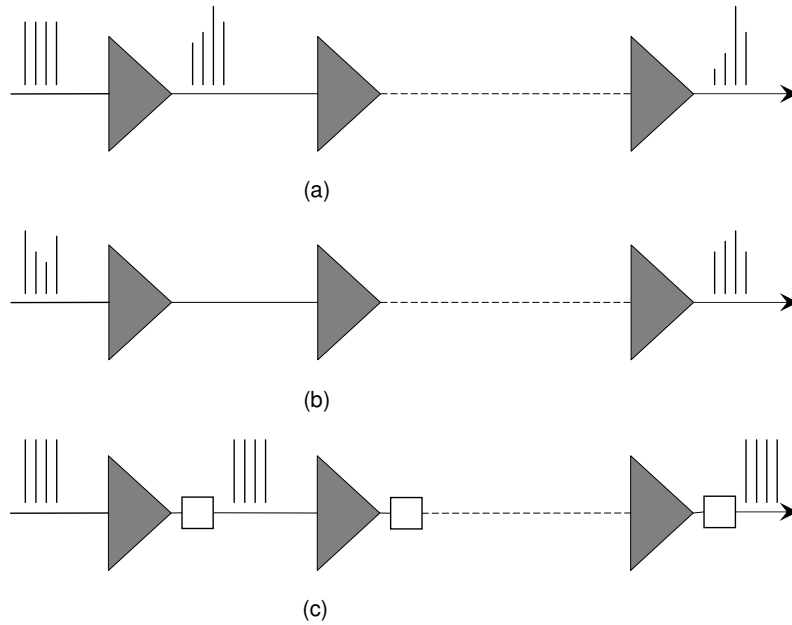


Figure 3.6: Effect of non-flat amplifier gains at different wavelength.

than the best channel. This effect is shown in Figure 3.6(a). Building amplifiers with flat gain spectra is there very important and is the best way to solve this problem. In practice, it is possible to design EDFAs to be inherently flat in the 1545 – 1560 nm wavelength range wherein many early WDM systems operate. However, systems with a larger number of channels will need to use the 1530 – 1545 nm wavelength range, where the gain of the EDFA is not flat.

At the system level, a few approaches have been proposed to overcome this lack of gain flatness. The first approach is to use pre-equalization, or pre-emphasis, as shown in Figure 3.6(b). Based on the overall gain shape of the cascade, the transmitted power per channel can be set such that the channels that see low gain are launched with higher powers. The goal of pre-equalization is to ensure that all channels are received with approximately the same OSNR and fall within the receiver’s dynamic range. However, the amount of equalization that can be done is limited, and other techniques may be needed to provide further equalization. In addition, this technique is difficult to implement in a network.

The second approach is to introduce equalization at each amplifier stage, as shown in Figure 3.6(c). After each amplification stage, the channels powers are equalized. This equalization may be done in many ways. One way is to de-multiplex the channels, attenuate each channel differently, and then multiplex them back together. This

Table 3.1: Physical impairments due to WB technology.

	Loss (dB)	CD (ps/nm)	PMD (ps)
Transit	16	± 10	0.3
Add	9.3	± 10	0.3
Drop	19.3	± 10	0.3

approach involves the use of considerable amount of hardware. It adds wavelength-tolerance penalties due to the added multiplexers and de-multiplexers. For these reasons, such an approach is impractical. Another approach is to use a multichannel filter, such as an acousto-optic tunable filter (AOTF). In an AOTF, each channel can be attenuated differently by applying a set of RF signals with different frequencies. Each RF signal controls the attenuation of a particular central wavelength, and by controlling the RF powers of each signal, it is possible to equalize the channel powers. However, an AOTF requires a large amount of RF drive power (of the order of 1 W) to equalize more than few (2 – 4) channels. Both approaches introduce several dBs of additional loss and some power penalties due to crosstalk. The preferred solution is to add an optical filter within the amplifier with a carefully designed pass-band to compensate for the gain spectrum of the amplifier in so as to obtain a flat spectrum at its output.

In BER-Predictor, two alternative schemes are possible. In the first scheme, gain equalizers are only located at the nodes whereas in the second schemes, gain equalizers are also provided inline, *i.e.*, after amplifiers cascading.

3.5 Optical Cross-Connect Related Issues

In current core optical networks, there are three possible technologies for the node architecture, namely the wavelength blocker (WB), the micro-electro-mechanical systems (MEMS), and the wavelength selective switch (WSS). The choice of the technology depends on the network connectivity, *e.g.*, for a network connectivity less than or equal to two, we use WBs. For higher connectivity, we can use either MEMS or WSS technologies. Tables 3.1, 3.2, and 3.3 summarize the physical impairments induced by the WB, MEM, and WSS technologies, respectively.

In BER-Predictor, a switching node is considered as a concatenation of an attenuator and a booster. The attenuator represents the loss due to traveling the

Table 3.2: Physical impairments due to MEM technology.

	Loss (dB)	CD (ps/nm)	PMD (ps)
Transit	18	± 20.25	0.43
Add/Drop	14	± 10.25	0.3

Table 3.3: Physical impairments due to WSS technology.

	Loss (dB)	CD (ps/nm)	PMD (ps)
Transit	12.8	± 10	0.4
Add	9.3	± 10	0.4
Drop	12.5	± 20	0.4

node with respect to the functioning mode, *i.e.*, “Transit”, “Add”, or “Drop”. In the current version of BER-Predictor, we neglect the chromatic dispersion and the polarization mode dispersion induced by the switching node; we only consider the power losses. In this thesis, we only consider the MEMS technology, hence, the losses in the switching nodes correspond to the values shown in Table 3.2.

3.6 Q factor Computation

At the end of a lightpath, the transmission parameters computed along the lightpath enable BER-Predictor to compute penalty induced by each considered transmission impairment, *i.e.*, penalties induced by chromatic dispersion, polarization mode dispersion, nonlinear phase shift, and amplified spontaneous emission. These four penalties are gathered into a single numeric value (Q factor) computed according to a polynomial function. The analytical relation between Q factor and the aforementioned penalties has been derived both from equations describing the physical phenomena, and experimental measurements (see [40] [41] and [42])⁷.

3.7 Summary

In this chapter, we have briefly described BER-Predictor. BER-Predictor gives an estimate of the BER for a given lightpath in a given WDM network. It computes the Q factor as a function of the penalties induced by the transmission impairments

⁷The analytical expression of Q factor was developed in Alcatel-Lucent Research and Innovation labs.

considered in this work, namely chromatic dispersion, polarization mode dispersion, nonlinear phase shift, and amplified spontaneous emission. In our problem of translucent network design, BER-Predictor enables to estimate the quality of transmission of a given lightpath and thus indicate whether a regeneration is required on the lightpath or not. Next chapter presents an empirical study that uses BER-Predictor to outline the limits of transparency in large-scale optical networks assuming realistic transmission systems.

*“All truths are easy to understand once they are discovered;
the point is to discover them.”
– Galileo Galilei (1564 - 1642)*

4 Limits of the Physical Layer: a Preliminary Study

In this chapter, we discuss the limits of transparency in real backbone optical networks. More precisely, we study the evolution of the quality of transmission (QoT) parameters as a function of the distance encompassed by the optical signal when no signal regeneration is performed. In this phase of our study, we only focus on quality of transmission. In other words, we do not deal in this chapter with the problem of routing and wavelength assignment. All numerical simulations are carried out by simply considering the shortest path for each possible source-destination pair in the network and by computing the values of the QoT parameters for all these shortest paths.

This chapter is organized as follows. Section 4.1 describes the elements of the numerical simulations carried out in this chapter such as the considered networks' topologies and the physical characteristics of the chosen technologies. Section 4.2 shows the quality of transmission evaluation considering a flat transmission system. The impact of the transmission system flatness is investigated in Section 4.3. In Section 4.4, we discuss the impact of deploying line dynamic gain equalizers on the quality of transmission.

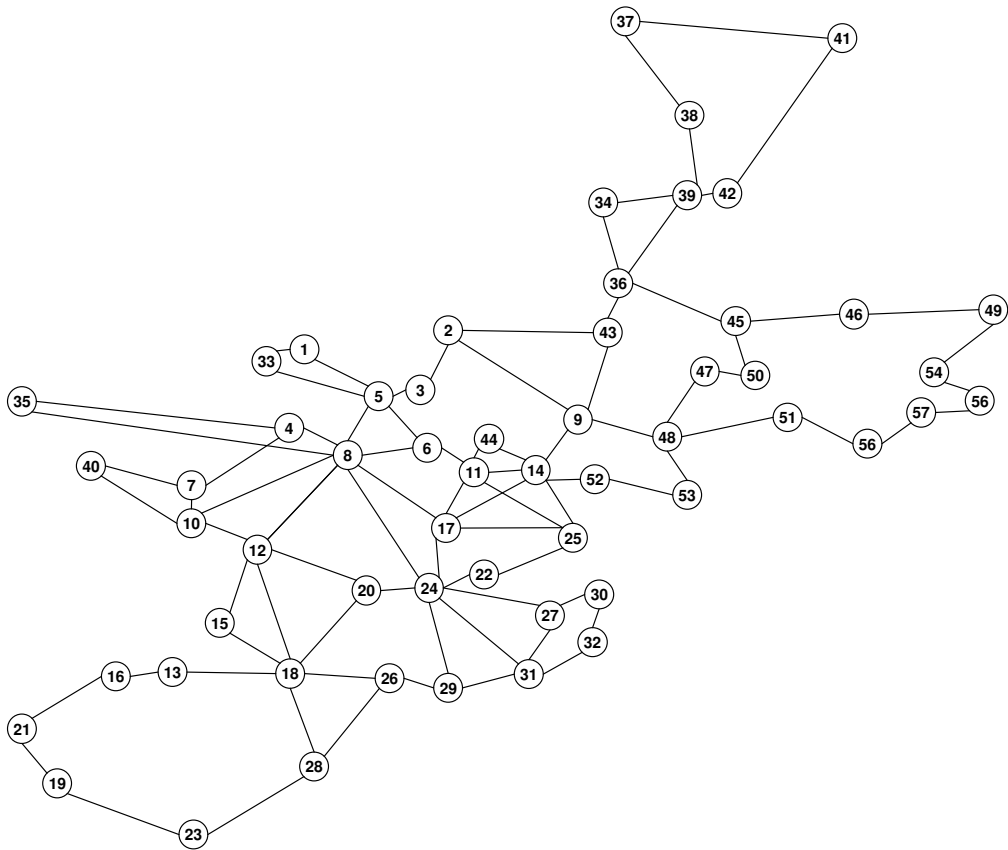


Figure 4.1: The European backbone network (EBN) topology.

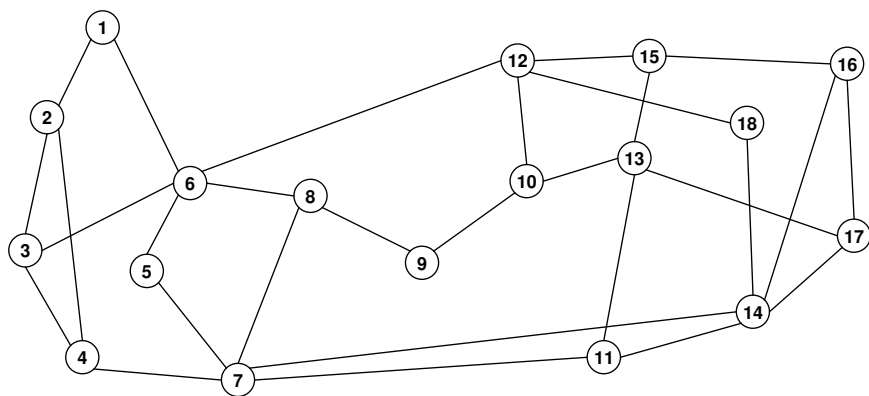


Figure 4.2: The American NSF backbone network (NSFNet) topology.

Table 4.1: Topological features of the EBN and the NSFNet networks.

	EBN	NSFNet
Number of nodes	57	18
Number of links	170	58
Shortest link (km)	26	300
Longest link (km)	680	2400
Average link length (km)	309	982

4.1 Simulations Assumptions

4.1.1 Network Topology

Since the network topology has an impact on the quality of transmission, we have chosen to investigate two network topologies with different sizes, average node connectivity, and average link lengths, namely the 57-node European backbone network (EBN) [44] and the 18-node American national scientific foundation backbone network (NSFNet) [45] shown in Figure 4.1 and Figure 4.2, respectively. The topological features of both networks are summarized in Table 4.1.

4.1.2 Physical Characteristics

In the following simulations, we assume that both the EBN and the NSFNet networks are deployed using the same technologies¹ ([15] and [2]). The networks' nodes are assumed to be MEMS-based optical cross connects (OXC) that affect the optical signal by inducing a loss of 13 dB. We assume that the network nodes are linked using standard single mode fibers (SMFs). Each fiber link has 40 available wavelengths over the C-band with 100 GHz channel spacing (Figures 4.3 and 4.4).

Chromatic dispersion is compensated using dispersion compensating fibers (DCFs) with a pre-compensation of -800 ps/nm and an inline residual dispersion of -100 ps/nm/span. Table 4.2 summarizes the physical characteristics of the SMF and DCF fibers at 1550 nm which is considered as a reference value enabling the lowest attenuation.

Optical line amplifiers are deployed every 80 km along a fiber link. All deployed amplifiers are erbium doped fiber amplifiers (EDFAs). The noise figure as well as

¹In all this document, the physical characteristics are always the ones given in this section unless it is explicitly mentioned in the text.

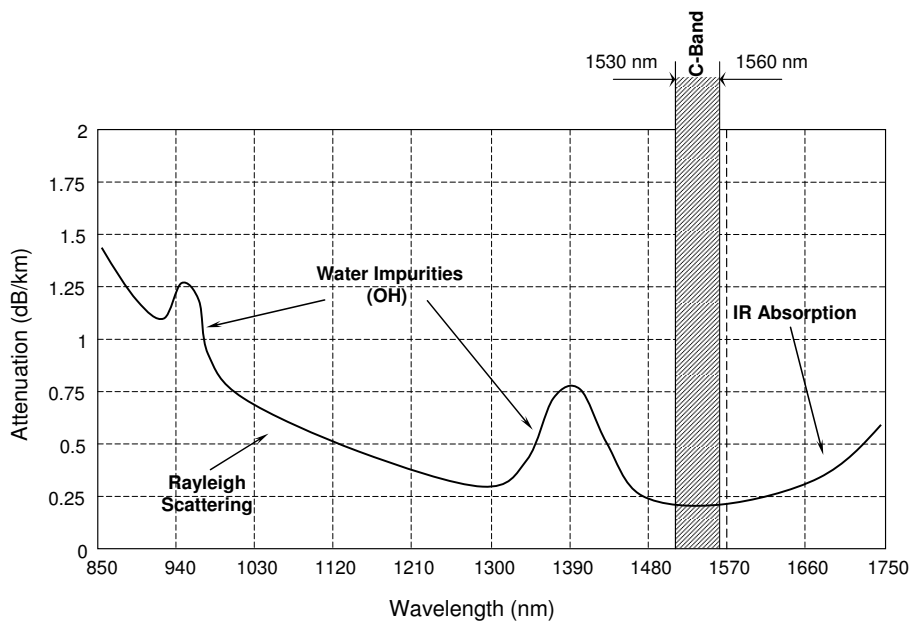


Figure 4.3: The C-Band region.

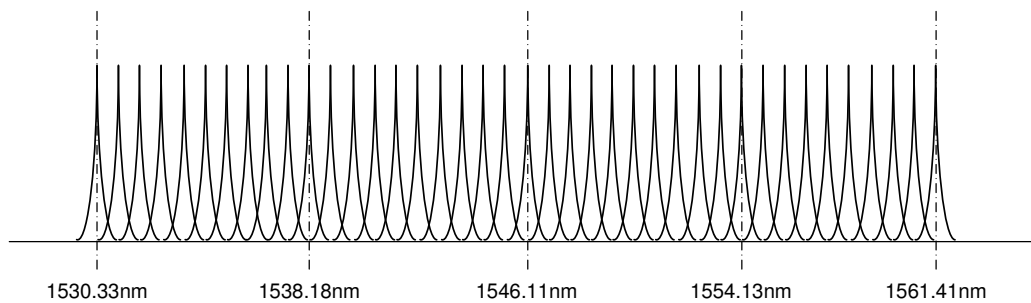


Figure 4.4: 40 wavelengths in the C-Band with 100 GHz channel spacing.

Table 4.2: Physical characteristics of SMF and DCF fibers at 1550 nm.

Fiber type	\mathcal{D} (ps/nm.km)	\mathcal{PMD} (ps/ $\sqrt{\text{km}}$)	Attenuation (dB/km)	Input power (dBm)
SMF	17	0.1	0.2	-1
DCF	-90	0.08	0.6	-7

Table 4.3: Physical characteristics of boosters and line amplifiers

Amplifier function	Noise Figure (dB)	Output power saturation (dBm)
Booster	6	22
Line amplifier	5.25	15

the output power saturation values of the boosters and the line amplifiers are given in Table 4.3.

4.2 Limits of Transparency for Flat Systems

In flat WDM transmission systems, fibers and optical amplifiers have the same physical characteristics at all the wavelengths whereas in non-flat WDM systems, these physical characteristics are not exactly the same for each wavelength.

In this section, we discuss the feasibility of transparency in real optical networks considering a flat WDM transmission system. The feasibility of transparency is investigated through the evaluation of the reach distance, *i.e.*, the distance that an optical signal can travel while conserving an acceptable OSNR. In this respect, we investigate the evolution of the four transmission impairments considered in this work with respect to the distance traveled by the optical signal. On the following figures, we plot the value of the considered parameter obtained at the end of each lightpath versus the length of the lightpath. Hence, a cloud of 3192 points and a cloud of 306 points are plotted for the EBN and the NSFNet networks, respectively.

Figure 4.5 shows the residual chromatic dispersion at the end of each considered lightpath with respect to the length of the route. As explained in Section 3.3.1, the chromatic dispersion is compensated gradually along each fiber link of the lightpath and roughly set to zero at each intermediate node (see Figure 3.3). Hence, a dispersion compensating module does not exactly compensate the amount of the chromatic dispersion accumulated along the fiber link. Consequently, residual dispersion accumulates along the route and results in the values presented in Figure

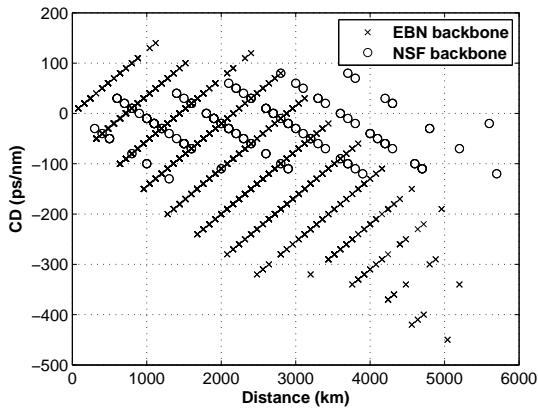


Figure 4.5: CD w.r.t. distance in a flat system.

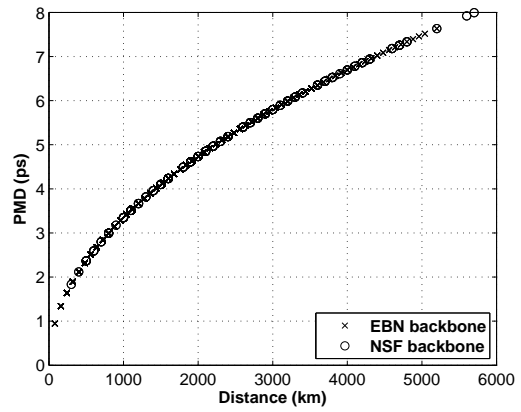


Figure 4.6: PMD w.r.t. distance in a flat system.

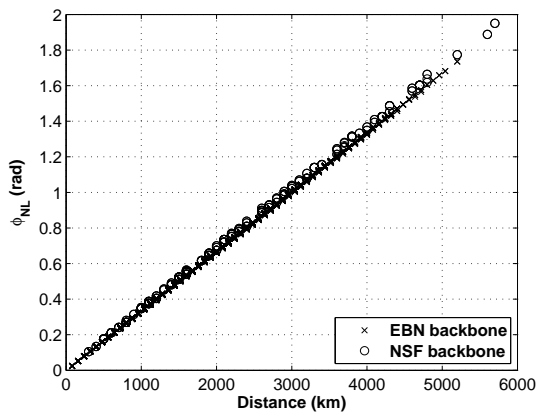


Figure 4.7: ϕ_{NL} w.r.t. distance in a flat system.

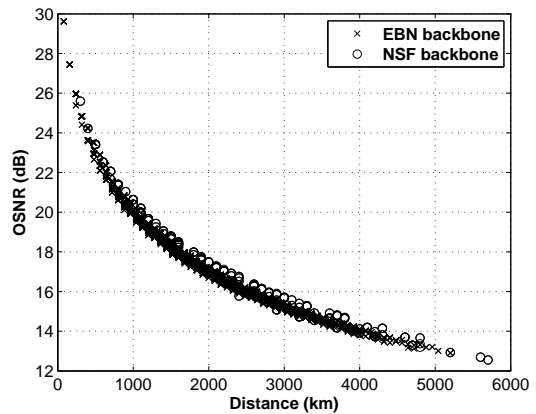


Figure 4.8: OSNR w.r.t. distance in a flat system.

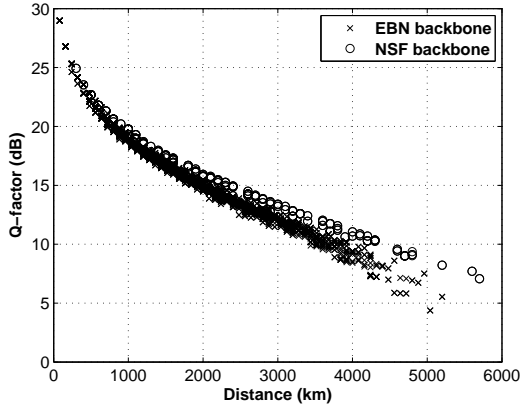
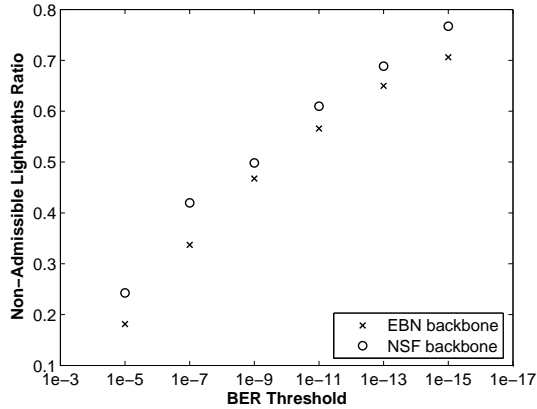
Figure 4.9: Q factor values w.r.t. distance.

Figure 4.10: Inadmissibility ratio w.r.t. distance.

4.5.

From Figure 4.5, we notice that the network topology has an impact on the residual chromatic dispersion: for a given length of lightpaths, the residual dispersion in the EBN network may be larger than the residual dispersion in the NSFNet network. This is due to the fact that the links of the EBN network are shorter than those of the NSFNet network. For comparable paths lengths, a lightpath in the EBN transits through more nodes than a lightpath in the NSFNet.

In Figure 4.6, we study the evolution of the polarization mode dispersion accumulated along the lightpaths with respect to the length of the route. The PMD evolves the same way in both the EBN and the NSFNet networks because it only depends on the distance traveled by the optical signal and not on the number of hops.

Figure 4.7 shows the evolution of the nonlinear phase shift with respect to the distance for both the EBN and the NSFNet networks. As the nonlinear phase shift mainly depends on the traveled distance and the input signal power and thus on the number of traveled amplifiers, the two clouds in Figure 4.7 are overlaid. Here, we notice that the nonlinear phase shift evolves as a monotonic function of the traveled distance.

The evolution of the amplified spontaneous emission is presented by means of the optical signal to noise ratio. For both the EBN and the NSFNet networks, Figure 4.8 shows the evolution of the OSNR versus traveled distance. Like the nonlinear phase shift, the OSNR depends on the number of traveled amplifiers. Consequently, for a given distance, the OSNR values are approximately the same for the two

considered networks.

In Figure 4.9, we plot the Q factor values for all the lightpaths with respect to their lengths. From the figure, we can see that the Q factor values in the NSFNet network are slightly better than those obtained in the EBN network. Once again, we can explain this result by the fact that the links of the EBN network are shorter than those of the NSFNet network so that to travel the same distance, the optical signal passes through more nodes in the EBN than in the NSFNet. In addition, considering a flat WDM transmission system and a BER threshold of 10^{-9} (Q factor of 15.59 dB), transparent connections of 1800 km can be achievable in the EBN network whereas a distance of 2200 km is reachable in the NSFNet network.

Admissibility, in terms of quality of transmission, is evaluated with respect to the BER threshold: a lightpath is admissible if its corresponding BER value is less than or equal to the BER threshold (Q factor value is greater than or equal to the Q factor threshold). In Figure 4.10, we plot the inadmissible lightpaths ratio for different values of the BER threshold. Assuming a BER threshold of 10^{-5} (Q factor of 12.59 dB), the inadmissible lightpaths ratio is about 18% in the EBN network and 24% in the NSFNet network. Considering a BER threshold of 10^{-15} (Q factor of 17.99 dB), these ratios become about 70% and 75%, respectively.

In both the EBN and the NSFNet networks, the obtained results show that considering a flat WDM transmission system, the quality of transmission behaves as a monotonic function with respect to the distance traveled by the optical signal. In addition, the network topology may have an impact on the quality of transmission because this latter depends on the number of traveled nodes as we have seen.

4.3 Impact of the System Flatness

Actually, optical components such as fibers and optical amplifiers do not behave exactly the same at each wavelength of the band. Physical characteristics such as dispersion, attenuation, amplifier gain, and noise figure depend on the considered wavelength.

In this section, we investigate the impact of the optical components flatness on the quality of transmission in real optical networks. In our simulations, fiber dispersion, amplifier gain and noise figure are obtained from experimental curves².

²These curves have been provided by Alcatel-Lucent Research and Innovation in the context of our collaboration in the RYTHME project.

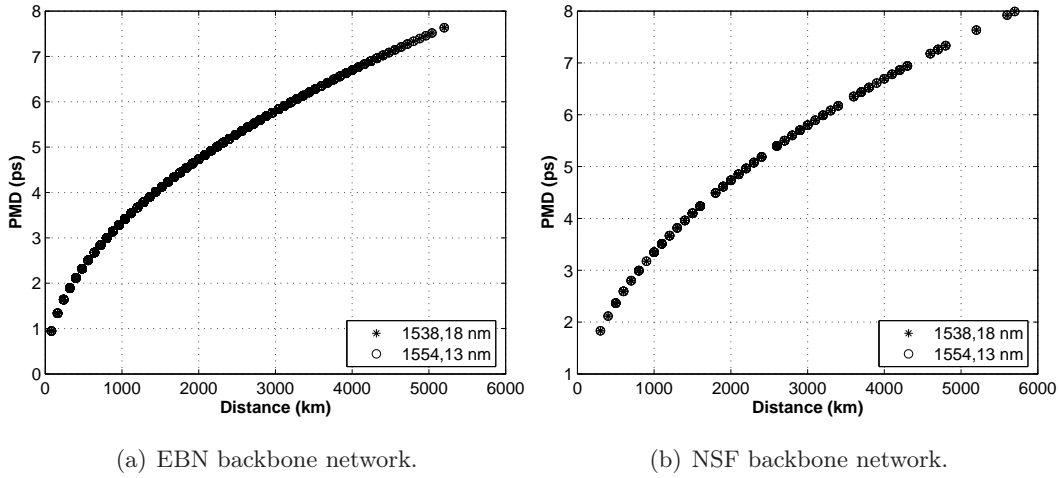


Figure 4.11: PMD w.r.t. distance in a non-flat system.

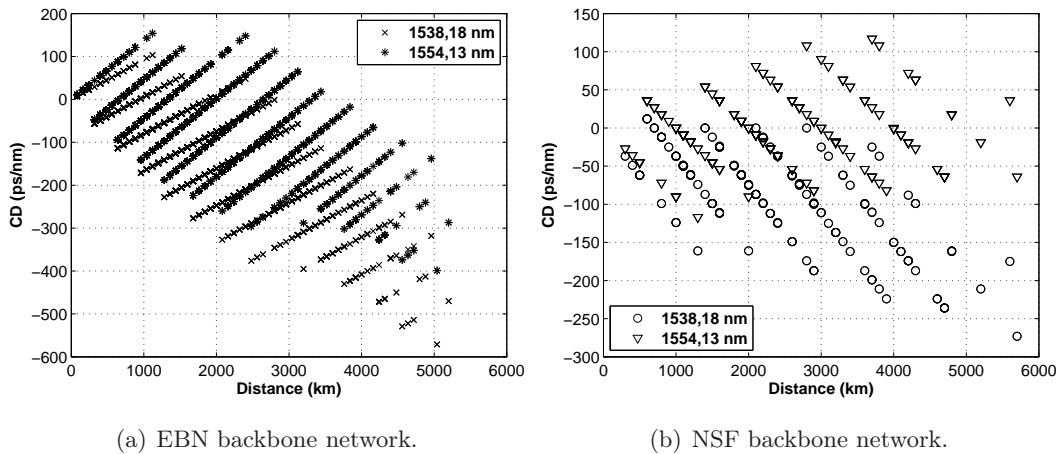


Figure 4.12: CD w.r.t. distance in a non-flat system.

Among the four transmission impairments considered in this work, it is well known that only the polarization mode dispersion does not depend on the wavelength. In Figure 4.11(a) and Figure 4.11(b), we plot the PMD values versus traveled distance for the EBN and the NSFNet networks, respectively. In both figures, the PMD is computed considering two different wavelengths from the C-band, namely the 1538.48 nm and 1554.13 nm wavelengths (see Figure 4.4). In both cases, the two clouds are overlaid and then confirm the wavelength independency of the PMD.

The impact of the non-flatness of the fiber is shown in Figure 4.12. Figure 4.12(a) and Figure 4.12(b) show the residual dispersion values with respect to traveled distance for the EBN and the NSFNet networks, respectively. In both cases, the

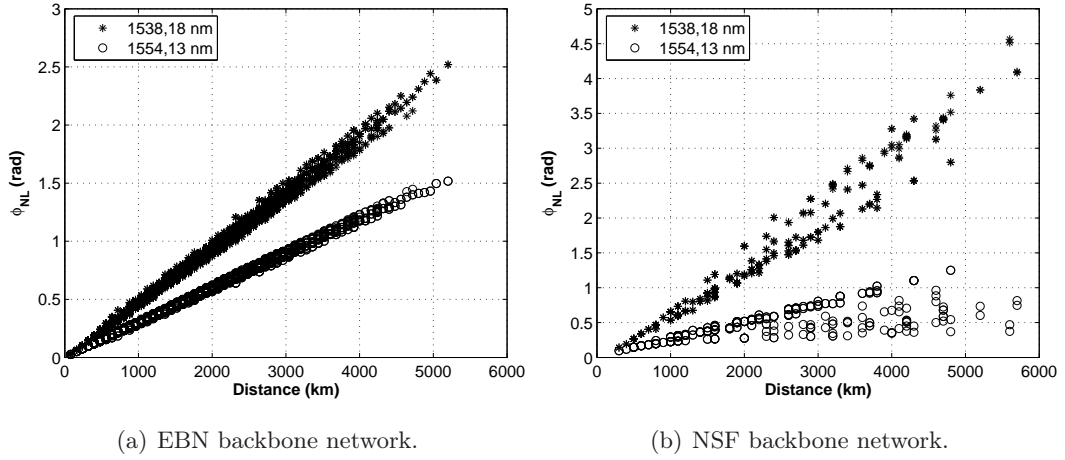


Figure 4.13: ϕ_{NL} w.r.t. distance in a non-flat system.

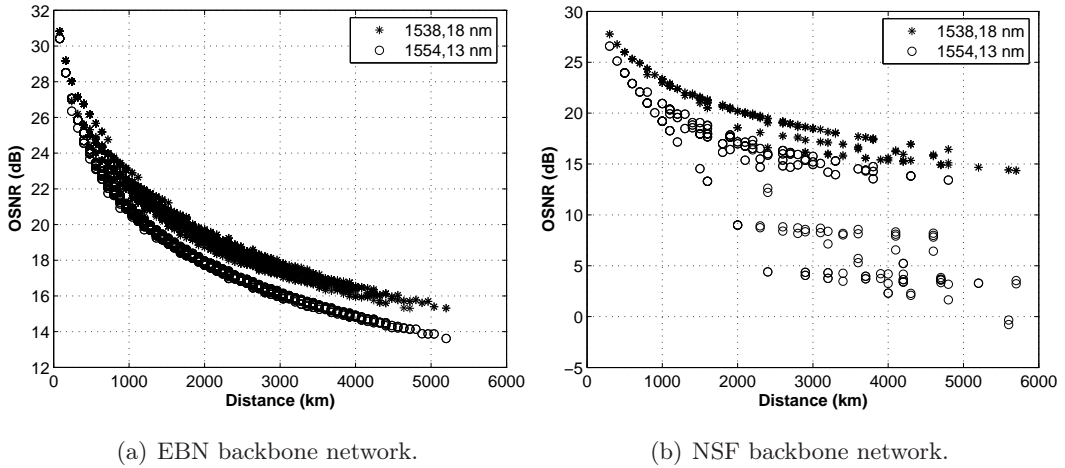


Figure 4.14: OSNR w.r.t. distance in a non-flat system.

non-flatness of the fiber results in a significant deviation in the residual dispersion values.

In Figure 4.13(a) and Figure 4.13(b), we observe the evolution of the nonlinear phase shift with respect to the distance considering the two wavelengths aforementioned. Here, we notice that there is an important difference between the nonlinear phase shift values obtained by each of them. By comparing the two figures, we state that the network topology has a significant impact on the evolution of the nonlinear phase shift: i) the difference between the two clouds in Figure 4.13(b) is more important than in Figure 4.13(a). This difference is even more noticeable at 1554.13 nm than at 1538.18 nm; ii) the clouds in Figure 4.13(a) are less scattered than in

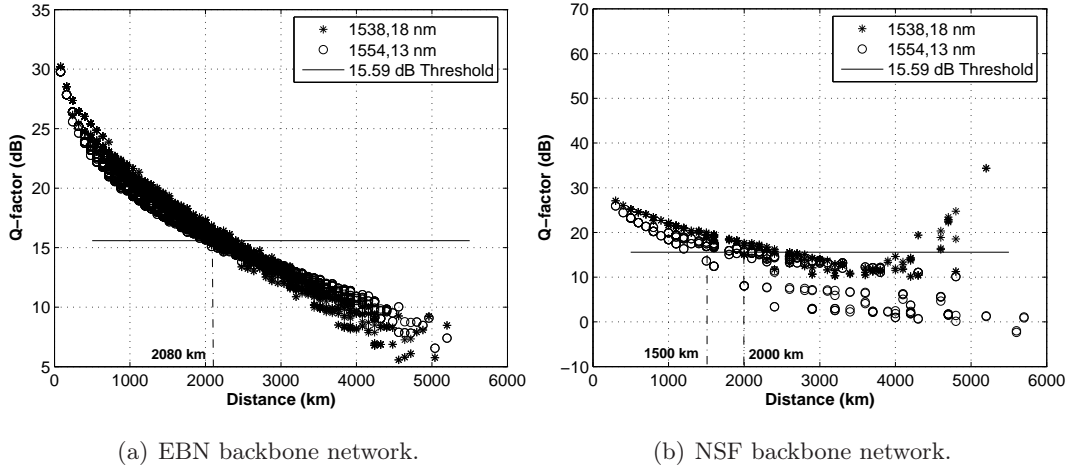


Figure 4.15: Q factor w.r.t. distance in a non-flat system.

Figure 4.13(b). Similarly to the nonlinear phase shift, the values of the optical signal to noise ratio are affected by the non-flatness of the transmission system and more precisely by the non-flatness of the optical amplifiers. As shown in Figure 4.14(a) and Figure 4.14(b), the network topology has an important impact on the evolution of the OSNR values.

In Figure 4.15(a) and Figure 4.15(b), we plot the values of the Q factor obtained, still considering the 1538.18 nm and 1554.13 nm wavelengths for the EBN and the NSFNet. For the EBN network, both the 1538.18 nm and the 1554.13 nm wavelengths can achieve a transparent connection of 2080 km length. On the other hand, for the NSFNet network, the 1538.18 nm wavelength outperforms the 1554.13 nm wavelength by achieving a transparent connection of 2000 km against 1500 km, respectively. Figure 4.15 leads us to two important conclusions. Firstly, the network topology has an important impact on the overall quality of transmission. Secondly, in the C-band, some wavelengths behave better than other ones with respect to the quality of transmission.

In order to evaluate the performance of all the C-band wavelengths (see Figure 4.4), we plotted the distance that can be achieved for each wavelength (without having to regenerate the signal). This is done for different values of the Q factor threshold as shown in Figure 4.16. These observations led us to develop impairment-aware wavelength assignment strategies that take into account the varying performance of the wavelengths in order to optimize the allocation of the wavelengths (see Chapter 6).

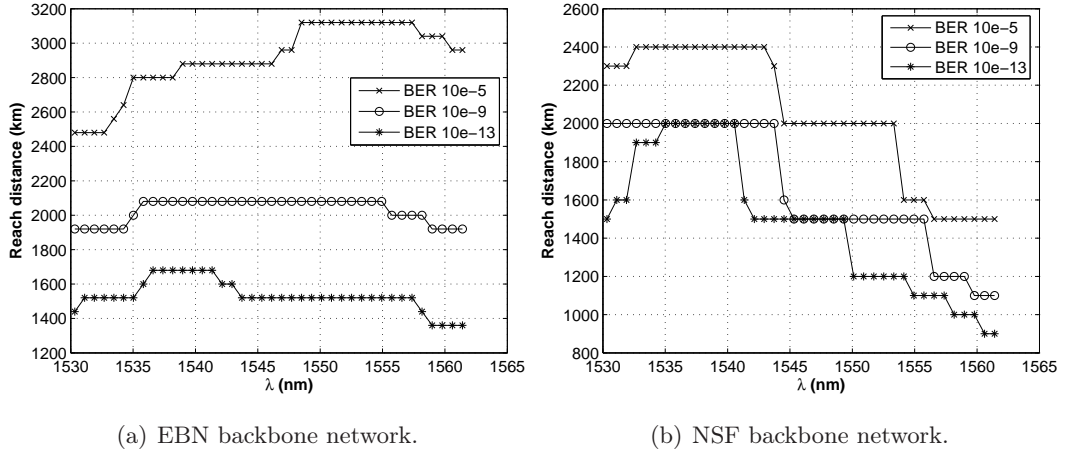


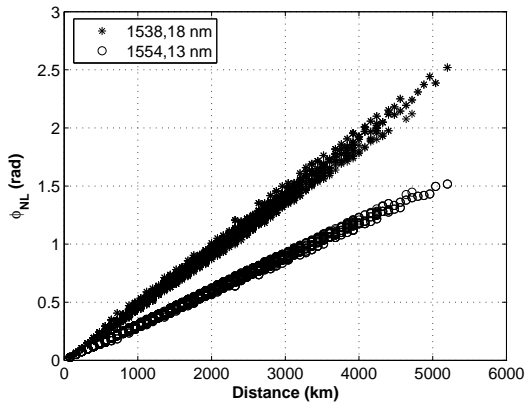
Figure 4.16: Reach distance w.r.t. wavelength for different BER-thresholds.

4.4 Impact of Gain Equalization

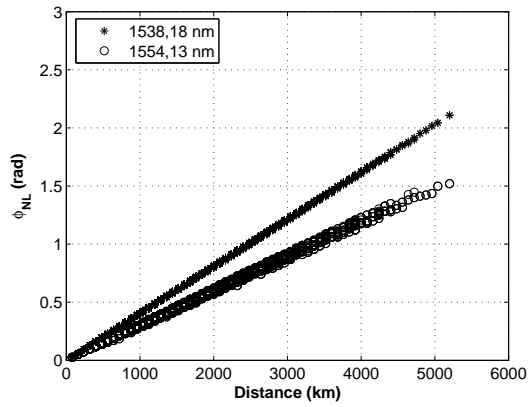
One possible approach to overcome the lack of flatness in the amplifier's gain, is to introduce dynamic gain equalizers at each amplification site (see Section 3.4.4). Up to now, we did not consider any inline equalization scheme in our study: dynamic gain equalization was only performed at the switching nodes.

In this section, we investigate the impact of deploying inline dynamic gain equalizers on the quality of transmission. Chromatic dispersion and polarization mode dispersion are not impacted by the gain equalization scheme. Consequently, we will only focus on the impact of gain equalization on the nonlinear phase shift and on the optical signal to noise ratio. In a first step, we deploy a gain equalizer at each fiber-span; this scheme is considered in the following as a reference scheme.

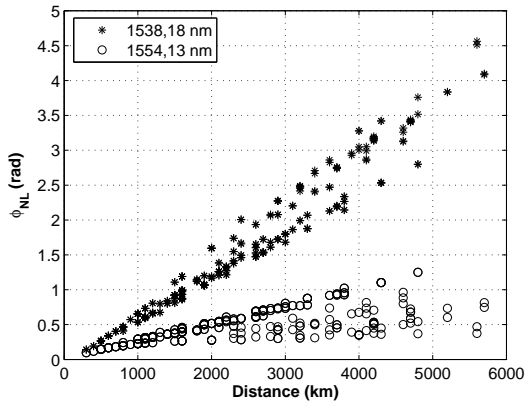
In Figure 4.17, we plot the nonlinear phase shift values versus the distance considering the 1538.18 nm and 1554.13 nm wavelengths when using a dynamic equalization scheme. Figures 4.17(a) and 4.17(b) refer to the EBN; they depict the evolution of Φ_{NL} with respect to the distance without/with line equalization, respectively. One notices that using an inline equalization scheme enables to reduce the dispersion of the clouds of points corresponding to the various lightpaths in the network. The same behavior is observed on Figures 4.17(c) and 4.17(d) considering the NSFNet. It is to be noticed that the impact of inline equalization is even more noticeable at 1538.18 nm where the slope of Φ_{NL} is sensibly reduced. Indeed, in the case of NSFNet, the average slope of the cloud referred to 1538.18 nm is reduced from 2.5 rad/4000 km to 1.5 rad/4000 km. Such an effect is interesting since it is desirable



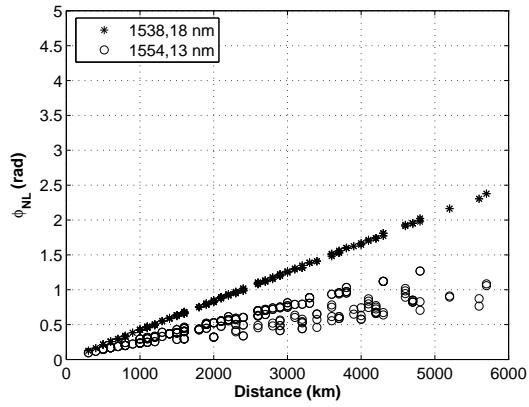
(a) EBN: without gain equalization scheme.



(b) EBN: using gain equalization scheme.



(c) NSFNet: without gain equalization scheme.



(d) NSFNet: using gain equalization scheme.

Figure 4.17: Impact of the gain equalization scheme on the values of ϕ_{NL} w.r.t. distance.

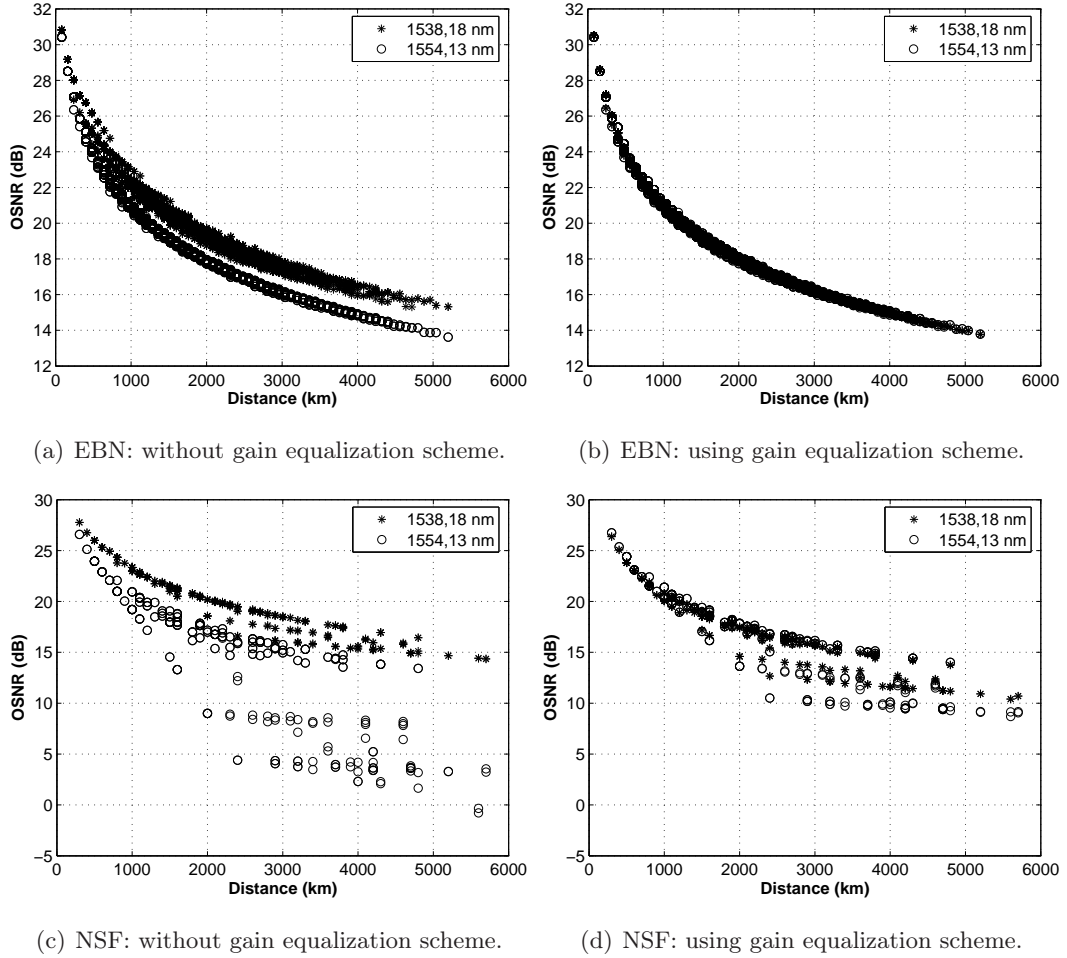


Figure 4.18: Impact of the gain equalization scheme on the values of OSNR w.r.t. distance.

to reduce the nonlinear effects.

Figures 4.18(a) and 4.18(b) depict the impact of inline equalization on the OSNR in the EBN network. Similarly to Φ_{NL} , inline equalization significantly reduces the clouds scattering. One observes that the cloud referring to 1538.18 nm overlaps the cloud referring to 1554.13 nm, lightly degrading OSNR when inline equalization is applied. In the case of NSFNet, the same phenomenon is observed.

In summary, the impact of deploying a dynamic gain equalization scheme on the quality of transmission can be numerically evaluated through the value of \mathcal{Q} factor. In Figure 4.19, we plot the values of \mathcal{Q} factor considering the 1538.18 nm and the 1554.13 nm wavelengths without/with gain equalization. Considering the average \mathcal{Q} factor value for each distance in the EBN network, we see that inline equalization does not have a significant impact on the network performance. In the

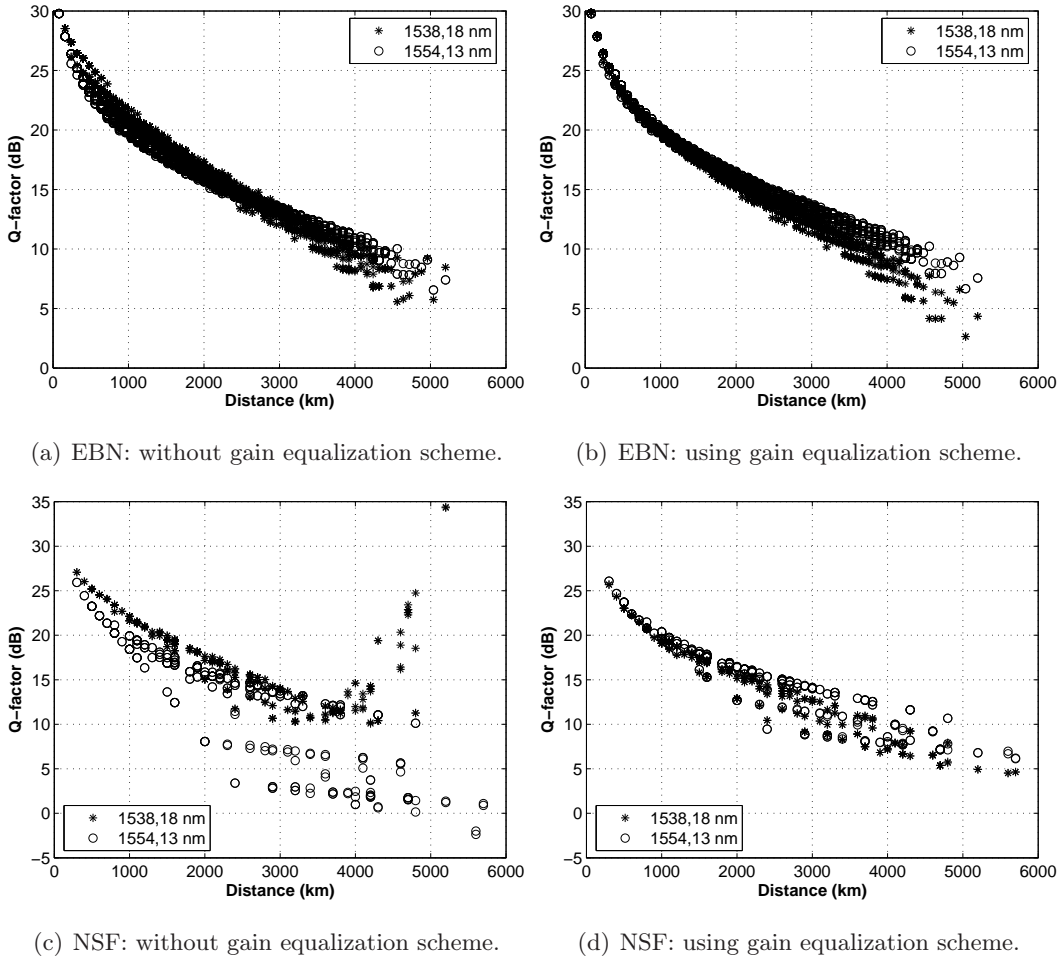


Figure 4.19: Impact of the gain equalization scheme on the values of Q factor w.r.t. distance.

case of NSFNet, the impact of inline equalization is mainly noticeable for distances greater than 3500 km. Indeed, without inline equalization, the Q factor diverges mainly due to the nonlinearities proper to 1538.18 nm. It is to be noticed that such divergence does not exist at 1554.13 nm. Applying inline equalization enables to totally cancel this Q factor divergence phenomenon.

From the previous figures, we state that the dynamic gain equalizers can provide a better homogeneity in the performance measures achieved by the available wavelengths. In order to adequately deploy the gain equalizers, we have investigated the impact of the number of optical amplifiers cascaded without gain equalization on the quality of transmission. In Figure 4.20, we compare two gain equalization schemes that deploy dynamic gain equalizers every 2 and 4 spans in the EBN network and every 5 and 10 spans in the NSFNet network. Each cloud on the figure represents

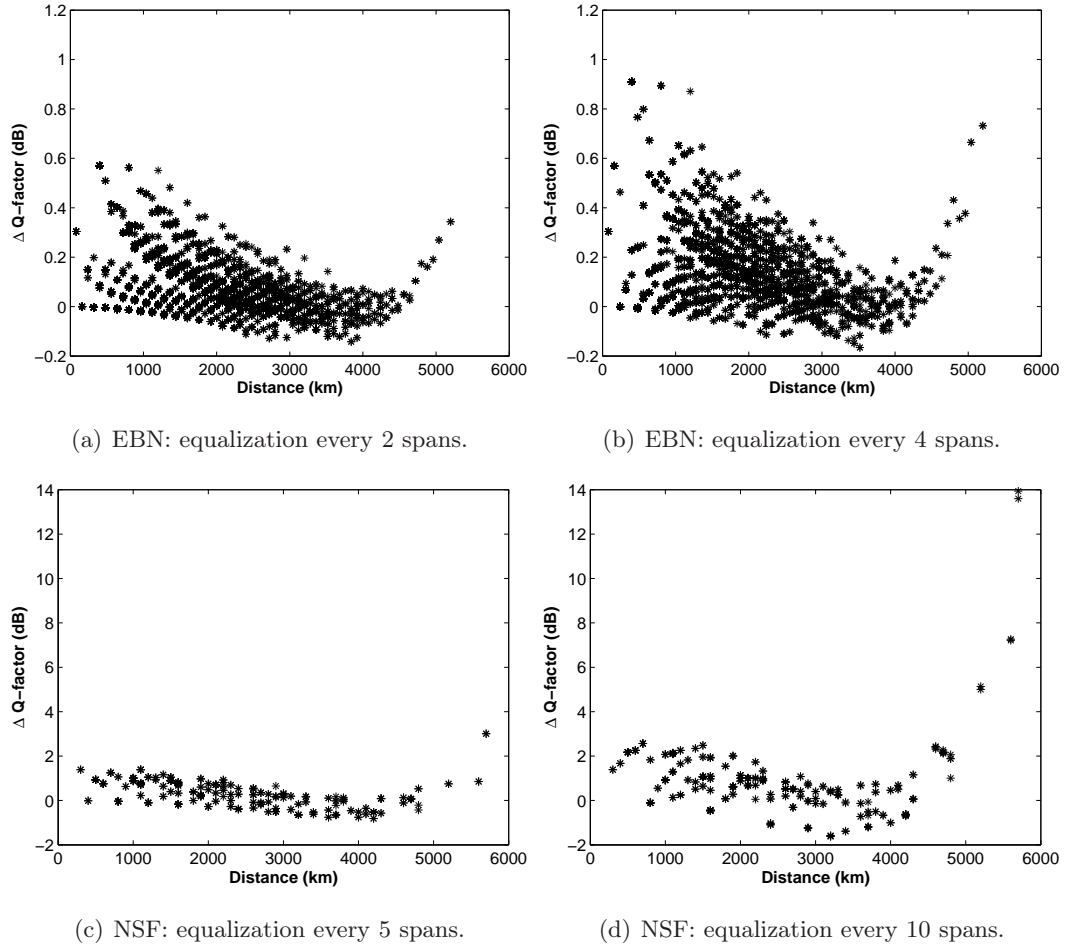


Figure 4.20: Impact of the equalizer placement on the values of Q factor.

the difference in the Q factor values between the corresponding equalization scheme and our reference scheme assuming the 1538.18 nm optical channel.

In the EBN network, both schemes achieve almost the same performance compared to the reference scheme. This result can be explained by the fact that the average length of the links (309 km, see Table 4.1) is very close to the average length of 4 spans (360 km). In other terms, considering 4 spans equalization scheme can be considered as equivalent, in the EBN, to the inherent equalization systematically applied at each switching node. The order of magnitude of ΔQ is very different between the EBN and the NSFNet. Indeed, the dispersion of ΔQ clouds is of the order of 0.7 dB in the case of EBN whereas it is of the order of 3 dB in the case of NSFNet.

4.5 Summary

In this chapter, we have studied the feasibility of transparency in real backbone networks. Quality of transmission, and thus the feasibility of a transparent lightpath is evaluated via its corresponding BER value. Four main transmission impairments are considered in order to provide an estimate of the BER, namely chromatic dispersion, polarization mode dispersion, nonlinear phase shift, and amplified spontaneous emission. We have investigated the impact of the system flatness on the optical signal quality. Simulation results have shown that firstly, the network topology has an important impact on the overall quality of transmission. Secondly, in the C-band, some wavelengths behave better than other ones with respect to the quality of transmission. One approach to overcome the non-flatness of the optical amplifier gain is to use an inline dynamic gain equalization scheme. We have addressed in this chapter the impact of using an inline equalization scheme on the network performance. Simulation results have shown that inline dynamic equalization provide a better homogeneity in the performance measures achieved by the available wavelengths.

*"All the forces in the world are not so powerful as an idea
whose the time has come."
– Victor Hugo (1802 - 1885)*

5 RWA Considering Physical Layer Constraints

Routing and wavelength assignment (RWA), survivability, control and management, traffic grooming and quality of transmission (QoT) are key issues in all-optical WDM network design. Within the framework of this thesis, we deal with RAW and QoT issues and investigate the idea of sparse regeneration in large-scale WDM networks. We propose new methods for the routing, regeneration placement and wavelength assignment taking into account the quality of transmission. In this chapter, we briefly describe each of these issues and review the solutions proposed in the literature to deal with these problems.

5.1 Routing and Wavelength Assignment

The routing and wavelength assignment (RWA) problem can be defined as follows. Given a network topology, a set of lightpath demands and a limited number of available wavelengths per optical fiber, we aim to determine the paths and wavelengths that should be assigned to the lightpath demands so that a certain performance metric is achieved.

The RWA algorithms, proposed in the literature, may be distinguished according to their performance metrics and traffic assumptions. Generally, the performance metrics fall under one of the following categories:

- Number of wavelengths required to set up the given set of lightpath demands

submitted to the network (see among others [1] [37]).

- Number of fibers handled at the switching nodes (see among others [46] [47]).
- Blocking probability, also called throughput, which is defined as the ratio of the number of blocked lightpath demands to the total number of lightpath demands (see among others [48] [49]).

The first two items refer to network planning whereas the third item refers to optimizing the utilization of network resources. The traffic assumptions generally fall into one of the following categories: static, incremental and dynamic [50] [51] [52]:

- Static traffic, also known as permanent traffic, assumes that the entire set of lightpath demands is known in advance, and the problem is then to set up lightpaths for these lightpath demands in a global fashion while minimizing network resources such as the number of wavelengths [53] or the number of fibers in the network [47]. Alternatively, one may attempt to set up as many of these demands as possible for a given fixed number of wavelengths per fiber-link [48]. The first approach refers to network planning while the second approach refers to the optimization of network resources. The RWA problem considering static traffic is known as the static lightpath establishment problem [52] [53] [54] [55].
- Incremental traffic assumes that the lightpath demands arrive in the network sequentially according to a given order. A (the) lightpath(s) is (are) established for each connection request, and the lightpath(s) remains (remain) in the network indefinitely. In this case, the objective is to minimize the rejection ratio of traffic demands in the network [52].
- Dynamic traffic assumes that the lightpath demands arrive in the network one by one. Two types of dynamic traffic can be distinguished: scheduled lightpath demands (SLDs) and random lightpath demands (RLDs) [36] [56] [57]. Scheduled lightpath demands are connection requests for which the setup and tear-down dates are known in advance [58]. Conversely, random lightpath demands are characterized by random arrival and life duration processes [59] [60]. In both cases, the objective is typically to minimize the rejection ratio of traffic demands. The problem of routing and wavelength assignment considering

dynamic traffic is known as dynamic lightpath establishment (DLE) problem [52] [53] [54] [55].

Numerous studies have investigated the routing and wavelength assignment problem for setting up a set of static lightpath demands [35] [48] [53]. These studies often set the SLE problem as an integer linear program (ILP) with the objective to minimize the resources required to establish the given set of lightpath demands (see among others [61] [31]). The ILP formulations turn out to be NP-complete problems [35] and therefore, they may only be solved for very small systems. For larger systems, meta-heuristic and heuristics methods are often proposed [53] [47]. In order to make the problem tractable, the SLE problem can be divided into two subproblems: the routing subproblem and the wavelength assignment subproblem [53] [62].

For the DLE problem, which is more difficult to solve than the SLE problem, heuristic methods are usually proposed [58] [59] [60]. As lightpaths are established and tear-down dynamically, routing and wavelength assignment decisions must be made at the time when a new connection request arrives in the network. It is possible that, for a given connection request, there may be insufficient network resources to set up a lightpath, in which case the connection request will be blocked. Once again, the routing and the wavelength assignment subproblems may be solved either jointly or separately [58] [59].

5.1.1 Separate Routing and Wavelength Assignment

As said previously, the routing and wavelength assignment may be processed within two separate steps. In this section, we give brief descriptions of the main algorithms proposed in the literature for the routing and wavelength assignment subproblems.

5.1.1.1 Routing Algorithms

Approaches to solve the routing subproblem can be broadly classified into three types: fixed routing (FR), fixed-alternate routing (FAR), and adaptive routing (AR) [63] [64] [65] [66] [67] [68].

Fixed Routing For each source-destination node pair in the network, a single path is calculated off-line and systematically used to route any connection request between this node pair [52] [62]. When a connection request is to be set up, the network attempts to establish a lightpath along the fixed path. It checks whether

a common wavelength is free all along the path. If none is free on this path, the connection request is blocked. If several wavelengths are available, a wavelength assignment algorithm can be used to select the adequate one. One example of such an approach is fixed shortest path routing wherein the shortest path is calculated using standard shortest path finding algorithms such as Dijkstra's algorithm [69].

A fixed routing approach is simple to implement and is characterized by a short set up time; however, it can potentially lead to high rejection ratios. In addition, fixed routing algorithms may be unable to handle fault situations where one or more links in the network fail. In order to minimize the rejection ratio in fixed routing networks, the predetermined paths need to be selected in a way to evenly balance the traffic load across the network links.

Fixed-Alternate Routing An extension of the fixed routing algorithm is known as fixed-alternate routing. For each source-destination node pair in the network, a set of \mathcal{K} -alternate shortest paths¹ ($\mathcal{K} > 1$), computed off-line, is provided [63] [64] [67] [72]. When a lightpath demand is to be set up, its \mathcal{K} -alternate candidate paths are explored in a fixed order and the first path with an available wavelength is selected. The order according to which the \mathcal{K} -alternate paths are considered is typically based on either path length or path congestion. If no adequate solution (path, wavelength) is found, the lightpath demand is blocked. If several wavelengths are available on the selected path, a wavelength assignment algorithm can be used to choose the adequate one.

Although this algorithm is slightly more complex than the fixed routing algorithm, it still remains simple and leads to short connection set-up times. In addition, it has better performance in terms of rejection ratio. However, the \mathcal{K} -alternate paths for a node pair may not include all the possible paths and the solution computed by the algorithm is not guaranteed to be optimal.

Adaptive Routing Also called unconstrained routing algorithm [63] [73] [74] [75] [76], the adaptive routing algorithm tries to set up the current lightpath demand on the best path (based on some criterion), chosen among all the possible paths. A cost is assigned to each link in the network based on the current network state, *e.g.*, wavelength availability on the link. A least-cost routing algorithm is then applied to

¹Among the most common \mathcal{K} -shortest paths finding algorithms, we mention the Epstein's [70] and the Yen's [71] algorithms.

find the least cost path for the current network.

Since the adaptive routing algorithm considers all possible paths, it results in better performance than the fixed routing or fixed-alternate routing algorithms. However, the algorithm has longer set up times than the fixed or fixed-alternate routing algorithms. Moreover, this algorithm is more suitable for centralized implementation and less amenable to distributed implementation.

As network traffic continues to scale up and become more bursty in nature, it is expected that a higher degree of multiplexing and flexibility will be required at the optical layer. Hence, lightpath establishment will become more dynamic in nature with connection requests arriving at higher rates and lightpaths being established for shorter time durations. In such situations, maintaining distributed global information may become infeasible. An alternative solution is to implement routing schemes which only rely on local information [52] [37].

A number of adaptive routing schemes exist which rely on local information rather than global information. The advantage of using local information is that the nodes do not have to maintain a large amount of state information; however, routing decisions tend to be less optimal than in the case of global information. One of the main local information based adaptive schemes is the least congested path routing algorithm [66] [65].

Least Congested Path Routing Similar to fixed-alternate routing, for each source-destination node pair in the network, a set of \mathcal{K} -alternate shortest paths is computed off-line. Among these paths, the least congested path routing (LCR) algorithm chooses the path with least congestion. The congestion of a path is determined from the number of wavelengths available on the entire path. When a lightpath demand is to be set up, the cost (congestion) of each of the \mathcal{K} -alternate shortest paths is computed. If several paths have the same cost, then the shortest path among them is chosen. Once the path is selected, a wavelength assignment algorithm is used to select the adequate wavelength. By selecting the least congested path, the algorithm tries to keep as many path-free wavelengths as possible in order to satisfy as many of the future lightpath demands as possible. It has been shown in [65] that LCR performs much better than fixed and fixed-alternate routing.

5.1.1.2 Wavelength Assignment Algorithms

If several wavelengths are available on a path between a source node and a destination node, a wavelength will be selected among them according to a wavelength assignment (WA) strategy. Due to the wavelength continuity constraint, the same wavelength must be used on the links spanned by a path. It is important that wavelength assignment enables to minimize rejection ratio for future connection requests.

Several heuristics for wavelength assignment have been proposed in the literature. Among others, we mention random wavelength assignment, first-fit, least-used wavelength, and most-used wavelength [62] [77] [78] [72] [79] [80] [81].

Random Wavelength Assignment (R) In this scheme, a wavelength is selected randomly (usually with uniform probability) among the available wavelengths [52] [37].

First-Fit Assignment (FF) In this scheme, the wavelengths are indexed *a priori* according to their increasing value in nanometer. When searching for available wavelengths, a lower-indexed wavelength is considered before a higher-indexed wavelength. In this manner, existing connections will be packed into the smallest indexed wavelengths, leaving the highly indexed wavelengths available for future demands.

The first-fit wavelength assignment strategy is very simple and has been widely adopted in literature [80] [73] [82]. It performs correctly in terms of blocking probability and fairness. Similar to random wavelength assignment, first-fit does not introduce any signaling overhead because it does not need any global knowledge of wavelength utilization in the network.

Least-Used Wavelength (LU) Another simple wavelength assignment algorithm is the least-used wavelength (LU) [66]. Among the wavelengths available on the considered path, the algorithm selects the wavelength that is the least used in the network. The least-used approach attempts to spread the load evenly across all wavelengths. Least-used assignment performs worse than random assignment in terms of blocking probability [37]. Moreover, it requires global information to compute the least-used wavelength as well as additional storage and computation costs.

Most-Used Wavelength (MU) This scheme is the opposite of the least-used wavelength scheme in that it attempts to select the most-used wavelength in the net-

work among the available ones. It outperforms the least-used approach significantly [62]. The communication overhead, storage and computation costs are all similar to their counterparts in least-used assignment. In addition, MU performs slightly better than first-fit by better packing connections into wavelengths and keeping the spare capacity of less-used wavelengths.

A number of more advanced wavelength assignment heuristics which rely on global network state information have been proposed [62] [81] [83]. It is assumed in these heuristics that the set of possible future lightpath connections is known in advance. For a given connection, the heuristics attempt to choose a wavelength which minimizes the number of future lightpaths that will be blocked by this connection. It is shown that these heuristics offer better performance than first-fit and random wavelength assignment.

5.1.2 Joint Routing and Wavelength Assignment

All the algorithms discussed so far select the route and the wavelength independently in two separate steps. Although these algorithms choose a route before choosing a wavelength, the reversed can also be done leading to new algorithms [84]. Unlike those algorithms, the joint wavelength-route (JWR) selection algorithm considers the cost of selecting every wavelength-route pair and chooses the least-cost pair.

The cost function used for a pair of route and wavelength takes into account factors such as the usage status of a wavelength in the network, the hop length of the route, or the congestion (or, equivalently, the number of free wavelengths) on the route.

The JWR algorithm uses an alternate routing approach. For every node pair p , a set of \mathcal{K} -candidate routes, computed off-line, is provided. These routes are denoted by $R_0^p, R_1^p, \dots, R_{\mathcal{K}-1}^p$. The set of candidate routes provided for a node pair is a subset of all the possible routes for the node pair. Let $A(w_i)$ denotes the number of links on which the wavelength w_i is currently available. Let $L(R_j^p)$ and $F(R_j^p)$ denote the hop length and number of free wavelengths on R_j^p , respectively. Then, the cost of a wavelength-route pair is given by:

$$C(w_i, R_j^p) = \alpha_1 A(w_i) + (1 - \alpha_1) \{ \alpha_2 [W - F(R_j^p)] + (1 - \alpha_2) L(R_j^p) \}, \quad 0 \leq \alpha_1 \text{ and } \alpha_2 \leq 1$$

Suitable values for the constants α_1 and α_2 can be chosen to achieve any desired cost function. For example, choosing a large value for α_1 (say, $\alpha_1 = 1$) will

prefer the most-used wavelength first. On the other hand, a smaller value for α_1 (say, $\alpha_1 = 0$) will prefer the least-cost route, ignoring the current level of usage of wavelengths. In short, this algorithm tries to combine the advantages of the MU, FAR, and LCP algorithms. A detailed description of simultaneous wavelength-path selection algorithms can be found in [84].

5.2 Physical Impairments Aware Routing

The RWA problem in all-optical networks has been presented in Section 5.1. Our discussions so far have assumed an ideal physical layer. However, in all-optical networks, transmission impairment, due to long-haul (LH) and ultra long-haul (ULH) optical components, may significantly affect the network performance. In this section, we discuss the impact of transmission impairment on the network performance and review solutions proposed in the literature to overcome physical impairments' effects.

5.2.1 Opaque versus Transparent versus Translucent Networks

In WDM *opaque* networks, data transmission occurs over point-to-point links so that the signal is regenerated at each intermediate node along the route via optical-to-electrical-to-optical (OEO) conversion. However, the operating expenses of such point-to-point system may be quite high, mainly due to the large amount of regenerators required at the nodes of a long-haul network. Recent technology advances lead to a trend in development of an all-optical - or *transparent* - network [85] [86] [87].

In WDM *transparent* networks, data is transmitted from its source to its destination in optical form. Switching and routing operations are performed in the optical domain without undergoing any optical-to-electrical (OE) conversion. In the absence of any wavelength conversion, the wavelength continuity constraint is imposed. In addition, these networks must face the technical difficulties in overcoming the transmission impairments introduced by optical components. Most studies reported in the literature neglect the transmission impairments' effects and assume that long-haul transparent networks are feasible. Actually, the optical signal undergoes various transmission impairments as it travels through the network (see Chapters 2 and Chapter 4). This fact leads to a new generation of studies that propose RWA algorithms taking transmission impairments into account.

WDM *translucent* networks, which use sparse regeneration, are a promising solution to achieve performance measures close to those obtained by fully opaque networks at a much lower cost [88] [6] [7] [9][8] [89]. Regeneration is performed at intermediate nodes only when it is necessary.

5.2.2 Impairment-Aware RWA in Transparent Networks

Compared to traditional impairment-unaware RWA, an impairment-aware RWA takes transmission impairments into account while computing and setting up a lightpath. In traditional algorithms, the connection request admission depends on resource availability, whereas the admission criterion in impairment-aware algorithms depends not only on resource availability but also on the lightpath's signal quality.

Several criteria could be used to evaluate the signal quality of a lightpath [90]. BER is a very appropriate criterion because it is a comprehensive parameter which takes all impairment effects into consideration [37]. The evaluation of BER is only possible once the lightpath is operational. In impairment-aware RWA, we aim to consider a predictive value of BER in the routing process. For that purpose, statistical model of transmission impairments has to be developed to evaluate the BER in advance (see Chapter 2).

Among several impairment-aware RWA algorithms proposed in the literature, we discuss the studies reported in [3] [4] [5].

5.2.2.1 Study of Huang et al.

Huang et al. propose in [3] two impairment-aware RWA (IRWA) algorithms, namely impairment-aware best-path (IABP) and impairment-aware first-fit (IAFF). Physical layer impairments are taken into account by constructing an integrated RWA model as shown in Figure 5.1.

The proposed algorithms are twofold: lightpath computation and lightpath verification. When a lightpath demand is to be set up, the algorithms use a network-layer module to find a candidate lightpath. If no route or wavelength is available, the lightpath demand is blocked due to lack of resources in the network layer. This type of blocking is referred to as *network resource blocking*. If routes and wavelengths are available for the candidate lightpath, a physical-layer module is used to verify the signal quality of the candidate lightpath. Transmission impairments are accumulated along the lightpath and the signal quality of the lightpath is estimated at the desti-

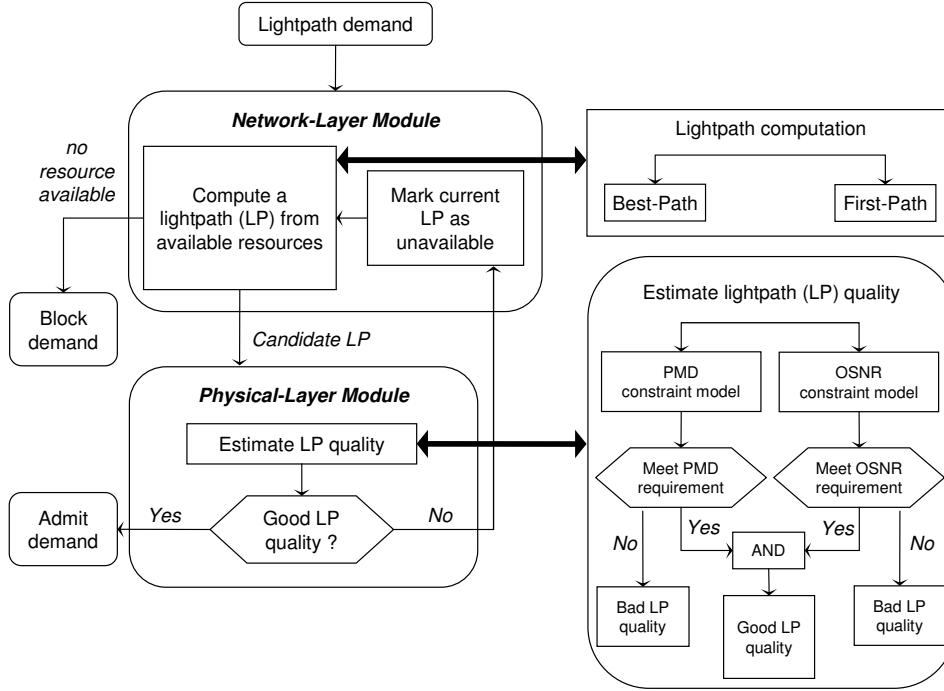


Figure 5.1: Integrated model of impairment-aware RWA algorithms.

nation's side. If the candidate lightpath satisfies a certain signal quality requirement, *e.g.*, BER of 10^{-9} , the lightpath demand is admitted using the candidate lightpath. Otherwise, the candidate lightpath is rejected and the network-layer module will try to find another candidate, and so forth. If no available lightpath can satisfy the signal quality requirement, the lightpath demand is blocked. This type of blocking is referred to as *physical layer blocking*. In this scope, we are mainly interested in the network-layer module. For more details about the physical-layer module, refer to [3].

Given a network topology (physical graph) $PG(N, L)$, a set of auxiliary wavelength-layered topologies (wavelength graph) $WG_w(N, L)$ is created, $w \in \{1, 2, \dots, W\}$, where:

- W is the maximum number of wavelengths available on a fiber link;
- N is the number of the network nodes;
- L is the number of the bidirectional links.

All wavelength-layered topology graphs (WGs) are initialized to be the same as the physical network topology graph (PG) where the link weight corresponds to the

fiber length. The routing decisions are made based on these auxiliary wavelength-layered graphs. Upon the arrival of a connection request, a candidate lightpath is computed as follows.

- Impairment-aware best-path (IABP) algorithm Based on the current state of the network, IABP applies a shortest path algorithm to find an available path P_w in each wavelength-layered graph $w, w \in \{1, 2, \dots, W\}$. A vector of path distances is defined as $D = \{D_w | w = 1, 2, \dots, W\}$. If no path is available in the w^{th} wavelength-layered graph WG_w , the D_w is set to ∞ . Otherwise, D_w is the total distance of path P_w .

After computing the shortest paths in all wavelength-layered graphs, IABP finds the minimum distance $D_w \in D$ and marks the candidate wavelength $\lambda = w$. If all the elements of D are ∞ , the connection request is blocked. At this step, the impairment-unaware algorithm is designated best-path (BP) algorithm.

If a candidate path P_λ exists, it is sent to the physical module to verify the signal quality. If the signal quality is estimated as "acceptable", the connection is set up using P_λ , and the network state is updated by specifying the links used by P_λ as occupied in the graph WG_λ . If the signal quality is estimated as "insufficient", D_λ is set to ∞ and D is browsed again. If no available wavelength guarantees an acceptable signal quality, the connection request is blocked.

- Impairment-aware first-fit (IAFF) algorithm The wavelength-layered graphs WG_s are considered one by one in increasing order. Unlike IABP, IAFF selects the first available shortest path P_w in WG_w . If no path is available in WG_w , the graph WG_{w+1} is considered and so on, until an available path is found. IAFF marks the candidate wavelength $\lambda = w$. If no path is available in all the wavelength-layered graphs WG_s , the connection request is blocked. At this step, the impairment-unaware algorithm is designated first-fit (FF) algorithm.

If a candidate path P_λ exists, it is sent to the physical module to verify the signal quality. If the signal quality is estimated as "acceptable", the connection is set up using P_λ , and the network state is updated by specifying the links used by P_λ as occupied in the graph WG_λ . If the signal quality is estimated as "insufficient", the graph WG_{w+1} is considered.

Simulations results reported in [3] show that, in realistic networks, impairment-

aware algorithms (IABP and IAFF) can achieve a significant improvement in blocking probability with respect to traditional impairment-unaware algorithms (BP and FF).

5.2.2.2 Study of Cardillo et al.

In [4], Cardillo et al. propose an impairment-aware algorithm called best OSNR (B-OSNR). It solves the RWA problem taking into account linear and nonlinear impairments.

- Best optical signal to noise ratio (B-OSNR) algorithm The B-OSNR is an impairment-aware algorithm that jointly solves the routing and wavelength assignment subproblems. Upon the arrival of a lightpath demand, a candidate lightpath is computed as follows. All possible lightpaths (path π , wavelength λ) are examined and the (π, λ) solution which guarantees the maximum OSNR is selected. Let $OSNR(\pi(s, d), \lambda_j)$ be the OSNR on path $\pi(s, d)$ using wavelength λ_j . One sets $OSNR(\pi(s, d), \lambda_j) = -\infty$ if λ_j is not usable on path $\pi(s, d)$ from node s to node d . Then, the path $\pi^{OSNR}(s, d)$ and the wavelength λ^{OSNR} is selected such that:

$$(\pi^{OSNR}(s, d), \lambda^{OSNR}) = \max_{(\pi \in \Pi(s, d)) \wedge (\lambda \in \Lambda)} OSNR(\pi, \lambda)$$

If the corresponding OSNR is above a given $OSNR_{min}$ threshold, then the lightpath is accepted and the corresponding wavelength λ is allocated on all links of path π . Otherwise, the lightpath demand is blocked.

As said before, the B-OSNR algorithm jointly assigns a path and a wavelength to a given lightpath demand. Its complexity grows linearly with the number of paths and the number of wavelengths that must be checked to find the best solution. Simulation results presented in [4] have shown that, when transmission impairments are considered, an accurate selection of path and wavelength which is driven by OSNR is mandatory. In particular, both load-independent and load-dependent effects can largely affect the rejection ratio. The former depend on the physical configuration and must be considered for any offered load to the network. There are mainly due to the inherent characteristics of devices and systems used along the considered lightpath. The latter depend on the number of lightpaths already established, *i.e.*, offered load, and are due to nonlinear effects.

5.2.2.3 Study of Deng et al.

In [5], Deng et al. study the impact of crosstalk on blocking performance in all-optical WDM networks. They propose four crosstalk-aware wavelength assignment strategies as variants of the well known random, first-fit, least-used and most-used wavelength assignment strategies. Crosstalk-aware wavelength assignment algorithms aim to minimize the crosstalk effect in the network: they choose the available wavelength that minimizes the crosstalk between the new and the existing lightpaths in order to reduce the rejection ratio. Let LP_i be a new lightpath that needs wavelength allocation, and let N^{LP_i} be the crosstalk factor associated to LP_i ²:

- **Crosstalk-aware random pick (C-RP) algorithm** This algorithm computes N^{LP_i} for all available wavelengths and chooses the wavelength that gives rise to the smallest N^{LP_i} . If multiple wavelengths provide the same N^{LP_i} value, then one among them is randomly selected.

- **Crosstalk-aware first-fit (C-FF) algorithm** In this scheme, the wavelengths are indexed according to their increasing value in nanometer and N^{LP_i} is computed for all available wavelengths. The wavelength that gives rise to the smallest N^{LP_i} is chosen. If multiple wavelengths provide the same N^{LP_i} value, then the one with the lowest index is selected.

- **Crosstalk-aware least-used (C-LU) algorithm** Among all available wavelengths on the requested path, the wavelength that gives rise to the smallest N^{LP_i} is chosen. If multiple wavelengths provide the same N^{LP_i} value, this scheme selects the wavelength that is used on the least number of links in the network.

- **Crosstalk-aware most-used (C-MU) algorithm** Among all available wavelengths on the requested path, the wavelength that gives rise to the smallest N^{LP_i} is chosen. If multiple wavelengths provide the same N^{LP_i} value, this scheme selects the wavelength that is used on the greatest number of links in the network.

Simulation results in [5] show that, compared to their traditional counterparts, the proposed crosstalk-aware algorithms can significantly reduce the rejection ratio caused by high BER values.

²Further details about the N^{LP_i} computation can be found in [5].

5.2.3 Impairment-Aware RWA in Translucent Networks

Many current studies suggest translucent optical networks as a solution to achieve performance measures close to those obtained in opaque networks at much lower cost. These studies support the idea of sparse electrical regeneration in large-scale optical networks [6] [7] [8] [9]. In such networks, an optical signal may be electrically regenerated if the BER value gets greater than a certain admissible threshold.

5.2.3.1 Study of Kim et al.

In [6], Kim et al. propose three heuristic algorithms to deal with the problem of regenerators placement under physical layer constraints. For each lightpath connecting node s to node d , one verifies whether the signal quality at node d is acceptable or not, according to the considered transmission impairments. In the latter case, one of the three following algorithms is applied:

- **Random placement algorithm (RPA)** Given a lightpath, the random placement algorithm (RPA) randomly chooses a first regeneration node among the intermediate nodes along the lightpath. BER is then evaluated on each lightpath segment. If the BER value exceeds a certain threshold at the end of the examined segment, then a new regeneration node is randomly chosen on the concerned lightpath segment. The algorithm simply keeps searching recursively until all the lightpath segments satisfy the quality of transmission requirement. In the worse case, all intermediate nodes between s and d become regeneration nodes (opaque network). The number of required regeneration nodes can be obtained using a recurrence relation. Further details can be found in [6].

- **Half placement algorithm (HPA)** Given a lightpath, the half placement algorithm (HPA) places a first regeneration node at the midpoint of the lightpath. In practice, this midpoint corresponds to nearest upstream node before the mid-distance between node s and d . BER is then evaluated on each lightpath segment. If the BER value exceeds a certain threshold along the examined lightpath segment, a new regeneration node is placed at the midpoints of the concerned lightpath segment. This process is recursively performed until all the lightpath segments satisfy the quality of transmission requirements. The number of required regeneration nodes can be obtained according to a recurrence relation as described in [6].

- **Linear placement algorithm (LPA)** Unlike the previous algorithm, the linear placement algorithm (LPA) assumes a limited regeneration capacity per node. Given a lightpath connecting node s to node d , one checks whether the signal quality at node d is acceptable or not. In the latter case, the signal quality is examined at the upstream nodes preceding the destination node. At the first intermediate node n_i where the signal quality becomes unacceptable, LPA determines if a regenerator is available at the upstream node n_{i-1} just before the considered node. If it is the case, a regenerator is effectively used in that node. Otherwise, the node n_{i-2} is considered as a potential regeneration node. This process is repeated for all candidate intermediate nodes on the given lightpath. Where no more nodes are available, the lightpath demand is rejected. The number of regeneration nodes can be obtained as described in [6].

Simulations carried out in [6] compare results obtained by the previous heuristics algorithms to a dynamic programming approach for minimal-cost placement (MCP). In this context, MCP refers to a routing and wavelength assignment solution that minimizes the number of required regenerators. Simulation results show that the MCP algorithm provide a better blocking performance than any other heuristic algorithms. In particular, the MCP algorithm is shown to outperform the other heuristic algorithms when lightpath demands have a long average hop distance. However, the MCP algorithm is the most complex with complexity of $O(H^3)$ where H is the number of hops. Further details about the MCP algorithm are provided in [6].

5.2.3.2 Study of Ramamurthy et al.

In [7] and [8], Ramamurthy et al. deal with the problem of sparse regeneration in translucent optical network assuming a limited regeneration capacity. Four regenerator placement algorithms are proposed, based either on network topology or on traffic prediction. Given a network topology $\mathcal{G}(\mathcal{V}, \mathcal{E})$ (\mathcal{V} nodes and \mathcal{E} links), N maximum number of regeneration sites, each site having X regenerators, a BER threshold BER_{th} , and LN_{max} which denotes the number of links that an optical signal can traverse without requiring any electrical regeneration. In this approach, the impact of quality of transmission is estimated under worst-case physical impairments and qualified by LN_{max} . For any couple source-destination in $(\mathcal{V} \times \mathcal{V})$, the shortest path in number of hops is adopted. The aim of this analysis is then to determine the location of the regeneration sites in order to minimize the number of rejected lightpath

demands.

- **Network Topology based Regenerator Placement** Without specific knowledge about future network traffic, the most useful information available for regenerator placement is the network topology. Indeed, the network topology partially reflects the long term traffic matrix. For instance, in general, the higher the generated traffic at node, the higher the physical degree of this node. Traffic demands are most likely to be generated at two categories of nodes. The first category corresponds to the nodes located at the “center” of a network. A node is considered as more “central” than another node if it is traversed by a greater number of shortest paths. The second category corresponds to the nodes having the higher physical degree than other nodes. Two regenerator placement algorithms that favor these two categories of nodes are developed.

- **Nodal degree first (NDF)** In NDF regenerator placement algorithm, each node is assigned an integer number equal to its in-degree. NDF algorithm selects the node with the maximum assigned number as a regeneration capable node and places X regenerator at that node. If multiple such nodes exist, one node among them is randomly selected. This process is repeated until the N groups of regenerators are placed.
- **Centered node first (CNF)** In CNF regenerator placement algorithm, each node is assigned a unique integer number between 1 and $|\mathcal{V}|$. The most “central” node is assigned the largest number. The nodes traversed by the same number of shortest paths are assigned numbers in random order. CNF algorithm selects the first N nodes, with respect to their assigned numbers, as the regeneration capable nodes and place X regenerators at each node.

- **Traffic Prediction based Regenerator Placement** When information about future network traffic is available, one may use traffic-prediction based regenerator placement algorithms. In [8], the authors employ a predefined wavelength routing algorithm on a large number of lightpath demands following a predicted traffic pattern and identify the nodes where regeneration demands are most likely. They propose two traffic-prediction based regenerator placement algorithms that favor the nodes with higher traffic loads and the nodes traversed by lightpath suffering signal quality degradation, respectively.

- **Traffic load prediction (TLP)** In TLP based regenerator placement algorithm, each node i is assigned an integer number C_i initialized to zero. TLP based algorithm runs a predefined wavelength routing algorithm on a number of randomly generated lightpath demands following a predicted traffic pattern. For each node i , the number C_i assigned to this node is incremented by one each time it is traversed by a new lightpath. After all nodes have been sorted in decreasing order of C , TLP based algorithm selects the first N nodes as regeneration capable nodes and places X regenerators at each of them. Although a higher traffic load does not necessarily mean a worse signal quality for the lightpaths that traverse a node, it tends to increase the noise inherent to crosstalk. In addition, the fact to place a larger number of regenerators at such nodes relax the wavelength continuity constraint and then improves the call admission ratio. In summary, TLP based algorithm selects the nodes with the highest transit traffic as regeneration capable nodes.
- **Signal quality prediction (SQP)** In SQP based regenerator placement algorithm, each node i is assigned an integer number C_i initialized to zero. SQP based algorithm runs a predefined wavelength routing algorithm on a number of randomly generated lightpath demands following a predicted traffic pattern. For each lightpath computed by the wavelength routing algorithm and for the j^{th} node from the source along the lightpath, an incremental value I_j is calculated according to:

$$I_j = \begin{cases} +1 & \text{if } ((j \bmod(LN_{max}) = 0) \vee ((j \pm 1) \bmod(LN_{max}) = 0)) \\ 0 & \text{otherwise} \end{cases} \quad (5.1)$$

I_j is then added to C_j assigned to this node. After all nodes being sorted in decreasing order of C , SQP based algorithm selects the first N nodes as regeneration capable nodes and places X regenerators at each node. SQP based algorithm is designed to favor the nodes and their immediate neighbors after every LN_{max} links along a predicted lightpath. In addition to every LN_{max}^{th} node, considering its immediate neighboring nodes may compensate for the error due to estimation of LN_{max} based on average link length. LN_{max} is constant in a given network, but may change for different networks.

In simulations, carried out in [8], the authors investigate the proposed algorithms considering different network topologies. Simulation results show that in the medium-sized network, the topology-based regenerators placement algorithms, NDF and CNF, yield better results followed by SQP and TLP, respectively. However, in the large-sized network, SQP yields the best performance followed by NDF, TLP, and CNF. In summary, the signal quality prediction based regenerator placement algorithm achieves good performance in all kind of network topologies. The topology based regenerator placement algorithms, NDF and CNF, may lead to the best results in some medium-sized irregular meshed topologies.

5.3 Summary

In this chapter, we presented routing and wavelength assignment algorithms for efficient connection provisioning with signal quality guarantees in all-optical networks. Under high data rate and long range, transmission impairments become predominant. In that case, appropriate techniques in both the physical and the network layers are required to mitigate the impairment effects on the network performance. Such impairment-aware RWA algorithms consider the transmission impairments when setting up a lightpath. In the context of realistic optical network, compared to impairment-unaware algorithms, impairment-aware algorithms efficiently provide connections with guaranteed signal quality while allowing a better utilization of network resources and significantly reducing rejection ratio.

Besides combating transmission impairments in all-optical networks, many related studies focus on sparse regeneration in translucent optical networks. Different methods and techniques have been proposed in the literature to allow lightpaths establishment with guaranteed signal quality. Without specific knowledge about future network traffic, a first approach consists in deducting from the network topology possible candidates for regeneration sites. In practice, since regenerator placement is part of the network planning phase, it seems to us more judicious to deduct regeneration sites from long term traffic matrices predictions.

In the context of translucent network design, we propose in the next chapter a new dimensioning tool called LERP for lightpath establishment and regenerator placement [89]. Given a network topology and a set of lightpath demands, LERP aims to satisfy the maximum number of lightpath demands while satisfying the quality of transmission requirement defined by the carrier. Quality of transmission

criterion is evaluated using BER-Predictor described in Chapter 3. In order to improve LERP performance in terms of the number of regenerators required in the network, we propose two new impairment-aware wavelength assignment strategies, namely min-BER-fit (MBF) and best-BER-fit (BBF) strategies.

"I hear and I forget. I see and I remember.

I do and I understand."

– Confucius (551 - 479 B.C.)

6 Regenerator Placement and Wavelength Assignment Strategies

6.1 Introduction

In the previous chapter, we have outlined how translucent optical networks could be considered as a promising solution to meet the fully opaque network performance at much lower cost. In such networks, 3R electrical regenerators are used at intermediate nodes only when it is necessary to improve the optical signal budget. In addition, we have underlined that the problem of regenerator placement is considered as part of the network planning objectives. In other terms, the problem of regenerator placement assumes a given network topology and a given long term static traffic matrix. In this stage, two approaches are possible for regenerator placement: i) one approach aiming to minimize the global amount of regenerators in the network while satisfying the largest amount of traffic demands, and ii) one approach aiming at the same objective assuming a fixed number of regeneration capable nodes in the network.

In this chapter, we propose an original tool for translucent optical network dimensioning. Our dimensioning tool, called LERP for lightpath establishment and regenerator placement, adopts the first of the two previous approaches. Several points characterize, to the best of our knowledge, the originality of this work. In the studies presented in Chapter 5, the authors seem to be more focusing on the problem of regenerator placement than on the optimization of network resources utilization. Indeed, their strategies consist first in placing regenerators in the network, and then in proceeding to routing and wavelength assignment of the lightpath demands. In

such a context, we have seen that the rejection of lightpath demands may be due to non-admissible quality of transmission along the path ([7] and [8]). LERP mixes iteratively the routing and wavelength assignment (RWA) process and the regenerator placement (RP) process in order to prevent any rejection ratio due to quality of transmission purposes. In other terms, LERP aims at minimizing both the amount of rejected lightpath demands due to lack of network resources, and the number of regenerators required to satisfy the quality of transmission constraints.

Concerning the routing and wavelength assignment process, we adopt a global and almost exhaustive optimization heuristic. In most studies represented in Chapter 5, routing and wavelength assignment is based on incremental traffic scenarios. We estimate that such an assumption of incremental traffic is far to be optimal in terms of network resources utilization. Instead, we propose to consider the combinatoric between a large amount of routing solutions, each routing solution corresponding in itself to an incremental scenario. In other terms, if D lightpath demands have to be routed in the network, $D!$ different incremental scenarios are possible. We choose among these $D!$ scenarios the one that enables the lowest traffic demand rejection ratio. For large values of D ($D > 10$), we have considered a subset of $D!$ possible incremental scenarios.

Another originality of our approach consists in reconsidering the global routing and wavelength assignment problem each time a regenerator is placed along a lightpath. Moreover, the regenerator placement decision is based on estimation of the BER along the considered lightpath. Such an estimation is provided by BER-Predictor which takes into account the effects of four transmission impairments (see Chapter 3).

In this chapter, we also propose new impairment-aware wavelength assignment strategies, namely min-BER-fit (MBF) and best-BER-fit (BBF). Via simulation results, we show that these new impairment-aware strategies which take into account the transmission system flatness, can improve the performance of LERP in terms of number of required regenerators in the network.

This chapter is organized as follows. Section 6.2 describes the problem of translucent network dimensioning. Section 6.3 describes the random search technique adopted in our approach to solve the problem of routing and wavelength assignment. Section 6.4 describes our strategy for regenerator placement. In section 6.5, we investigate the impact of employing inline dynamic gain equalization scheme on

the network performance. In Section 6.6, we describe and investigate the proposed wavelength assignment strategies. New research work directions are discussed in Section 6.6.3.

6.2 Description of the Problem

We state the problem of lightpath establishment and regenerator placement with guaranteed quality of transmission as follows.

Given:

- a physical network topology $\mathcal{G} = (\mathcal{V}, \mathcal{E})$, where \mathcal{V} represents vertices (network nodes) and \mathcal{E} represents edges joining these vertices (network links). We assume that each edge is made of two contra-directional optical links, and each node corresponds to either a transparent or a translucent switching node;
- a set of permanent lightpath demands (PLDs);
- W available wavelengths per fiber-link;
- an admissible threshold of the BER in the network BER_{th} ;

determine a:

- feasible routing and wavelength assignment solution that minimizes the number of rejected PLDs (maximizes the network throughput);
- feasible regenerator placement solution that minimizes the number of required regenerator in order to satisfy the quality of transmission requirement for each PLD.

Figure 6.1 gives a schematic view of the global problem including the optical signal quality evaluation. Given a network topology $\mathcal{G} = (\mathcal{V}, \mathcal{E})$, a set of W wavelengths available per fiber-link, and a lightpath p connecting two nodes, BER-Predictor provides an estimate of the optical signal quality carried by any wavelength $\lambda \in W$ at the destination node. In our approach, for each possible node-pair in the network, BER-Predictor provides an estimate of the signal quality for K alternative paths connecting these two nodes and for all wavelengths. This process is done off-line before proceeding to the routing, wavelength assignment and regenerator placement.

Given a network topology $\mathcal{G} = (\mathcal{V}, \mathcal{E})$, a set of W wavelengths available per fiber-link, a set of K alternative paths for each possible node-pair in the network,

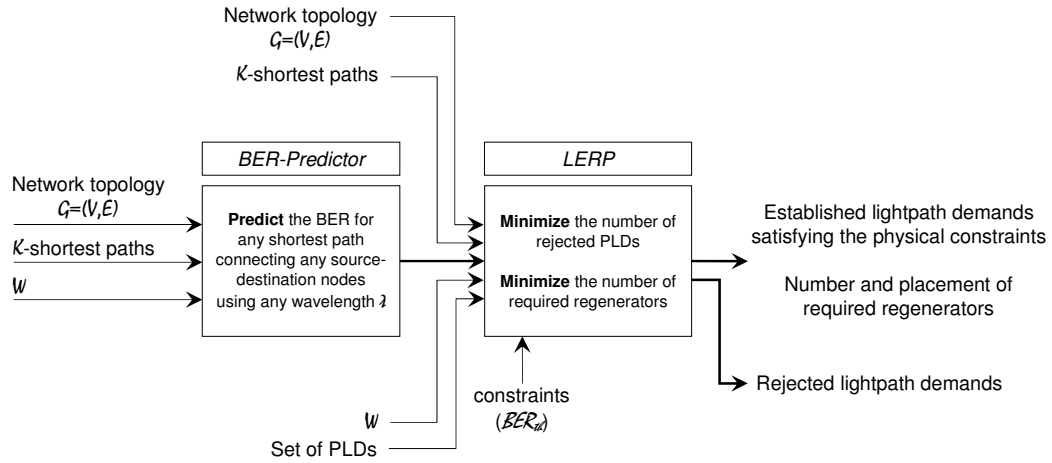


Figure 6.1: Lightpath establishment and regenerator placement with guaranteed quality of transmission.

a set of permanent lightpath demands, and an admissible BER_{th} in the network, LERP aims to establish the maximum number of lightpath demands so that the BER value on each established lightpath is less than or equal to the admissible threshold. If it is necessary (*i.e.*, the BER value exceeds the admissible threshold), one (several) regenerator(s) is (are) placed along the route in order to meet the quality of transmission requirement.

6.3 Routing and Wavelength Assignment

In our approach, the problem of routing and wavelength assignment is solved using a heuristic algorithm based on a random search (RS) technique [89]. Before explaining the principles of the RS-based algorithm, we describe the sequential routing and wavelength assignment algorithm (seqRWA).

6.3.1 Notations

In this chapter, we use the following notations and typographical conventions.

Index conventions

- i , j , and p as subscripts usually denote a demand index, a link index, and a route index, respectively.

The parameters

- $\mathcal{G} = (\mathcal{V}, \mathcal{E}, \xi)$ is an arc-weighted symmetrical graph representing the network topology with vertex set \mathcal{V} (representing the network nodes), arc set \mathcal{E} (representing the network links) and weight function $\xi : \mathcal{E} \rightarrow \mathbb{R}_+$ mapping the physical length of the links (or any other cost of the links defined by the network operator).
- $N = |\mathcal{V}|$ denotes the number of vertices (network nodes) of the graph representing the network topology.
- $L = |\mathcal{E}|$ denotes the number of arcs (network links) of the graph representing the network topology.
- W denotes the number of available wavelengths (*i.e.*, WDM channels) per fiber-link. We assume that all the network links have the same number of available wavelengths.
- D denotes the number of permanent lightpath demands (PLDs) to be set up.
- The PLD numbered i , denoted $p_i, 1 \leq i \leq D$, corresponds to a connection demand between two nodes in the network; p_i is defined by a tuple (s_i, d_i, π_i) where $s_i \in \mathcal{V}, d_i \in \mathcal{V}$ are respectively the source node and destination node of the lightpath demand, and π_i is the number of requested lightpaths to be established from s_i to d_i .
- R_i denotes the set of available routes connecting the source node and the destination node of p_i . For each $p_i, 1 \leq i \leq D$, we compute beforehand K -alternate shortest paths connecting the source node to the destination node of the PLD according to Epstein's algorithm [70] (if as many paths exist, otherwise we consider the available ones).
- $P = \{R_1 \cup R_2 \cup \dots \cup R_D\}$ is the set of available routes considering all the K -alternate shortest paths computed between all PLDs to be set up.
- $P_{i,k}$ denotes the k^{th} alternate shortest path in R_i connecting the source node to the destination node of p_i .
- $c_j^\omega \in \{1, +\infty\}$ is the cost of using wavelength λ_ω on link $j \in \mathcal{E}$. If λ_ω is free on link j , $c_j^\omega = 1$. $c_j^\omega = +\infty$ otherwise.

- $C_{i,k}^\omega = \sum_{j \in P_{i,k}} c_j^\omega$ is the cost of using wavelength λ_ω on $P_{i,k}$. $C_{i,k}^\omega < +\infty$ if λ_ω is a path-free wavelength on $P_{i,k}$. $C_{i,k}^\omega = +\infty$ otherwise.
- $\gamma_{i,k}^\omega = 1$, $1 \leq i \leq D$, $1 \leq k \leq K$, $1 \leq \omega \leq W$, if wavelength λ_ω is a path-free wavelength along the k^{th} alternate path $P_{i,k}$, connecting the source to the destination node of p_i (corresponds to $C_{i,k}^\omega < +\infty$). $\gamma_{i,k}^\omega = 0$ otherwise (corresponds to $C_{i,k}^\omega = +\infty$).
- $\sigma_{i,k} = \sum_{\omega=1}^W \gamma_{i,k}^\omega$, $1 \leq i \leq D$, $1 \leq k \leq K$, is the number of path-free wavelengths along $P_{i,k}$.
- $\mathbf{A} = (a_{pi})$ is a binary $P \times D$ matrix in which $a_{pi} = 1$ if the p -th path joins the PLD p_i and 0 otherwise;
- $\mathbf{B} = (b_{pj})$ is a binary $P \times L$ matrix in which $b_{pj} = 1$ if the link j belongs to the path p , and 0 otherwise.

The variables

- $\varphi = (\varphi_i)$, $i \in \{1, \dots, D\}$ is a line-vector in which φ_i denotes the number of connections established for the PLD p_i ;
- $\mathbf{C} = (c_{pw}) : P \times W$ is the route and wavelength assignment matrix, in which $c_{pw} = 1$ if a connection has been established using the path p and the wavelength w , 0 otherwise.

6.3.2 Sequential RWA (seqRWA)

The seqRWA algorithm considers the connection requests in an arbitrary order. On each shortest path, able to support the current connection request, we look for as many path-free wavelengths as the number of requested lightpaths. In the case where no enough path-free wavelengths are available, some lightpath demands are rejected. If the number of available wavelengths on a path is higher than the number of request lightpaths, wavelengths are assigned according to a standard first-fit scheme [82]. The assigned wavelengths are reserved on all the links of the path and become then unavailable for any other paths sharing a link with this path. The pseudo code of seqRWA is presented in 6.1.

Synopsis 6.1 Pseudo-code of the sequential RWA algorithm**Input:** ρ, D, R_i, W **Output:** Rejected PLDs(* Sequentially route the PLDs set according to ρ and compute the number of rejected PLDs *)

1 rejectedPLDs := 0

2

for $i := 1$ to D do2.1 Find the corresponding PLD $p_i, 1 \leq i \leq D$ (* Consider in turn the \mathcal{K} -alternate shortest paths associated to PLD p_i *)2.2 $k := 1$

2.3 FLAG := 0

2.4

while ($k \leq \mathcal{K}$) and (FLAG = 0) do

2.4.1

for $\omega := 1$ to W do2.4.1.1 Compute $\gamma_{i,k}^\omega$

endfor

2.4.2

if $\sigma_{i,k} \geq \pi_i$ then

2.4.2.1 FLAG := 1

endif

2.4.3 $k := k+1$

endwhile

2.5

if (FLAG = 0) then

(* The PLD cannot be set up. There are not enough path-free wavelengths on any of the considered shortest paths associated to PLD p_i *)

2.5.1 rejectedPLDs := rejectedPLDs+1

else

(* The PLD is set up. Instantiate the lightpaths. Update paths' cost. In the case when $\sigma_{i,k} > \pi_i$, the wavelengths are selected according to a First-Fit scheme *)2.5.2 $\omega := 1$ 2.5.3 $p := 1$

2.5.4

while ($\omega \leq W$) and ($p \leq \pi_i$) do

2.5.4.1

if $C_{i,k}^\omega \leq +\infty$ then2.5.4.2 $C_{i,k-1}^\omega := +\infty$ 2.5.4.3 $p := p + 1$

endif

2.5.5 $\omega := \omega + 1$

endwhile

endif

endfor

End.

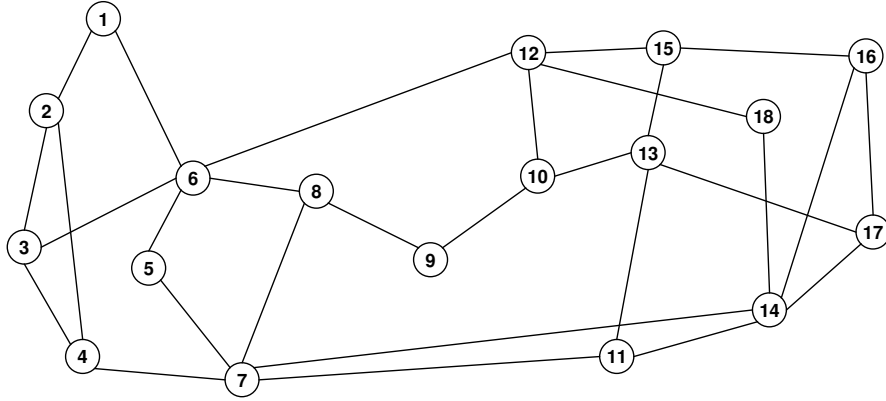


Figure 6.2: The American NSF backbone network (NSFNet) topology.

6.3.3 Random Search Based RWA (RS-based RWA)

We notice that the solution given by seqRWA highly depends on the ordering in which the lightpath demands are routed. The objective of the random search technique is to find a solution that minimizes the number of rejected demands among numerous solutions obtained by the seqRWA algorithm. Let Ω be the set of $D!$ possible permutations of the set $\{1, 2, \dots, D\}$, each permutation, denoted ρ_D^r , $1 \leq r \leq m$ and $m \leq D!$, indicates an ordering of the lightpath demands to be routed. Let Ω' be a subset of Ω containing the permutations already investigated. The RS-based RWA algorithm is carried out as follows.

1. Select randomly an initial solution $\rho_D^1 \in \Omega$; $\Omega' := \{\rho_D^1\}$.
2. Repeat m times (for $r = 1 \rightarrow m$):
 - (a) select randomly $\rho_D^r \in \{\Omega \setminus \Omega'\}$;
 - (b) $\Omega' := \Omega' \cup \{\rho_D^r\}$;
 - (c) $C_{\rho_D^r}$ is the number of rejected PLDs inherent to ρ_D^r ;
3. Select in Ω' the vector $\rho_D^{r_0}$, $1 \leq r_0 \leq m$ that enables to minimize the number of rejected lightpath demands. If two or more vectors in Ω' give the same minimum number of rejected PLDs, one selects the solution that minimizes the number of used WDM channels.

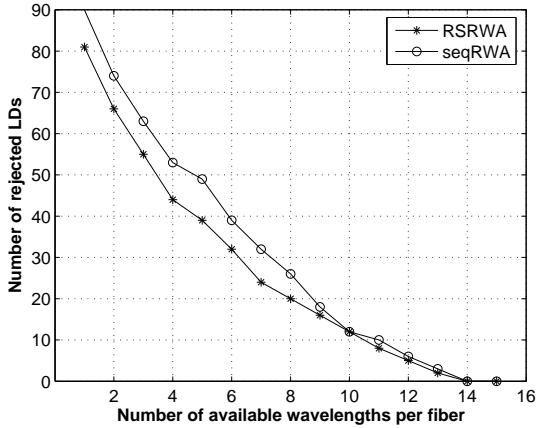


Figure 6.3: Number of rejected demands.

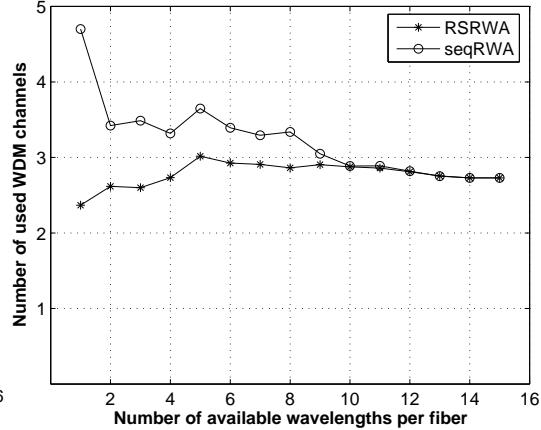


Figure 6.4: Used WDM channels per demand.

6.3.4 seqRWA versus RS-based RWA

Numerical simulations have been done in order to show the interest of using the RS-based RWA algorithm instead of the seqRWA algorithm. In these simulations, we considered the 18-node NSFNet network, depicted in Figure 6.2, and ten traffic matrices of 100 lightpath demands. These matrices are generated randomly according to a uniform distribution.

In Figure 6.3, we plotted the number of rejected demands obtained by both seqRWA and RS-based RWA algorithms for different values of W . From the figure, we notice that the RS-based RWA rejects less demands than the seqRWA. This benefit can reach an order of 20%. Indeed, for $W = 5$, seqRWA throws back 50 demands, while 40 demands are rejected by RS-based RWA. For large values of W , seqRWA and RS-based RWA naturally converge towards the same values.

In Figure 6.4, we plotted the number of consumed WDM channels considering different values of W . Here, let us recall that the number of WDM optical channels consumed by a PLD corresponds to the number of hops followed by the PLD. From Figure 6.4, we notice that RS-based RWA enables shorter paths (in the number of hops) than seqRWA. For instance, when $W = 2$, the average lightpath length is 2.7 hops using RS-based RWA against 3.5 hops using seqRWA. Again, one observes that the behavior of the two algorithms converge for large values of W . Actually, in the presence of sufficient number of wavelengths, demands can be routed on shorter lightpaths since the probability to find a free wavelength on these lightpaths becomes important. Thus, the ordering of demands routing has no more a major impact.

6.3.5 RS-based RWA versus ILP Formulation

The problem of static routing and wavelength assignment can be also formulated as an integer linear program (ILP) ([1], [52]). According to notations defined in Section 6.3.1, the problem can be formulated as follows.

$$\text{Maximize } \sum_{i=1}^D \varphi_i \quad (6.1)$$

subject to:

$$C^T B \leq \mathbb{1}_{W \times L} \quad (6.2)$$

$$\varphi = \mathbb{1}_W C^T A \quad (6.3)$$

$$\varphi_i \leq \pi_i, i \in \{1, 2, \dots, D\} \quad (6.4)$$

$$\varphi_i \in \mathbb{N}, i \in \{1, 2, \dots, D\} \quad (6.5)$$

$$c_{ij} \in \{0, 1\}, i \in \{1, 2, \dots, P\}, j \in \{1, 2, \dots, W\} \quad (6.6)$$

where $\mathbb{1}_{W \times L}$ (resp. $\mathbb{1}_W$) is the $W \times L$ (resp. $1 \times W$) matrix in which all the elements are 1. Equation 6.2 specifies that a wavelength can be used at most once on a given link. Equation 6.3 defines φ according to the route and wavelength assignment matrix C . Equation 6.4 ensures that the number of established connections is lower than the number of requested connections. Equations 6.5 and 6.6 correspond to domain constraints.

Actually, the resolution of the exact model may be untractable for large size instances. In order to assess the efficiency of the proposed RS-based algorithm, this latter has been applied on several problem instances. The obtained results have been compared to those provided by the exact model (the optimal ones)¹. This study has proved that the RS-based algorithm is efficient to solve the routing and wavelength assignment problem especially when large number of wavelengths are available per fiber-link. Indeed, it gives near optimal solutions in short time. It is interesting to use this approximative method if the number of source-destination pairs is large, since, in this case, the exact model fails to find a solution in reasonable time.

¹This comparison has been done in collaboration with Lucile Belgacem [10].

6.4 Regenerator Placement

Once the RWA problem has been solved, the quality of transmission of all admissible lightpaths must be tested. Our first approach for regenerator placement, also called sLERP for simple LERP, was inspired from the trace-back regenerator allocation strategy proposed in [8].

6.4.1 Simple Lightpath Establishment and Regenerator Placement

The Q factor value associated to each established lightpath is computed off-line using BER-Predictor. The quality of transmission evaluation treats sequentially the admissible lightpaths composed of at least two hops. Single hop lightpaths are directly considered as satisfying the quality of transmission constraint. Let us index from 1 to n the nodes along a lightpath made of $(n - 1)$ successive hops, nodes 1 and n corresponding to the source and to the destination nodes respectively. We test the quality of transmission at each of the $(n - 1)$ intermediate nodes along such a lightpath, excepted at node 2. If the evaluated BER at node i is lower than BER_{th} , then a regenerator has to be placed at node $i - 1$, else, the quality of transmission is evaluated at node $(i + 1)$. In case of non-admissible quality at node i , a new lightpath originated at node $(i - 1)$ and ended at node n is considered. By convention, this new lightpath uses the same route and the same wavelength as the initial lightpath from 1 to n . We then investigate the signal quality along this new lightpath. Again, if the evaluated BER at an intermediate node j , with $j > i$, along this new lightpath is lower than BER_{th} , then a second regenerator has to be placed at the preceding node. Such a process is repeated recursively until the destination n can be reached with an acceptable BER.

In summary, for any admissible lightpath, the sLERP tool enables to place as many regenerators as necessary in order to provide an acceptable BER at destination. The route and the wavelength assignment obtained after the RWA phase for an admissible lightpath remain unchanged after a regenerator placement.

6.4.2 Lightpath Establishment and Regenerator Placement

LERP is an improved version of sLERP aiming at optimizing the number of required regenerators and at maximizing the amount of admissible lightpaths. Figure 6.5 illustrates the block diagram of the LERP tool. The LERP tool operates in three

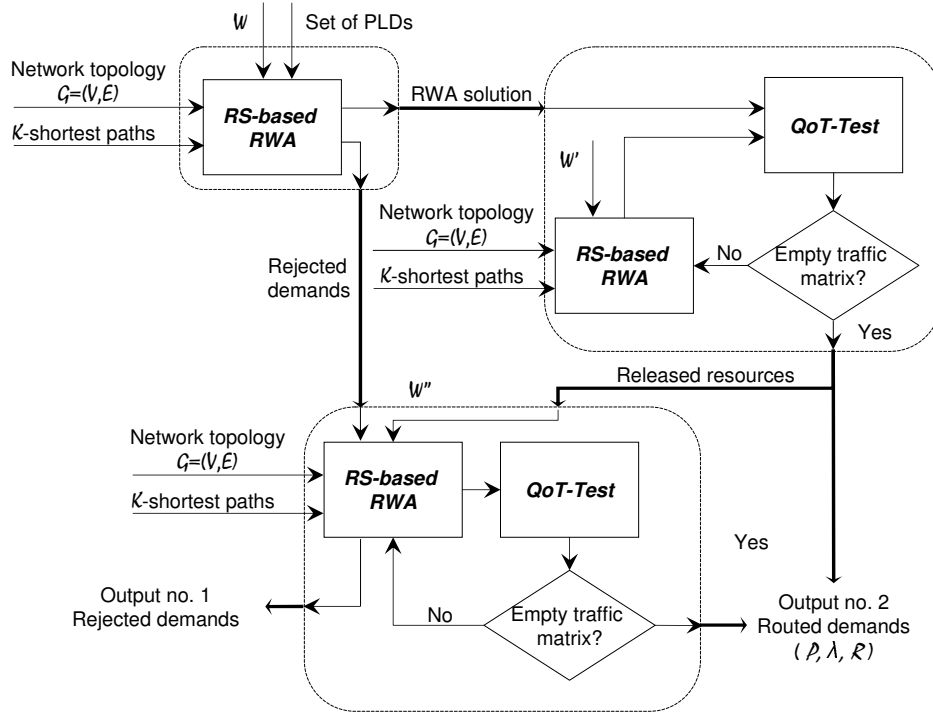


Figure 6.5: Synopsis of LERP.

successive steps corresponding to the three boxes represented in dotted line on the figure.

1. *First step:*

In a first step, an RS-based RWA scheme (see the upper left side of Figure 6.5) enables to determine a first set of admissible lightpaths². The list of rejected lightpath demands because of lack of network resources obtained after this first step is stored in order to be reconsidered during the last step of the LERP tool.

2. *Second step:*

The main difference between LERP and sLERP consists in using a more sophisticated approach for regenerator placement. This approach called QoT-Test tries to optimize regenerator placement by reconsidering the route and the wavelength of a lightpath in case of regenerator placement. The aim of the second step of LERP is to determine a list of admissible and acceptable lightpaths³. Let us index from 1 to n the nodes along a lightpath made of

²In the following, we use the adjective "admissible" when a lightpath may benefit of the same wavelength along its route.

³In the following, we use the adjective "acceptable" when an admissible lightpath is also feasible

$(n - 1)$ successive hops. For each admissible lightpath between s and d , we thus investigate the signal quality, hop by hop starting from the third node of the path (similarly to sLERP, we assume that QoT is systematically admissible after a single hop). The QoT-Test module evaluates the feasibility of each admissible lightpath in considering sequentially these lightpaths in the same order as they are provided by the RS-based RWA initial module (upper left side of Figure 6.5). For each admissible lightpath, as soon as a regenerator is required, we consider a residual lightpath in charge of linking the regeneration site to the destination. In general, once all the admissible lightpaths have been tested, some of them are acceptable end-to-end while some others need a regeneration site. A new traffic matrix made of the list of the residual lightpaths is then considered. This new matrix is used as a new input of a second RS-based RWA module (see upper right side of Figure 6.5). In other terms, LERP reconsiders the route and the wavelength to be assigned to a residual lightpath, whereas sLERP assumes that a residual lightpath reuse the same route and the same wavelength as its associated initial lightpath. It has to be noted that the number of available wavelengths per fiber link used as an input of this second RS-based RWA module is not the same as the one used as an input of the first RS-based RWA module. Indeed, we have to subtract for each fiber link from W the number of consumed optical channels by the acceptable lightpaths. Once the residual lightpaths have been processed by the second RS-based RWA module, again, the feasibility of this second list of admissible lightpaths is investigated by means of the QoT-Test tool. From this second RWA, a second list of residual lightpaths may be established. The same process is repeated iteratively until all the residual lightpaths become acceptable. It is important to note that, unlike the first RS-based RWA module, the second RS-based RWA module does not reject any traffic demand. We refer to W' as the new network capacity during this second step of LERP. Strictly speaking, the value of W' is updated at each iteration of the loop represented in this second box of LERP.

3. *Third step:*

In this last step, we reconsider the list of the rejected demands obtained at the end of the first step. We try then to reroute these demands on the same

in terms of QoT.

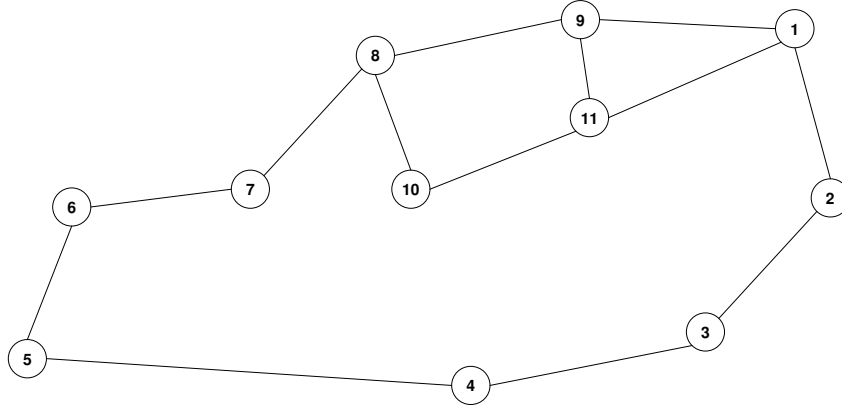


Figure 6.6: 11-node network topology.

topology by means of a third RS-based RWA module. Similarly to the second RS-based RWA module, this third RS-based RWA module uses the same network topology but not the same network resources as the first RS-based RWA module. In other terms, the number of available wavelengths per fiber link is given by W to which we subtract the number of used wavelengths at the end of the second step. Available resources are referred in this step to W'' .

At the end of the three steps of the LERP tool, we obtain the list of admissible and acceptable traffic demands. For each traffic demand, we have the list of the successive lightpaths that are used to join the source s to the destination d via a list of regeneration sites. For each lightpath, LERP provides the physical route and the assigned wavelength. It is important to note that step 2 enables to release network resources since the wavelength continuity constraint is relaxed as soon as we use a regenerator.

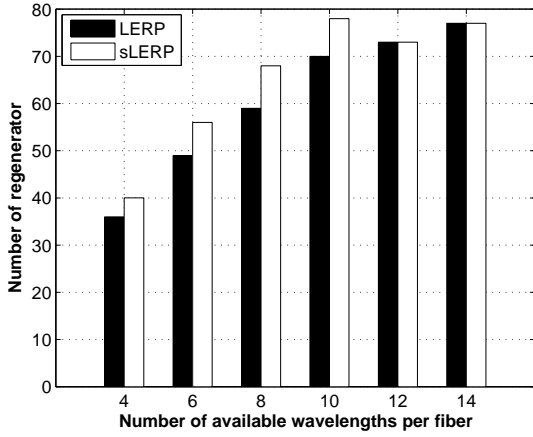
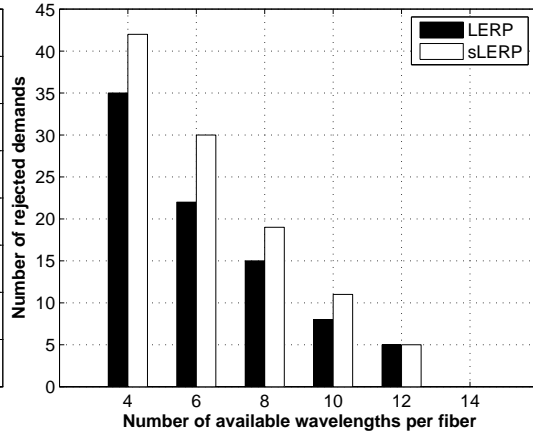
6.4.3 Illustrative Example

Let us consider the 11-node network topology extracted from the NSFNet (Figure 6.6), and the set of lightpath demands given in Table 6.1. We assume that 2 wavelengths are available by fiber-links ($W = 2$).

Let us recall that a path $P_{i,k}$ refers to the k^{th} shortest path associated to the i^{th} lightpath demand. In this example, we assume $\mathcal{K} = 2$. $P_{i,k}$, $1 \leq i \leq 9$ and $1 \leq k \leq 2$, computed according to the Epstein's algorithm, are given in Table 6.1. The result of step 1 gives the list of admissible lightpaths $\{P_{1,1}, P_{2,1}, P_{3,2}, P_{4,2}, P_{5,1}, P_{7,1}, P_{8,1}\}$ and the list of rejected lightpath demands $\{p_6, p_9\}$.

Table 6.1: The set of PLDs to be set up

p_i	s_i	d_i	$P_{i,1}$	$P_{i,2}$
1	2	8	$P_{1,1} = 2 - 1 - 9 - 8$	$P_{1,2} = 2 - 1 - 11 - 9 - 8$
2	9	3	$P_{2,1} = 9 - 1 - 2 - 3$	$P_{2,2} = 9 - 11 - 1 - 2 - 3$
3	8	4	$P_{3,1} = 8 - 9 - 1 - 2 - 3 - 4$	$P_{3,2} = 8 - 7 - 6 - 5 - 4$
4	1	5	$P_{4,1} = 1 - 2 - 3 - 4 - 5$	$P_{4,2} = 1 - 9 - 8 - 7 - 6 - 5$
5	8	2	$P_{5,1} = 8 - 9 - 1 - 2$	$P_{5,2} = 8 - 9 - 11 - 1 - 2$
6	9	5	$P_{6,1} = 9 - 8 - 7 - 6 - 5$	$P_{6,2} = 9 - 11 - 10 - 8 - 7 - 6 - 5$
7	5	2	$P_{7,1} = 5 - 4 - 3 - 2$	$P_{7,2} = 5 - 6 - 7 - 8 - 9 - 1 - 2$
8	3	6	$P_{8,1} = 3 - 4 - 5 - 6$	$P_{8,2} = 3 - 2 - 1 - 9 - 8 - 7 - 6$
9	4	1	$P_{9,1} = 4 - 3 - 2 - 1$	$P_{9,2} = 4 - 5 - 6 - 7 - 8 - 9 - 1$

**Figure 6.7:** Number of required regenerators.**Figure 6.8:** Number of rejected demands.

At step 2, we investigate the feasibility of admissible lightpaths. In this example, 3 regenerators are required at the end of step 2: one at node 5 for $P_{3,2}$, one at node 7 for $P_{4,2}$, and one at node 4 for $P_{7,1}$. At the end of step 3, lightpath demands $\{p_6, p_9\}$ are reconsidered with updated network resources (W''). It appears that demand p_9 may be accepted on its first shortest path $P_{9,1}$ because the regeneration of $P_{7,1}$ at node 4 has relaxed the wavelength continuity constraint.

6.4.4 sLERP versus LERP

Numerical simulations have been done in order to outline the benefit of LERP against sLERP. Once again, we consider the NSFNet network shown in Figure 6.2 and ten traffic matrices of 100 demands generated randomly according to a uniform distri-

bution. First, we vary the value of W and we compute the number of regenerators to be placed in the network using both sLERP and LERP algorithms.

In Figure 6.7, we plot the average number of required regenerators versus W for both LERP and sLERP. We observe that LERP requires a lower amount of regenerators than sLERP up to $W = 10$. For larger values of W , LERP and sLERP tends to the same performance. Figure 6.8 depicts the evolution of the number of rejected lightpath demands versus W for both LERP and sLERP. For a given value of W , sLERP induces a larger amount of rejected demands than LERP. Again, for large values of W , both algorithms tends to the same results.

Indeed, the segmentation of lightpaths and the new routing computed for segments of the lightpaths requiring regeneration, allow to forward demands on shorter lightpaths. This implies that there is less chance that the quality of transmission degrades too much, and consequently, the number of regenerators to place is smaller. In fact, some rejected demands due to lack of wavelengths, can be routed after the regenerator placement phase. When placing regenerators, the wavelength continuity constraint is relaxed. Using the LERP algorithm, we can relax this constraint thanks to the rerouting phase, where connections requiring regeneration can change wavelength. However, in sLERP, the lightpaths established by the RS-based RWA do not change, and no wavelength conversion is performed at nodes presenting regenerators. For the same reason as before, the performance of both algorithms becomes comparable for higher values of W .

From both figures, one can notice that for a given value of W the ratio of the number of required regenerators to the number of established lightpaths is systematically lower for LERP than for sLERP. For instance, when $W = 4$, this ratio is of about 53% and 68% for LERP and sLERP, respectively. In other terms, the efficiency of regeneration is greater under LERP than under sLERP.

6.5 Impact of Dynamic Gain Equalization

As it has been shown in Chapter 4, using dynamic gain equalization can significantly impact the network performance in terms of quality of transmission. In this section, we investigate the impact of employing an inline gain equalization scheme on the number of required regenerators in the network [91]. We want to assess the economical benefit of using equalization as a complement to regeneration. We will compare the number of required regenerators in the considered optical network with

Table 6.2: A set of three traffic demands

<i>Demand</i> (p_i)	<i>Source</i> (s_i)	<i>Destination</i> (d_i)	<i>Route</i> (P_i)
p_1	2	4	2 – 3 – 4
p_2	1	6	1 – 2 – 3 – 6
p_3	3	7	3 – 4 – 7

Table 6.3: \mathcal{Q} factor value w.r.t. the used wavelength

<i>Demand</i> (p_i)	<i>Route</i> (P_i)	λ (nm)	\mathcal{Q}_{WE} (dB)	\mathcal{Q}_E (dB)
p_1	P_1	1561.41	11.42	14.17
		1553.32	14.95	17.26
		1545.32	15.77	17.93
		1540.55	17.49	18.09
p_2	P_2	1561.41	5.71	10.03
		1553.32	11.49	13.92
		1545.32	12.19	14.36
		1540.55	13.19	13.71
p_3	P_3	1561.41	-0.24	5.70
		1553.32	6.92	13.50
		1545.32	9.39	14.56
		1540.55	12.69	13.83

and without inline equalization and try to evaluate the cost ratio between the two solutions.

6.5.1 Numerical example

A numerical example may clarify how the LERP algorithm works with and without employing inline gain equalizers. Considering the NSFNet network (see Figure 6.2) and the set of demands described in Table 6.2, we assume that four wavelengths are available on each fiber-link, namely $\lambda_1 = 1561.41$ nm, $\lambda_2 = 1553.32$ nm, $\lambda_3 = 1545.32$ nm, $\lambda_4 = 1540.55$ nm. For each route P_i , we compute the \mathcal{Q} factor corresponding to each wavelength with (\mathcal{Q}_E) and without (\mathcal{Q}_{WE}) equalization as shown in Table 6.3.

In Figure 6.9, we present solutions provided by LERP with and without inline gain equalization. In Figure 6.9(a), black disks labeled with an “R” stand for required regenerators at intermediate nodes. The solution computed by LERP requires two

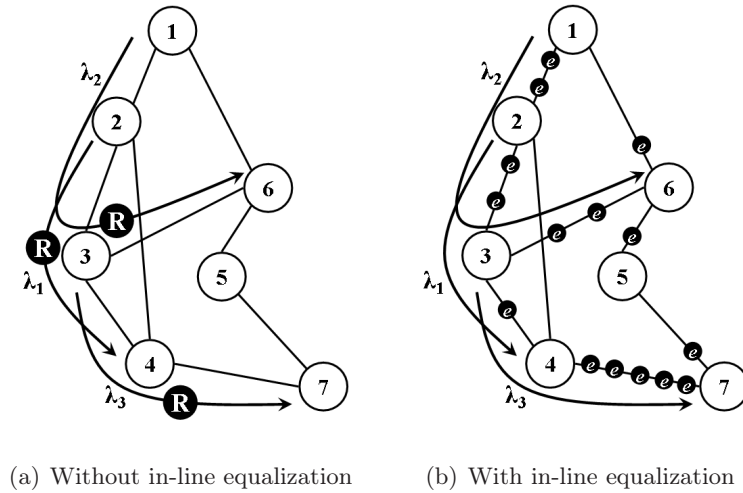


Figure 6.9: Solutions computed without/with in-line gain equalization.

regenerators at node 3 (one for the demand routed on λ_1 and one for the demand routed on λ_2) and one regenerator at node 4 (for the demand routed on λ_3). In Figure 6.9(b), black disks labeled with an “e” stand for inline gain equalizers considering an equalization scheme that deploys an equalizers every 5 fiber-spans. One can notice that once the equalization scheme has been set, the number of equalizers is set once for all in the network. Figure 6.9(b) shows, for example, that the equalization scheme requires 5 equalizers between node 4 and node 7. The BER threshold is assumed to be 10^{-5} which corresponds to a Q factor value of 12.6 dB.

From both Figures 6.9(a) and 6.9(b), one notices that without inline gain equalization, the obtained solution requires 3 regenerators whereas none regenerator is required when using an inline gain equalization. Inline equalization may then highly reduce the number of regenerators required to ensure quality of transmission. In the following subsection, we will investigate the economical impact of a tradeoff between regeneration and equalization.

6.5.2 Numerical Simulations

Several numerical simulations have been carried out to show the effect of employing an inline gain equalization scheme. These simulations have been achieved considering the NSFNet network (see Figure 6.2). The network is assumed to be deployed using standard single-mode fibers (SMF) covering the C-band with 100 GHz spacing (providing 40 wavelengths on each fiber-link). Double-stage EDFA amplifiers

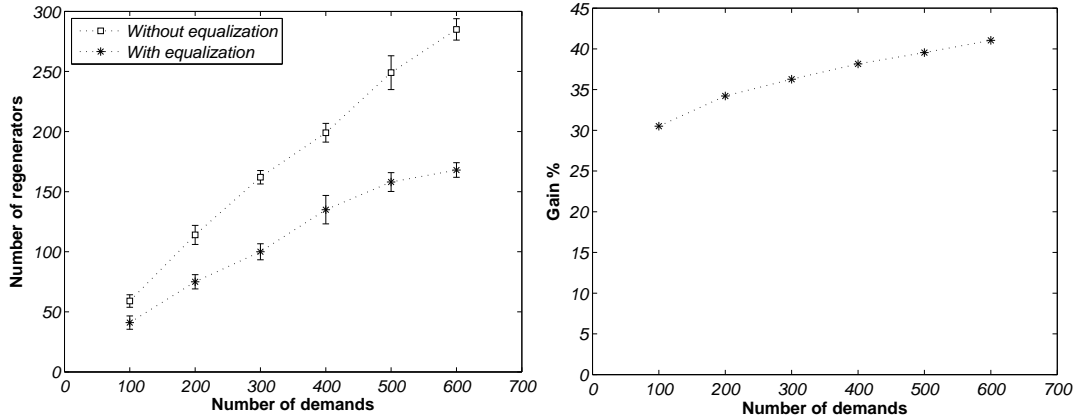


Figure 6.10: Number of regenerators w.r.t. traffic load without/with equalization. **Figure 6.11:** Gain in the number of regenerators w.r.t. traffic load.

are deployed every 80 km. Gain equalizers are deployed every 5 spans, i.e. every 400 km. As already mentioned, the number of equalizers installed in the network only depends on the network topology and on the equalization scheme. Hence, this number (here 122 equalizers) is set once for all.

Simulation results have been obtained considering permanent traffic matrices generated randomly according to a uniform distribution. In our simulation scenarios, we consider various traffic loads where matrices of 100 to 600 demands are used. For each traffic load, we deal with 10 different matrices. Hence, each result presented in this section is the mean value of the results gathered 10 different simulations.

First, we are interested in the impact of employing an inline gain equalization scheme on the number of required regenerators. Figure 6.10 shows the mean values of the number of regenerators required to establish lightpaths for various traffic loads with and without equalization. Vertical lines refer to the confidence intervals, i.e. mean value \pm standard deviation. Regenerators are placed considering a typical BER threshold value of 10^{-5} . We assume that the system uses forward error correction (FEC), therefore the system can achieve an end-to-end BER of about 10^{-20} whilst the effective BER is of about 10^{-5} . Figure 6.10 shows that inline gain equalization becomes more interesting for heavy traffic loads⁴. Using equalization leads to a gain of about 30% in the number of required regenerators for low traffic loads whereas this gain is of about 40% for heavy traffic loads (Figure 6.11). This can be explained by the fact that an equalizer is a mutualized equipment able to serve

⁴We have voluntarily limited the number of submitted demands to 600. This value corresponds to upper limit over which demands may be rejected.

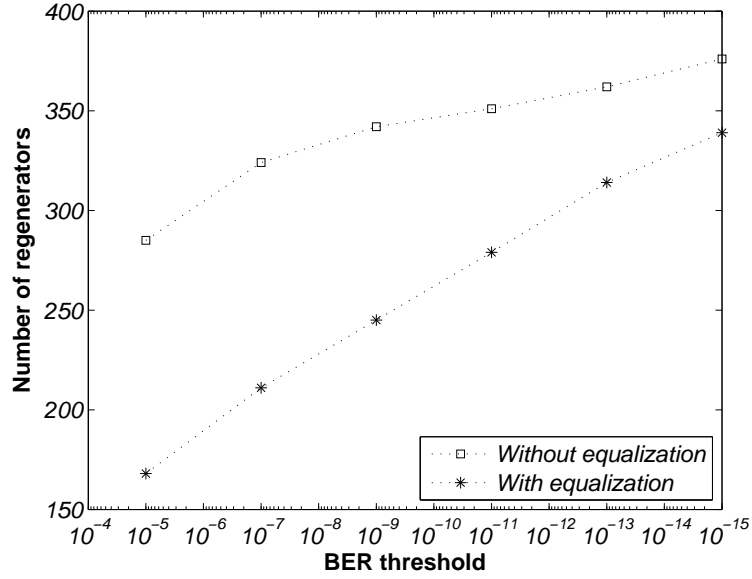


Figure 6.12: Number of regenerators w.r.t. BER-threshold without/with equalization.

multiple wavelengths simultaneously. At the opposite, a regenerator is a dedicated equipment serving a single optical channel.

Figure 6.12 shows the mean values of the number of regenerators required to satisfy 600 demands for various values of the BER threshold. As expected, in both cases (with/without gain equalization), the number of regenerators increases as the quality of transmission requirement increases. We see that the gain in the number of regenerators decreases with BER threshold. For instance, we see that a gain of about 10% compared to 40% is obtained for BER threshold of 10^{-15} and 10^{-5} , respectively.

In Figure 6.13, we observe the gain in the network cost offered by inline gain equalizers. Let us first define some variables and parameters:

- C_E is the cost of a gain equalizer;
- C_R is the cost of a regenerator;
- α is the ratio of an equalizer's cost to a regenerator's cost, and as such $\alpha = C_E/C_R$;
- N_E is the number of equalizers deployed in the networks (for the considered example network and equalization scheme $N_E = 122$);
- N_R is the number of regenerators required when no equalizers are used;

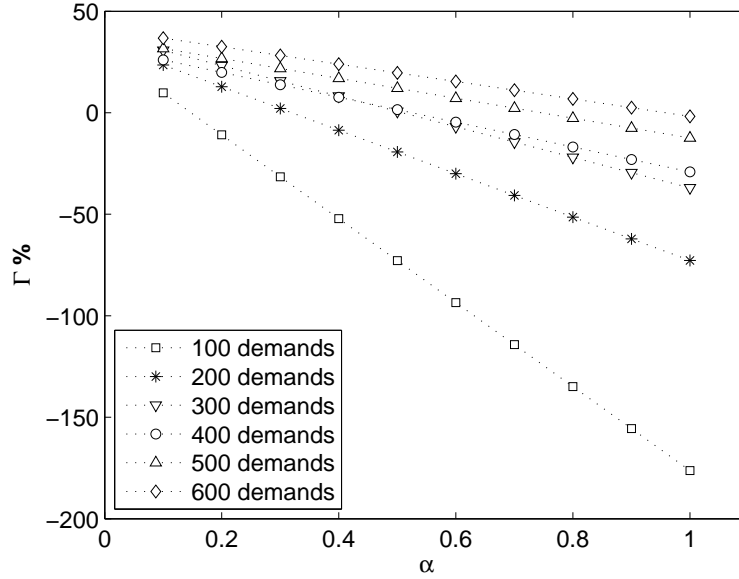


Figure 6.13: Network cost gain w.r.t. device cost ratio (equalizer's cost/regenerator's cost).

- N_{RE} is the number of regenerators that are required when using equalizers.

We define Γ as the gain in the network cost achieved by using inline gain equalizers. Therefore, Γ can be defined as:

$$\Gamma = \frac{C_R N_R - C_R N_{RE} - C_E N_E}{C_R N_R} \quad (6.7)$$

Thus,

$$\Gamma = 1 - \frac{N_{RE}}{N_R} - \alpha \frac{N_E}{N_R} \quad (6.8)$$

Figure 6.13 shows the value of the gain Γ as a function of α for various traffic loads. One can notice that for heavy traffic loads and for α of about 0.1, the use of inline gain equalizers can achieve a benefit of about 37% in the network cost whereas the benefit is null for $\alpha = 1$. It is understandable that heavy traffic loads lead to better benefits when using inline equalization. Indeed, again, an equalizer improves the full bunch of wavelengths. The higher the traffic load, the higher the mutualization benefit of the equalizers (the more the equalizer is profitable).

6.6 Impairment-Aware Wavelength Assignment Strategies

In the previous section, we have seen that dynamic gain equalization provides a better homogeneity in the BER distribution over the wavelengths on a given path. In other terms, dynamic gain equalization facilitates wavelength assignment for LERP. Motivated by the simulation results presented in Section 6.5.2, we propose new impairment-aware wavelength assignment strategies, namely min-BER-Fit (MBF) and best-BER-Fit (BBF) [92]. In the following, we describe both the MBF and BBF strategies and we recall the standard FF strategy which will serve as a basis for comparison.

1. *First-Fit (FF) Strategy:*

All the available wavelengths are indexed according to their increasing values in nanometer. The first available wavelength with the lowest index is selected.

2. *Min-BER-Fit (MBF) Strategy:*

For each path, all available wavelengths are sorted according to their Q factor value. The wavelength with the highest Q factor is selected from the set of available wavelengths.

3. *Best-BER-Fit (BBF) Strategy:*

For each path, all available wavelengths are sorted according to their Q factor value. The first wavelength with the nearest admissible Q factor value to the threshold is selected. This approach enables to remain available the wavelengths with higher Q factor values for longer lightpaths.

6.6.1 Numerical example

We reconsider Example 6.5.1 in order to clarify how these different wavelength assignment strategies work. Considering the 18-node north American backbone network (see Figure 6.2) and the set of demands described in Table 6.2, we assume that four wavelengths are available on each fiber-link, namely $\lambda_1 = 1561.41$ nm, $\lambda_2 = 1553.32$ nm, $\lambda_3 = 1545.32$ nm, $\lambda_4 = 1540.55$ nm. For each route P_i , we compute the Q factor corresponding to each wavelength as shown in Table 6.3.

Solutions provided by the three strategies are given in Figure 6.14. By using the FF strategy, 3 regenerators are needed, two of them being placed at node 3 (Figure

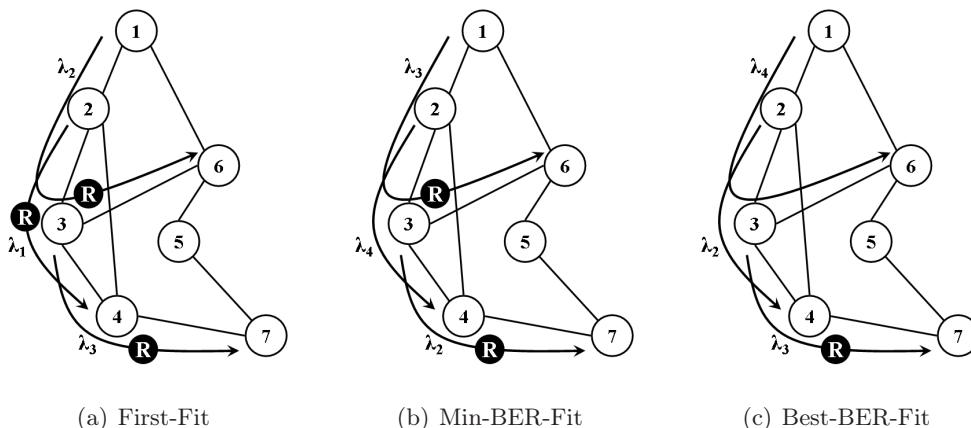


Figure 6.14: Solutions to Example 6.5.1 computed by the three WA strategies.

6.14(a)). MBF uses 2 regenerators whereas BBF only uses one regenerator (Figures 6.14(b) and 6.14(c) respectively). This result is due to the fact that BBF uses λ_2 first, thus allowing the use of λ_4 for the longest route.

6.6.2 Numerical Simulations

Several numerical simulations have been carried out in order to assess the improvements provided by our new wavelength assignment strategies. The simulations are carried out considering the NSFNet network (see Figure 6.2). The network is assumed to be deployed using standard single-mode fibers (SMF) covering the C-band with a spacing 100 GHz (providing 40 wavelengths on each fiber-link). Double-stage EDFA amplifiers are deployed every 80 km. Gain equalizers are only deployed at the network nodes.

Simulation results have been obtained considering permanent traffic matrices generated randomly according to a uniform distribution. In our simulation scenarios, we consider various traffic loads where matrices of 100 to 700 demands are used. For each traffic load, we deal with 10 different matrices. Hence, each result presented in the following is the mean value of 10 experiments.

First, we compare the wavelength assignment strategies in terms of number of required regenerators. Figure 6.15 shows the mean values of the number of regenerators required to establish lightpaths for various traffic loads. Vertical lines refer to the confidence intervals, i.e. mean value \pm standard deviation. Regenerators are placed considering a typical BER threshold value of 10^{-5} . We assume that the sys-

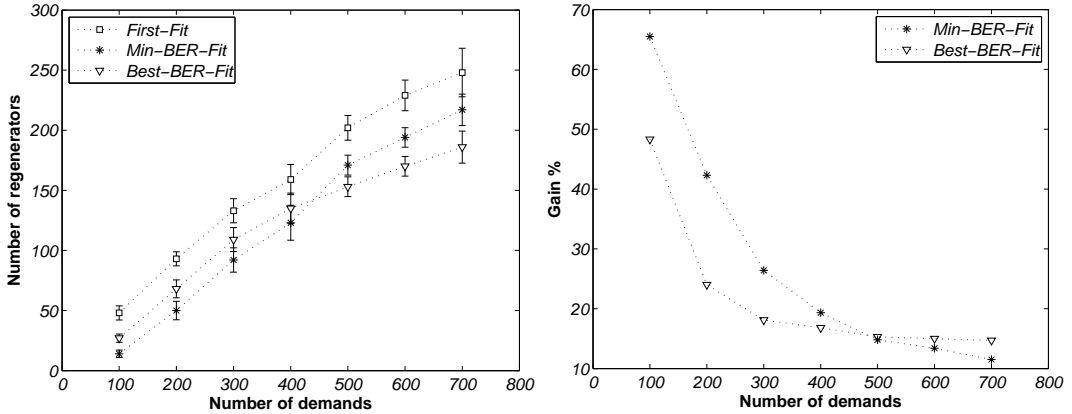


Figure 6.15: Number of regenerators w.r.t. traffic load. **Figure 6.16:** Gain against FF strategy w.r.t. traffic load.

tem uses a forward error correction (FEC) code, therefore the system can achieve an end-to-end BER of about 10^{-20} whilst the effective BER is of approximately 10^{-5} . Figure 6.15 shows that for low traffic loads, Min-BER-Fit is the best strategy whereas Best-BER-Fit is the best one for high traffic loads. As shown in the example of Section 6.6.1, the MBF strategy first consumes the wavelengths achieving the best performance. Such wavelengths are no longer available for the most stringent lightpaths under heavy traffic loads. In any case, both the MBF and BBF strategies always outperform the FF strategy.

In Figure 6.16, we plot the gain in the mean value of the number of regenerators achieved by both the MBF and BBF strategies w.r.t. the First-Fit strategy. We notice an average benefit of 66% and 50% achieved by MBF and BBF respectively for low traffic loads. Nevertheless, for heavy traffic load, BBF provides up to a 15% gain in the number of regenerators whereas MBF only provides a gain of 11.5%.

Figure 6.17 shows the mean values of the number of regenerators required to satisfy 400 demands for various values of the BER threshold and considering the three wavelength assignment strategies. As expected, the number of regenerators increases for all strategies with BER requirement. Once again, we notice that MBF and BBF strategies outperform the FF strategy. Considering a low threshold (below 10^{-6}) the MBF strategy outperforms the BBF strategy which confirms the results shown in Figure 6.15.

In Figure 6.18, we compare the FF, MBF, and BBF strategies in terms of number of required regenerators. In this figure, the simulation scenarios are different from those reported in Figure 6.15. Our motivation is to outline the capacity of a

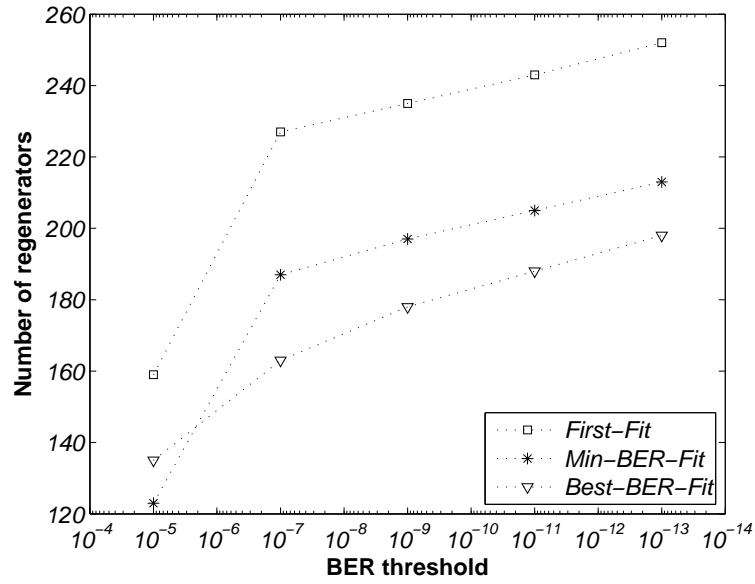


Figure 6.17: Number of regenerators w.r.t. BER_{th} .

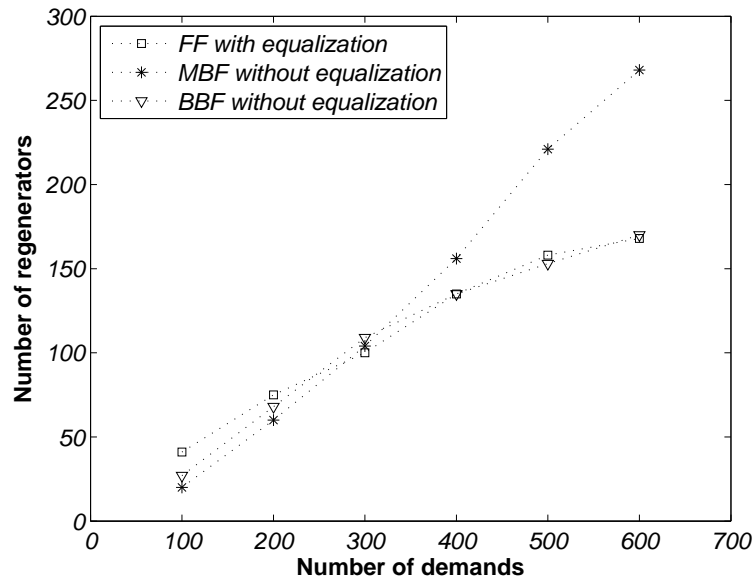


Figure 6.18: Number of regenerators w.r.t. traffic load.

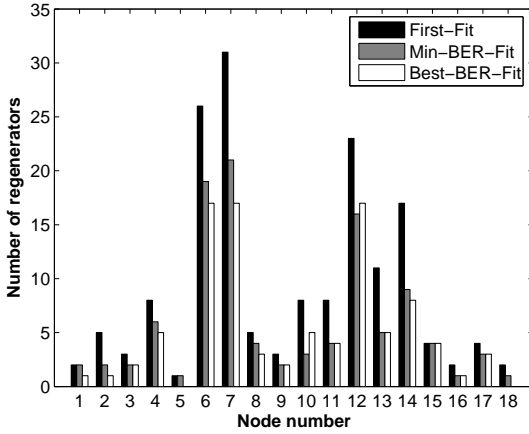


Figure 6.19: Geographical distribution of the regenerators w.r.t. WA strategies.

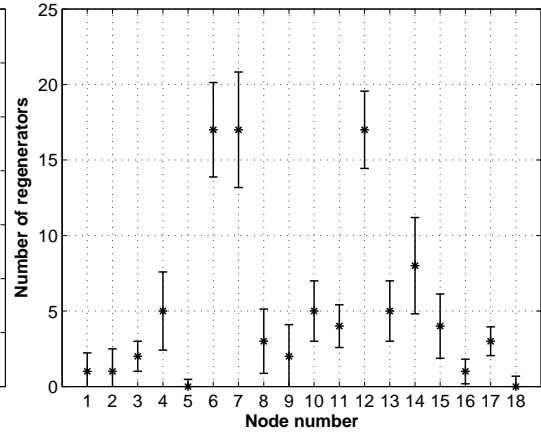


Figure 6.20: Location distribution of regenerators for different traffic matrices.

suitable wavelength assignment strategy to compensate for the absence of inline gain equalization. For that purpose, let us compare the performance of MBF and BBF strategies without inline equalization with the performance of FF strategy with inline equalization. Under low traffic loads, the three approaches drive to comparable results in terms of required regenerators. For higher offered loads (more than 300 demands), one notices that dynamic equalization applied to FF strategy gives roughly the same results as BBF without dynamic equalization. In addition, we observe that the performance of MBF decreases considerably at high loads.

In conclusion, for low traffic loads, for which the deployment of inline equalizers is not profitable (see Figure 6.13), an impairment-aware wavelength assignment strategies may compensate for the absence of gain equalizers.

6.6.3 Aggregated versus Distributed Regenerator Placement

In LERP, we aim to minimize the global amount of regenerators for a given traffic matrix and a given network topology. A carrier may be interested in a tradeoff between minimizing the number of regenerators and minimizing the number of regeneration sites. This observation led us to investigate the potential correlation between network topology and the regenerator placement. Let us consider the NSFNet network (see Figure 6.2) and a traffic load of 400 demands. Ten traffic matrices corresponding to this traffic load are randomly generated according to a uniform distribution. A BER threshold of 10^{-5} is considered assuming FEC.

In Figure 6.19, we depict the geographical distribution of the regenerators' loca-

tions for the three WA strategies proposed in Section 6.6. The histogram plotted in Figure 6.19 corresponds to the average results obtained considering the ten traffic matrices. On one side, we notice that nodes 6 and 7 contain the highest number of regenerators. On the other side, we notice that nodes 6 and 7 are the nodes with the highest physical degree (5). Moreover, the links connecting nodes 6 and 7 to their neighbors have an important length, especially the links $7 - 14$, $7 - 11$ and $6 - 12$. The lightpath using these links via nodes 6 or 7 have a high probability to require regenerators. Voluntarily, we have imposed that two demands linking the same couple source-destination use the same route. By this way, we expect to better outline the impact of wavelength assignment on regenerator placement. The MBF strategy leads to the lowest global number of required regenerators but the BBF strategy leads to a better-balanced regenerator distribution. A balanced distribution is worthwhile considering that in practical node implementations, the number of regenerators is limited (regenerators are often provided in racks).

Actually, other factors, such as traffic distribution, also have an impact on the regenerators' location. In Figure 6.20, we show the geographical distribution of regenerators for 10 different traffic matrices with 400 demands. Actually, we provide the mean values of the number of regenerators at each node as well as the confidence intervals under the BBF strategy. We notice that the traffic distribution fluctuations result in little fluctuations in the regenerators's locations while the shape of the distribution remains the same. Thus, we may suggest that the network topology actually is the key factor explaining the regenerators' locations.

6.7 Summary

This chapter unifies the multiple concepts that have been introduced in the previous chapters of this thesis. Mainly two aspects have been considered, the impact of physical layer impairments on quality of transmission in realistic WDM transmission systems and the optimization techniques on which relies optical network design. In this chapter, we have proposed an original dimensioning tool called LERP, enabling to optimize network resources utilization while satisfying quality of transmission requirements. Compared to other similar studies, LERP is able to minimize the number of required regenerators for a given static matrix and a given network topology. For that purpose, unlike similar tools (like sLERP) that clearly separate the RWA phase from regenerator placement phase, LERP interleaves these two phases itera-

tively. Concerning the RWA strategy, a random search approach has been adopted. We have seen that this approach enables better performance than sequential RWA and provides near optimal solution compared to an ILP formulation. The impact of dynamic inline equalization has been investigated. We have shown that using an inline equalization scheme could reduce significantly the number of required regenerators. The tradeoff between equalization and regeneration has been evaluated for large range of cost ratio between a regenerator and an equalizer. At evidence, the main benefit of equalization is inherent to its mutualization whereas a regenerator is dedicated to a single wavelength. Two innovating wavelength assignment strategies have been compared to the traditional first-fit strategy applied to the LERP algorithm. We can conclude that for low traffic loads, equalization is not cost-effective and can be replaced by a judicious wavelength assignment strategy, namely the BBF strategy. Finally, we have considered the correlation between the physical topology and the regenerator placement. Nodes with the highest physical degree and with the longest average distance from their first neighbors seem to be well suited for an *a priori* regenerator placement.

*"Ye shall know the truth,
and the truth shall make you free."*

– Bible, John 8:32

7 Conclusions and Future Work

7.1 Conclusions

The aim of this thesis was to contribute to the feasibility of translucent optical networks on which will rely next generation carriers' networks. Before this thesis, most of impairment-aware routing and wavelength assignment strategies were characterized by a clear separation between the RWA phase and the quality of transmission evaluation phase. These strategies were considering individually the impact of several physical layer impairments. In this thesis, we have proposed an innovative impairment-aware dimensioning tool, called LERP, that iteratively combines the two phases in order to optimize network resources utilization while minimizing the global amount of required regenerators. LERP is able to evaluate the quality of transmission of a given lightpath by means of a sophisticated tool, called BER-Predictor, that takes into account the simultaneous impact of chromatic dispersion, polarization mode dispersion, nonlinear phase shift, and amplified spontaneous emission.

LERP is based on a random search RWA algorithm combined with a procedure called QoT-Test, in charge of quality of transmission evaluation and regenerator placement. The QoT-Test uses itself the BER-Predictor tool. We have shown through numerous simulations the suitability of LERP to deal with large size and realistic backbone networks. In this matter, we have systematically adopted the well known 18-node north American backbone (NSFNet) since it is considered as a reference model in the community. We have compared, for similar scenarios and network configurations LERP with a more traditional approach referred to as sLERP. Unlike sLERP, LERP reconsider the route and the wavelength assignment after a regener-

ator placement. For instance, assuming four wavelengths per fiber link ($W = 4$), a gain of about 13% can be achieved in the number of required regenerators. In addition, LERP also enables to increase the network resources utilization by achieving a gain of about 12% in the number of admissible lightpaths. We have checked that the larger W , the lower the relative gain in terms of number of required regenerators and in terms of admissible lightpaths.

We have then investigated the benefit of using inline dynamic gain equalization. Considering the NSFNet network with $W = 40$ and operating in the C-band with inter-channel spacing of 100 GHz, dynamic gain equalization leads to a benefit of about 30% in the number of required regenerators under low traffic loads whereas this gain is of about 40% for heavy traffic loads. We have also investigated the cost benefit of a tradeoff between electrical regeneration and dynamic equalization. Simulation results show that dynamic gain equalization is mainly interesting under high offered loads. This result is intuitive since an equalizer is a mutualized equipment able to deal with multiple parallel WDM channels. At the opposite, an electrical regenerator is a dedicated equipment that deals with one optical channel at a time.

The basic version of LERP uses a standard first-fit wavelength assignment strategy. We have proposed two innovative impairment-aware wavelength assignment strategies, namely min-BER-fit (MBF) and best-BER-fit (BBF). In these strategies, for each lightpath, available wavelengths are sorted according to their Q factor value. MBF selects the wavelength with the highest Q factor whereas BBF selects the wavelength with the lowest Q factor above the admissible threshold. Simulation results show that an average benefit of about 60% and about 50% is achieved by MBF and BBF respectively under low traffic loads. Under heavy traffic load, BBF provides up to a 15% gain in the number of regenerators whereas MBF only provides a gain of about 10%. We have outlined that BBF can compensate for the absence of dynamic gain equalization under any traffic load.

The proposed tools in this thesis, LERP and its variants, have potential applications for both network carriers and equipment manufacturers. Indeed, the quality of transmission is evaluated on the basis of realistic characteristics of transmission equipment currently available on the market.

7.2 Perspectives

At the end of Chapter 6, we have briefly discussed the necessary tradeoff for a carrier between aggregated and distributed regenerator placement. We have concluded from a set of random scenarios that a correlation is probably existing between the physical degree of a node and its average distance from its first neighbors, and its potential role of regeneration. In our opinion, such an intuitive conclusion deserves deeper and more rigorous analysis.

One of the originalities of LERP that has not been mentioned in the previous section deals with crosstalk. Indeed, the analytical expression adopted for the \mathcal{Q} factor computation including the impact of nonlinear phase shift, takes into account a worst case scenario relatively to crosstalk. This worst case scenario corresponds to the simultaneous presence of W active optical channels per fiber. We intend to take into account the impact of crosstalk by considering a new wavelength assignment strategy aiming at reducing the intra-channel and inter-channel interference. Preliminary investigations have also been carried out during this thesis to extend LERP to the computation of primary and backup lightpaths [11]. The problem of shared backup in the context of impairment-aware RWA is a complex problem that will need a particular attention.

All these perspectives will be part of a new European project called DICONET wherein I shall be personally involved.

List of Publications

- [1] S. Al Zahr, M. Gagnaire, and N. Puech, Impact of wavelength assignment strategies on hybrid WDM network planning, in *Procs. of DRCN '07*, La Rochelle, France, October 2007. IEEE Communications Society.
- [2] † S. Al Zahr, N. Puech, and M. Gagnaire, Gain equalization versus electrical regeneration tradeoffs in hybrid WDM networks, in *Procs. of ConTEL '07*, Zagreb, Croatia, June 2007. IEEE Communications Society.
- [3] M.-A. Ezzahdi, S. Al Zahr, M. Koubaa, N. Puech, and M. Gagnaire, LERP: a quality of transmission dependent heuristic for routing and wavelength assignment in hybrid WDM optical networks, in *Procs. of ICCCN '06*, Arlington, VA, USA, October 2006. IEEE Communications Society.
- [4] S. Al Zahr, M. Gagnaire, and M.-A. Ezzahdi, Impact of quality of transmission on protection schemes in hybrid WDM optical networks, in *Procs. of EUNICE '06*, Stuttgart, Germany, September 2006. IEEE Communications Society.
- [5] N. Puech, S. Al Zahr, and M. Gagnaire, Wavelegth-dependent quality of transmission in WDM transparent optical networks, in *Procs. of ICT '06*, Funchal, Madeira, Portugal, May 2006. IEEE Communications Society.
- [6] S. Al Zahr, M. Gagnaire, N. Puech, and M. Koubaa, Physical layer impairments in WDM core networks: a comparison between a north-American backbone and a pan-European backbone, in *Procs. of BROADNETS '05*, Boston, MA, USA, October 2005. IEEE Communications Society.

† This paper has received the Best Student Paper Award.

Glossary

SYMBOLS 1-9

2R Re-amplifying, Re-shaping.

3R Re-amplifying, Re-shaping, and Re-timing.

A

ADM Add/Drop Multiplexer.

AOTF Acousto-Optic Tunable Filter.

AR Adaptive Routing.

ASE Amplified Spontaneous Emission.

ATM Asynchronous Transfer Mode.

AWG Arrayed Waveguide Grating.

B

B-OSNR Best Optical Signal to Noise Ratio.

BBF Best-BER-Fit.

BER Bit Error Ratio.

C

- C-FF** Crosstalk-aware First-Fit.
- C-LU** Crosstalk-aware Least-Used wavelength.
- C-MU** Crosstalk-aware Most-Used wavelength.
- C-RP** Crosstalk-aware Random Pick.
- CD** Chromatic Dispersion.
- CNF** Centered Node First.

D

- DBR** Distributed Bragg Reflector.
- DCF** Dispersion Compensating Fiber.
- DCM** Dispersion Compensating Module.
- DFB** Distributed Feed Back.
- DGCD** Differential Group Delay.
- DLE** Daynamic Lightpath Establishment.
- DWDM** Dense Wavelength Division Multiplexing.

E

- EBN** European Backbone Network.
- EDFA** Erbium Doped Fiber Amplifier.
- E/O** Electrical-to-Optical.
- EXC** Electrical Cross-connect.

F

- FAR** Fixed-Alternate Routing.
- FDM** Frequency Division Multiplexing.
- FEC** Forward Error Correction.
- FF** First-Fit.
- FR** Fixed Routing.
- FWM** Four Wave Mixing.

H

- HPA** Half Placement Algorithm.

I

- IABP** Impairment-Aware Best-Path.
- IAFF** Impairment-Aware First-Fit.
- ILP** Integer Linear Program.
- IP** Internet Protocol.
- IRWA** Impairment-aware Routing and Wavelength Assignment.
- ISI** Inter-Symbol Interference.

J

- JWR** Joint Wavelength-Route.

L

- LASER** Light Amplification by Stimulated Emission of Radiation.
- LCR** Least Congested Routing.
- LD** Lightpath Demand.
- LED** Light-Emitting Diodes.

LERP Lightpath Establishment and Regenerator Placement.

LH Long-Haul.

LPA Linear Placement Algorithm.

M

MBF Min-BER-Fit.

MCM Multi-Carrier Modulation.

MCPA Minimal-Cost Placement Algorithm.

MEMS Micro-Electro-Mechanical System.

MLM Multi-Longitudinal Mode.

MMF Multi-Mode Fiber.

MU Most-Used.

N

NDF Nodal Degree First.

NF Noise Figure.

NRZ Non Return to Zero.

NSFNet National Science Foundation Network.

O

OA Optical Amplifier.

OADM Optical Add/Drop Multiplexer.

OBS Optical Burst Switching.

OCS Optical Circuit Switching.

ODFA Optical Doped Fiber Amplifier.

O/E Optical-to-Electrical.

OEO	Optical-to-Electrical-to-Optical.
OPS	Optical Packet Switching.
OSNR	Optical Signal to Noise Ratio.
OTDM	Optical Time Division Multiplexing.
OXC	Optical Cross-connect.
P	
PG	Physical Graph.
ϕ_{NL}	Nonlinear Phase Shift.
PLD	Permanent Lightpath Demand.
PMD	Polarization Mode Dispersion.
PSK	Phase-Shift Keying.
Q	
QoT	Quality of Transmission.
R	
RF	Radio Frequency.
RLD	Random Lightpath Demands.
ROA	Raman Optical Amplifier.
RP	Regenerator Placement.
RPA	Random Placement Algorithm.
RS	Random Search.
RWA	Routing and Wavelength Assignment.
RZ	Return to Zero.

S

SBS Stimulated Brillouin Scattering.

SDH Synchronous Digital Hierarchy.

seqRWA sequential Routing and Wavelength Assignment.

SLA Semiconductor Laser Amplifier.

SLD Scheduled Lightpath Demands.

SLE Static Lightpath Establishment.

sLERP simple Lightpath Establishment and Regenerator Placement.

SLM Single-Longitudinal Mode.

SMF Standard single Mode Fiber.

SONET Synchronous Optical NETwork.

SPM Self-Phase Modulation.

P

SQP Signal Quality Prediction.

S

SRS Stimulated Raman Scattering.

T

TDM Time Division Multiplexing.

TLP Traffic Load Prediction.

U

ULH Ultra Long-Haul.

W

WA Wavelength Assignment.

WB Wavelength Blocker.

WDM Wavelength Division Multiplexing.

WG Wavelength-layered Graph.

WSS Wavelength Selective Switch.

X

XPM Cross-Phase Modulation.

Bibliography

- [1] R. Ramaswami and K. N. Sivarajan. *Optical networks: a practical perspective*. Morgan Kaufmann Publishers, 2002.
- [2] A. Gumaste and T. Antony. *DWDM network designs and engineering solutions*. Cisco Press, 2003.
- [3] Y. Huang, J. P. Heritage, and B. Mukherjee. Connection provisioning with transmission impairment consideration in optical WDM networks with high-speed channels. *IEEE/OSA Journal on Lightwave Technology*, 23(3):982–993, 2005.
- [4] R. Cardillo, V. Curri, and M. Mellia. Considering transmission impairments in wavelength routed networks. In *Proc. International Conference on Optical Networking Design and Modeling (ONDM)*, pages 421–429, 2005.
- [5] T. Deng, S. Subramaniam, and J. Xu. Crosstalk-aware wavelength assignment in dynamic wavelength-routed optical networks. In *Proc. International Conference on Broadband Communications, Networks, and Systems (Broadnets)*, pages 140–149, 2004.
- [6] S-W. Kim and S-W. Seo. Regenerator placement algorithms for connection establishment in all-optical networks. *SPIE Optical Network Magazine*, 1(1):47–60, 2000.

- [7] B. Ramamurthy, S. Yaragorla, X. Yang. Translucent optical WDM networks for the next-generation backbone networks. In *Proc. Global Telecommunications Conference (GLOBECOM)*, volume 1, pages 60–64, 2001.
- [8] X. Yang, B. Ramamurthy. Sparse regeneration in translucent wavelength-routed optical networks: architecture, network design and wavelength routing. *Photonic Network Communications*, 10(1):39–50, 2005.
- [9] E. Yetginer and E. Karasan. Regenerator placement and traffic engineering with restoration in GMPLS networks. *Photonic Network Communications*, 6(2):139–149, 2003.
- [10] L. Belgacem, S. Al Zahr, and N. Puech. Routing and Wavelength Assignment in WDM Optical Networks: Exact Resolution vs. Random Search Based Heuristics. Technical Report 2008D002, Institut TELECOM/TELECOM ParisTech, 2008.
- [11] S. Al Zahr, M. Gagnaire, and M.-A. Ezzahdi. Impact of quality of transmission on protection schemes in hybrid WDM optical networks. In *Proc. IEEE EUNICE Conference*, 2007.
- [12] K. C. Kao and G. A. Hockham. Dielectric-fiber surface waveguides for optical frequencies. *Institution of Electrical Engineers*, 133(2):1151–1158, 1996.
- [13] F. P. Karpon, D. B. Keck, and R. D. Maurer. Radiation losses in glass optical waveguides. *Applied Physics Letters*, 17(10):423–425, 1970.
- [14] J. B. MacChesney, P. B. O'Connor, F. V. DiMarcello, J. R. Sompson, and P. D. Lazay. Preparation of low loss optical fibers using simultaneous vapor phase deposition and fusion. In *Proc. Congress on Glass*, volume 6, 1974.
- [15] G. P. Agrawal. *Fiber optic communication systems*. Wiley-Interscience Publication, 1997.
- [16] ITU-T. Characteristics of a single-mode optical fiber cable. Recommendation G.652, International Telecommunication Union, 1997.
- [17] J. S. Cook and O. I. Szentesi. North American field trials and early applications in technology. *IEEE Journal on Selected Area in Communications*, 1(2):393–397, 1983.

-
- [18] A. Moncalvo and F. Tosco. European field trials and early applications in technology. *IEEE Journal on Selected Area in Communications*, 1(3):398–403, 1983.
- [19] H. Ishio. Japanese field trials and early applications in technology. *IEEE Journal on Selected Area in Communications*, 1(3):404–419, 1983.
- [20] J. R. Stauffer. FT3C - a lightwave system for metropolitan and intercity applications. *IEEE Journal on Selected Area in Communications*, 1(3):413–419, 1983.
- [21] ITU-T. Characteristics of a dispersion-shifted single-mode optical fiber cable. Recommendation G.653, International Telecommunication Union, 1997.
- [22] J. X. Cai et al. 2.4 Tb/s (120 x 20 Gb/s) Transmission over transoceanic distance with optimum FEC overhead and 48 percent spectral efficiency. In *Proc. Optical Fiber Communications (OFC)*, pages PD20/1–3, 2001.
- [23] B. Bakhsi et al. 1 Tb/s (101 x 10 Gb/s) Transmission over transpacific distance using 28 nm C-band EDFAs. In *Proc. Optical Fiber Communications (OFC)*, pages PD21/1–3, 2001.
- [24] G. Vareille, F. Pitel, and J. F. Marcero. 3 Tb/s (300 x 11.6 Gb/s) Transmission over 7380 km using 28 nm C+L-band with 25 GHz channel spacing and NRZ format. In *Proc. Optical Fiber Communications (OFC)*, pages PD22/1–3, 2001.
- [25] B. Zhu et al. 3.08 Tb/s (77 x 42.7 Gb/s) Transmission over 1200 km of Non-Zero dispersion shifted fiber with 100 km spans using C-L-band distributed raman amplification. In *Proc. Optical Fiber Communications (OFC)*, pages PD23/1–3, 2001.
- [26] ITU-T. Spectral grids for WDM application: DWDM frequency grid. Recommendation G.694-1, International Telecommunication Union, 2002.
- [27] J. R. Stauffer. Which core technology for your network? *BT Technology Journal*, 20(4):19–26, 2002.
- [28] K. Grobe, M. Donhauser, M. Wiegand, and J. McCall. Optical metropolitan DWDM networks: an overview. *BT Technology Journal*, 20(4):27–44, 2002.

- [29] O. Gerstel, R. Ramaswami, and S. Foster. Merits of hybrid optical networking. In *Proc. Optical Fiber Communications (OFC)*, pages 33–34, 2002.
- [30] D. F. Grosz, A. Agarwal, S. Banerjee, A. P. Kiing, D. N. Maywar, A. Gurevich, T. H. Wood, C. R. Lima, B. Faer, J. Black, C. Hwu. 5.12 Tb/s (128 x 42.7 Gb/s) Transmission with 0.8 bit/s/Hz spectral efficiency over 1280 km of standard single-mode fiber using all-raman amplification and signal filtering. In *Proc. European Conference on Optical Communications (ECOC)*, volume 5, pages 1–2, 2002.
- [31] R. Ramaswami. Optical fiber communication: from transmission to networking. *IEEE Communications Magazine*, 40(5):138–147, 2002.
- [32] B. Doshi, D. Einstein, R. Nagarajan, G. N. Srinivasa Prasanna, C. Baatar, N. Blackwood, M. Sharma, S. Jothipragasam, A. Alfakih, and N. Raman. Crosstalk-aware wavelength assignment in dynamic wavelength-routed optical networks. In *Proc. International Telecommunication Network Strategy and Planning Symposium*, pages 537–546, 2002.
- [33] M. Islam. Raman amplifiers for telecommunications. *IEEE Journal of Selected Topics in Quantum Electronics*, 8(3):548–559, 2002.
- [34] Y. Zhou, A. Lord, and E. Sikora. Ultra-long-haul WDM transmission systems. *BT Technology Journal*, 20(4):61–70, 2002.
- [35] I. Chlamtac, A. Ganz, and G. Karmi. Lightpath communications: an approach to high bandwidth optical WAN's. *IEEE Transactions on Communications*, 40(7):1171–1182, 1992.
- [36] J. Kuri. *Optimization problems in WDM optical transport networks with scheduled lightpath demands*. PhD thesis, École Nationale Supérieure des Télécommunications, Paris, France, 2003.
- [37] B. Mukherjee. *Optical WDM Networks*. Springer, 2006.
- [38] A. Morea. *Contribution à l'étude des réseaux optiques translucides: évaluation de leur faisabilité technique et de leur intérêt économique*. PhD thesis, École Nationale Supérieure des Télécommunications, Paris, France, 2006.
- [39] J. G. Proakis. *Digital Communications*. McGraw Hill, 2001.

- [40] Denis Penninckx and A. Audouin. Physical performance in all-optical transparent networks. In *Proc. Conference Photonics in Switching (CPS)*, page PS.Tu.B2, 2003.
- [41] S. Al Zahr, M. Gagnaire, N. Puech, and M. Koubàa. Physical layer impairments in WDM core networks: a comparison between a north-American backbone and a pan-European backbone. In *Proc. International Conference on Broadband Communications, Networks, and Systems (Broadnets)*, pages 335–340, 2005.
- [42] N. Puech, S. Al Zahr, and M. Gagnaire. Wavelength-dependent quality of transmission in WDM transparent optical networks. In *Proc. International Conference on Telecommunications (ICT)*, 2006.
- [43] Y. Frignac and S. Bigo. Numerical optimization of residual dispersion in dispersion-managed systems at 40 Gbit/s. In *Proc. Optical Fiber Communications (OFC)*, 2000.
- [44] E. Harroff . France Telecom opens European Backbone Network. *Lightwave Magazine*, 17(2), 2000.
- [45] D.L. Mills and H-W. Braun. The NSFNET backbone network. In *Proc. Conference of the Special Interest Group on Data Communication (SIGCOMM)*, pages 191–196, 1987.
- [46] P. Winkler and L. Zhang. Wavelength assignment and generalized interval graph coloring. In *Proc. Symposium on Discrete Algorithms*, pages 830–831, 2003.
- [47] C. Nomikos, A. Pagourtzis, K. Potika, and S. Zachos. Fiber cost reduction and wavelength minimization in multifiber WDM networks. In *Proc. Networking*, pages 150–161, 2004.
- [48] R. Ramaswami and N. Sivarajan. Routing and wavelength assignment in all-optical networks. *IEEE Transactions on Communications*, 3(5):489–500, 1995.
- [49] T. E. Stern and K. Bala. *Multiwavelength optical networks: a layered approach*. Prentice Hall PTR, 1999.
- [50] O. Gerstel and S. Kutten. Dynamic wavelength allocation in all-optical ring networks. In *Proc. International Conference on Communications (ICC)*, volume 1, pages 432–436, 1997.

- [51] J.Y. Yoo and S. Banerjee. Design, analysis, and implementation of wavelength-routed all-optical networks: routing and wavelength assignment approach. *IEEE Communications Surveys, Broadband Network area*, 1997. <http://home.att.net/sbanerjee/publications.html>.
- [52] H. Zang, J. P. Jue, and B. Mukherjee. A review of routing and wavelength assignment approaches for wavelength-routed optical WDM networks. *Optical Network Magazine*, 1(1):47–60, 2000.
- [53] D. Banerjee and B. Mukherjee. A practical approach for routing and wavelength assignment in large wavelength-routed optical networks. *IEEE Journal on Selected Area in Communications*, 14(5):903–908, 1996.
- [54] J. P. Jue. *Optical networks: recent advances*, chapter Lightpath establishment in wavelength-routed WDM optical networks. Kluwer Academic Publishers, 2001.
- [55] Y. Zhu and R. Lin. Algorithms for lightpath establishment in wavelength-routed networks. In *Proc. Optical transmission, switching, and subsystems*, volume 5281, pages 334–341, 2004.
- [56] M. Koubàa. *Routing, protection and traffic engineering in WDM all-optical networks*. PhD thesis, École Nationale Supérieure des Télécommunications, Paris, France, 2005.
- [57] E. A. Doumith. *Traffic engineering in multi-protocol multi-granularity networks*. PhD thesis, École Nationale Supérieure des Télécommunications, Paris, France, 2007.
- [58] J. Kuri, N. Puech, M. Gagnaire, E. Dotaro, and R. Douville. Routing and wavelength assignment of scheduled lightpath demands. *IEEE Journal on Selected Area in Communications*, 21(8):1231 – 1240, 2003.
- [59] M. Koubàa, N. Puech, and M. Gagnaire. Routing and spare capacity assignment for scheduled and random lightpath demands in all-optical transport networks. In *Proc. Conference on Next Generation Internet Networks (NGI)*, pages 18–20, 2005.
- [60] E. A. Doumith and M. Gagnaire. Impact of traffic predictability on WDM EXC/OXC network’s performance. *IEEE Journal on Selected Areas in Communications*, 25(5):895–904, 2007.

-
- [61] I. Chlamtac, A. Ganz, and G. Karmi. Lightnet: Lightpath based solutions for wide bandwidth WAN's. In *Proc. International Conference on Computer Communications (INFOCOM)*, volume 3, pages 1014–1021, 1990.
- [62] S. Subramaniam and R. A. Barry. Wavelength assignment in fixed routing WDM networks. In *Proc. International Conference on Communications (ICC)*, volume 1, pages 406–410, 1997.
- [63] K. Bala and T. E. Stern. Algorithms for routing in a linear lightwave network. In *Proc. International Conference on Computer Communications (INFOCOM)*, volume 1, pages 1–9, 1991.
- [64] H. Harai, M. Murata, and H. Miyaraha. Performance of alternate routing methods in all optical switching networks. In *Proc. International Conference on Computer Communications (INFOCOM)*, volume 2, pages 516–524, 1997.
- [65] L. Li and A.K. Somani. Dynamic wavelength routing using congestion and neighborhood information. *IEEE ACM Transactions*, 7(5):779–786, 1999.
- [66] K. Chan and T. P. Yum. Analysis of least congested path routing in WDM lightwave networks. In *Proc. International Conference on Computer Communications (INFOCOM)*, volume 2, pages 962–969, 1994.
- [67] S. Ramamurthy and B. Mukerjee. Fixed-alternate routing and wavelength conversion in wavelength-routed optical networks. *IEEE ACM Transactions*, 10(3):351–367, 2002.
- [68] S. Ramamurthy. *Optical design of WDM network architectures*. PhD thesis, University of California, Davis, CA, USA, 1998.
- [69] E. W. Dijkstra. A note on two problems in connexion with graphs. *Numerische Mathematik*, 1(1):269–271, 1959.
- [70] D. Epstein. Finding the k shortest paths. *SIAM Journal of Computing*, 28(2):652–673, 1998.
- [71] J. Y. Yen. Finding the lengths of all shortest paths in n-node nonnegative-distance complete networks using $12n^3$ additions and n^3 comparisons. *Journal of the ACM*, 19(3):423–424, 1972.

- [72] A. Birman and A. Kershenbaum. Routing and wavelength assignment methods in single-hop all-optical networks with blocking. In *Proc. International Conference on Computer Communications (INFOCOM)*, volume 2, pages 431–438, 1995.
- [73] A. Mokhtar and M. Azizoglu. Adaptive wavelength routing in all-optical networks. *IEEE ACM Transactions*, 6(2):197–206, 1998.
- [74] R. Ramaswami and A. Segall. Distributed network control for wavelength routed optical networks. In *Proc. International Conference on Computer Communications (INFOCOM)*, volume 1, pages 138–147, 1996.
- [75] H. Zang, L. Sahasrabudde, J. P. Jue, S. Ramamurthy, and B. Mukherjee. Connection management for wavelength-routed WDM networks. In *Proc. Global Telecommunications Conference (GLOBECOM)*, volume 2, pages 1428–1432, 1999.
- [76] J. P. Jue and G. Xiao. An adaptive routing algorithm with distributed control scheme for wavelength-routed optical networks. In *Proc. International Computer Communication Conference (ICCC)*, pages 192–197, 2000.
- [77] I. Chlamtac, A. Ganz, and G. Karmi. Purely optical network for Terbit communication. In *Proc. International Conference on Computer Communications (INFOCOM)*, volume 3, pages 887–896, 1989.
- [78] R. A. Barry and S. Subramanian. The MAX-SUM wavelength assignment algorithm for WDM ring networks. In *Proc. Optical Fiber Communications (OFC)*, pages 121–122, 1997.
- [79] G. Jeong and E. Ayanoglu. Comparison of wavelength-interchanging and wavelength selective cross-connects in multiwavelength all-optical networks. In *Proc. International Conference on Computer Communications (INFOCOM)*, volume 1, pages 156–163, 1996.
- [80] E. Karasan and E. Ayanoglu. Effects of wavelength routing and selection on wavelength conversion gain in WDM networks. *IEEE ACM Transactions*, 6(2):186–196, 1998.

-
- [81] X. Zhang and C. Qiao. Wavelength assignment for dynamic traffic in multi-fiber WDM network. In *Proc. International Conference on Computer Communications and Networks (ICCCN)*, pages 479–485, 1998.
- [82] X. Sun, Y. Li, I. Lambadaris, and Y. Q. Zhao. Performance analysis of first-fit wavelength assignment algorithm in optical networks. In *Proc. International Conference on Telecommunications (ICT)*, volume 2, pages 403–409, 2003.
- [83] E. Karasan and E. Ayanoglu. Performance of WDM transport networks. *IEEE Journal on Selected Area in Communications*, 16(7):1081–1096, 1998.
- [84] C. S. R. Murthy and M. Gurusamy. *WDM Optical Networks: Concepts, Design and Algorithms*. Prentice Hall, 2002.
- [85] M. Sharma, M. Soulliere, A. Boskovic, and L. Nederlof. Value of agile transparent optical networks. In *Proc. Optical Fiber Communications (OFC)*, pages 293–294, 2002.
- [86] I. Tomkos. Transport performance of WDM metropolitan area transparent optical networks. In *Proc. Optical Fiber Communications (OFC)*, pages 350–352, 2002.
- [87] A. Willner, M. C. Cardakli, O. H. Adamczyk, Y. Song, and D. Gurkan. Key building blocks for all-optical network. *IE-ICE Transactions in Communications*, E83-B(10):2166–2177, 2000.
- [88] B. Ramamurthy, H. Feng, D. Data, J. P. Heritage, and B. Mukherjee. Transparent vs. opaque vs. translucent wavelength-routed optical networks. In *Proc. Optical Fiber Communications (OFC)*, pages 59–61, 1999.
- [89] M.A. Ezzahdi, S. Al Zahr, M. Koubàa, N. Puech, M. Gagnaire. LERP: a quality of transmission dependent heuristic for routing and wavelength assignment in hybrid WDM networks. In *Proc. International Conference on Computer Communications and Networks (ICCCN)*, pages 125–130, 2006.
- [90] P. C. Becker, N. A. Olsson, and J. R. Simpson. *Erbium-doped fiber amplifiers: fundamentals and technology*. Academic Press: Optics and Photonics, 1999.
- [91] S. Al Zahr, N. Puech, and M. Gagnaire. Gain equalization versus electrical regeneration tradeoffs in hybrid WDM networks. In *Proc. International Conference on Telecommunications (ConTEL)*, 2007.

- [92] S. Al Zahr, M. Gagnaire, and N. Puech. Impact of wavelength assignment strategies on hybrid WDM network planning. In *Proc. Design of Reliable Communication Networks (DRCN)*, 2007.